NASA-CR-197330

JPL Publication 94-15

Synthesis of a Large Communications Aperture Using Small Antennas

G. M. Resch
T. A. Cwik
V. Jamnejad
R. T. Logan
R. B. Miller
D. H. Rogstad

July 1, 1994

NASA
National Aeronautics and Space Administration

Jet Propulsion Laboratory
California Institute of Technology
Pasadena, California

JPL Publication 94-15

Synthesis of a Large Communications Aperture Using Small Antennas

G. M. Resch
T. A. Cwik
V. Jamnejad
R. T. Logan
R. B. Miller
D. H. Rogstad

July 1, 1994

National Aeronautics and
Space Administration

Jet Propulsion Laboratory
California Institute of Technology
Pasadena, California

The research described in this publication was carried out by the Jet Propulsion Laboratory, California Institute of Technology, under a contract with the National Aeronautics and Space Administration.

ABSTRACT

In this report we compare the cost of an array of small antennas to that of a single large antenna assuming both the array and single large antenna have equal performance and availability. The single large antenna is taken to be one of the 70-m antennas of the Deep Space Network.

The cost of the array is estimated as a function of the array element diameter for three different values of system noise temperature corresponding to three different packaging schemes for the first amplifier. Array elements are taken to be fully steerable paraboloids and their cost estimates were obtained from commercial vendors. Array loss mechanisms and calibration problems are discussed. For array elements in the range 3 to 35 m there is no minimum in the cost versus diameter curve for the three system temperatures that were studied.

PREFACE

The motivation for this study can be traced entirely to the refusal of the 3.7-m antenna on the Galileo spacecraft to deploy properly. That antenna was intended to transmit X-band science data to Earth at a rate of 134 kbs as the spacecraft orbited the planet Jupiter and made successive encounters with the Jovian satellites. Loss of this antenna means that only an omnidirectional S-band antenna is available for mission support and represents a 47-dB reduction in communications capability.

During the spring and summer of 1992, the Galileo team tried various "tricks" to coax the antenna open but to no avail. The Galileo project manager asked the Tracking and Data Acquisition (TDA) Office if other support options were available, just in case the antenna never opened. A study team was formed, led by Leslie J. Deutsch, that quickly developed a list of "wild ideas" by which the mission data return capabilities could be enhanced at S-band. The most significant enhancements involved modifying the spacecraft in some way, such as using data compression. On the ground, the enhancements involved arraying as many antennas as possible and reducing the system temperature on each of these antennas.

As a member of that Wild Ideas team, along with Don Brown, Bruce Crow, and Dave Rogstad, we investigated arraying possibilities. One of the first things we did was to review what was then a 2-year-old study that estimated the cost of a new 70-m Beam Waveguide antenna, and we calculated that the cost of new collecting aperture would be approximately $26,000 per square meter, if it were purchased as individual 70-m apertures. It did not require a mathematical whiz to estimate that new aperture to make up the 47-dB link loss would cost more than the entire NASA budget for the next century, even assuming a generous discount for buying 70-m antennas in quantity, and therefore was unlikely ever to be funded.

I recalled a memo written by Barry Clark [1966] exploring something he called the "Kilodish Array," as a possible configuration for what later became the Very Large Array. Basically, he pointed out that by using TV dish antennas, a large collecting aperture could be assembled inexpensively, but the electronics cost was large and restricted future expansion capabilities. A quick scan of the *Los Angeles Times* revealed an advertisement touting a 3-m satellite dish with receiver for $1699, or an aperture cost of roughly $239 per square meter. The difference in aperture cost was intriguing, and I soon found that several of my colleagues had previously noted this factor-of-ten cost discrepancy and wondered, as I did, if there might be a cost advantage for the Deep Space Network to array small antennas—not just for Galileo but for all the DSN's various activities.

The idea of a massive array of small antennas to address the Galileo problem disappeared under the onslaught of restrictive budget and schedule realities, but it was decided to explore the

concept further with a design study and cost estimate. Hence, this study was born and the concept was nicknamed MOAA—the mother of all arrays. Like any conservative team leader, I recruited people who were much smarter than I. We met weekly, parceled out assignments, shared crazy ideas, told a lot of jokes, and generally had a good time. Everybody on the team contributed, all criticism was constructive, and we all developed a deep respect for each other's ideas. I count the experience as the most pleasurable job assignment I have had in my career at JPL and hope that my fellow team members enjoyed it even half as much as I did.

The report is laid out in pretty much the temporal order in which we developed arguments and analysis. As a result, the reader may notice some inconsistency in the development. For instance, one of the requirements that we adopted was to synthesize the equivalent aperture of three 70-m antennas. I think it is safe to say that all the team members began the study with the belief that arraying small antennas would be much less expensive than building large 70-m apertures, and it would then be possible to consider such a large undertaking. You will note that in the end, the cost for synthesizing only one 70-m aperture is estimated.

During several of our initial team meetings there were questions as to how or why the DSN does certain things a particular way, i.e., a questioning of the "conventional wisdom," and the historical summary in the first chapter addresses these questions. In the current environment there is much discussion of re-engineering the DSN, and I think that it would be helpful if more people understood the historical development of the DSN before they begin to implement fundamental changes. We agonized much more about uplink arraying than is indicated by the short section in the text and discussed the cost aspects with colleagues in the transmitter group. However, any follow-on effort should re-examine this issue with respect to cost effectiveness.

I owe a huge thanks to Les Deutch, William Rafferty, Charles Stelzried, and Hugh Fosque for providing encouragement and financial support for this study. I suspect they knew I wanted to do this study so badly that I would have worked for free but they paid me anyway. I am particularly indebted to them for the understanding they have shown as to why this report is a year late.

Don Brown, Rick Green, Richard Mathison, and Bruce Crow all provided early encouragement that was both needed and appreciated. A very special thanks is due to Robert Clauss and David Fort for their help and advice in several areas. Bob Clauss was a constant source of provocation and constructive criticism. Some of his words are found verbatim in the report in regard to low-noise amplifier performance and cost. Dave Fort was an active consultant on questions concerning the correlator, combiner, and array performance. George Morris and Jack Fanselow both contributed unconventional ideas and encouragement. Fred McLaughlin reminded me that he and Bob Stevens had noticed that small antennas do not seem to follow the

diameter to the 2.7-power law. Larry Rauch reviewed a draft of this report and suggested several improvements and caught a host of errors—thank you Larry.

During the course of the study I received so many good suggestions and ideas from so many people that I no longer remember all of them. If you are among this number, please accept my apologies along with my sincere gratitude.

George M. Resch

TABLE OF CONTENTS

FIGURES

TABLES

1.0 INTRODUCTION

This report documents the results of a design study whose objective was to develop a quantitative understanding of the performance, cost, and technical risks associated with synthesizing a large aperture from an array of smaller apertures. Such an array would support the communication links to any spacecraft engaged in solar system exploration. The study represents the conceptual exploration of a particular evolutionary path that is open to the Deep Space Network (DSN).

The product of the study is a model that relates the total acquisition cost of an array to the diameter of the elemental apertures in the array. This cost is a function of the total antenna gain divided by total system temperature, i.e., denoted as G/T. The functional performance benchmark used in the study is taken from DSN Document 810-5, Module TCI-10 [1991], for the 70-m antenna network. The cost benchmark is taken from a previous study documented by Brunstein [1990].

The rationale for this study is based on the premise that changing technology acts to reduce the cost of the electronics as a function of time while the cost of a single large antenna is dominated by steel and labor, which increase as a function of time at least as fast as inflation. It was reasoned that as the fractional cost of electronics decreased, smaller antenna diameters would minimize the total system cost. It follows that a study such as this one should be done periodically to determine the optimum array element diameter.

The term "system" that is used throughout the document consists of antennas, radio- and intermediate-frequency amplification, signal distribution, combiner electronics, and the monitor and control needed to operate the array in a synchronous fashion. Although we believe the particular array design that will be discussed would perform and support all DSN responsibilities (e.g., planetary radar, radio science, etc.), the functional requirements were dominated by telemetry considerations. It must be kept in mind throughout this document that although much of the discussion is focused on the performance and cost of a receive-only array, the total system concept would more likely include a single 34-m-class antenna having both uplink and downlink capabilities. For instance, the new 34-m Beam Waveguide (BWG) with an active uplink capability would be arrayed with some number of receive-only antennas.

This section contains a very brief historical review of some of the factors that have influenced the design of the current DSN. The rationale behind the study is discussed, and there is a short summary of some of the reasons why the study avoided uplink capability in the array. The overall requirements and goals of the array are outlined, and finally there is a description of the approach used in the study and identification of who was primarily responsible for what.

1.1 HISTORY

"I know no way of judging the future but by the past"
-Patrick Henry

In the early 1960's, the National Aeronautics and Space Administration (NASA) began a major expansion of the DSN in order to support the planetary exploration program. The primary requirements for this network were: (1) support operations under all reasonably anticipated weather conditions, (2) support continuous 24 hr/day communications, and (3) support both a low-gain/broad-beam and a high-gain/narrow-beam communications link. The latter requirement arose from the supposition that most spacecraft would be equipped with a high-gain/narrow-beam antenna to support high data rate links, as well as a nearly omnidirectional/low-gain antenna to be used during spacecraft emergencies.

These requirements were driven primarily by the then current state-of-the-art in spacecraft design. The result was a network of deep-space stations spaced approximately 120° apart in longitude that could provide 24 hr/day communications. The implication of communications gaps were mission penalties in the form of increased spacecraft weight, complexity, and lower reliability as a result of greater data storage requirements. In addition, there is the possibility that a spacecraft emergency during a gap could lead to an unrecoverable failure. Perhaps more important, by the early 1960's, a successful operations scenario was established for planetary missions that took full advantage of continuous contact with a continuously operating spacecraft, a scenario that continues to the present day.

The overall goal of the expansion in the 1960's, and the goal that persists to this day, is to achieve a design balance between Earth support equipment and spacecraft capability so as to provide the most cost-effective <u>total</u> system cost to NASA. In such a balanced design, every dollar invested in the ground stations would lead to an increase in returned data (integrated over the station lifetime), that would be exactly the same as the increase in data resulting from the same dollar investment in spacecraft development. While there is no readily available metric to measure progress toward this goal, the sentiment is highly worthwhile.

In late 1965, P. Potter, W. Merrick, and A. Ludwig [1965] published a report documenting the major considerations that had gone into the evolution of the DSN in the early part of that decade. Their concerns were the economic balancing of ground antenna aperture with potential improvements in spacecraft performance, the use of large single antennas versus arrays of smaller antennas, and the optimum frequency of the communications link. Based on an approximately 2-yr. study, they concluded that a single antenna of the 65-m diameter class was the most economically

feasible approach for the next 10 to 15 years. Further, either a steerable paraboloid of approximately 65 m diameter or an array of such antennas would be the optimum aperture implementation, depending on the number and capability of spacecraft launched in the 70's and 80's. It is relevant to note that this study considered arraying in some detail. Finally they judged that the optimum frequency of operation would be approximately 2 GHz.

In the late 1970's, the DSN again considered a major expansion and embarked on a study of what was termed the Large Advanced Antenna Station or LAAS for short, and was documented in a status report issued in 1978 [Haglund, 1978]. Prior to 1977 it was thought that the next major addition to the DSN would be implementation of a second subnet of 64- to 100-m antennas, as the earlier study had concluded. However, in March 1977 it was postulated that an antenna array rather than a single antenna aperture would be more cost-effective for the prospective LAAS, and the study was expanded to include this possibility. On May 16, 1978, JPL recommended to what was then the Office of Space Tracking and Data Acquisition (currently the Office of Space Operations) that if a large advanced antenna station was to be built, it should be built with multiple apertures (i.e., an array) because the life-cycle cost and technical risk were significantly less than for a single large aperture.

The antenna diameters that were considered in the LAAS study were 100 m for the large single aperture and 25 m to 38 m for the array elements. Three companies, E-Systems Inc., Ford WDL, and Harris Corp., were contracted to provide detailed performance and cost estimates for the antennas while electronics performance and costs were estimated internally at JPL. The study report alluded to an attempt to investigate the cost advantages of even smaller antenna elements and stated that "this approach did not prove practical due to antenna-related electronics costs."

Brunstein [1990] documented a study that addressed the question, "Would an array of smaller antennas with performance equivalent to a 70-m antenna be cheaper to build than a 70-m BWG (Beam Waveguide) antenna?" The study considered an array of four 34-m antennas that was functionally equivalent to 70-m capabilities for commanding, telemetry, radio science, and Very Long Baseline Interferometry (VLBI). The study concluded that the array was not cheaper. The total cost for the array and the 70-m antenna, including all electronics, was approximately the same or at least within the estimation errors of the budgeting process.

In the discussions that followed the Brunstein memo, it was realized that the arraying approach enjoyed an enormous practical advantage over the single large antenna. The array could be constructed one element at a time and the capital investment spread out over several years. This is the strategy that the DSN has planned for the next decade. A 34-m subnet of High-Efficiency (HEF) antennas has already been constructed. The Construction of Facilities plan for the next decade calls for new 34-m BWG antennas at Goldstone and Canberra. In principle, the 34-m antennas at Goldstone could be combined to provide the equivalent capability of a 70-m antenna.

1.2 RATIONALE

"You can never plan the future by the past."
- Edmund Burke

The primary reason that the DSN is evolving today is exactly the same as it was 30 years ago —to support NASA's planetary exploration program. While some considerations remain the same, there have been other fundamental changes in the forces that drive this evolution.

First, and foremost, the content and constraints on the planetary exploration program have changed. The planetary program has almost transitioned from the reconnaissance stage to the exploration stage. We have had flybys of all the planets except one, and have begun the systematic discovery and understanding of processes, history, and planetary evolution. The next phase that we must anticipate is intensive *in situ* study that will involve landers, rovers, atmospheric balloons, sample returns, and possible landings by astronauts.

Second, the range of responsibilities assigned to the DSN has expanded. Near-Earth missions that cannot be tracked by the Tracking and Data Relay Satellite System (TDRSS) and international cooperative missions have greatly expanded the list of spacecraft that keep the network busy. In fact, the missions in this category constitute the largest segment of future support requests.

Finally, technology has changed. Thirty years ago the selection of 64 m as the "best" antenna diameter was made largely on the judgment that 64 m was the largest antenna that could safely be constructed within cost, performance, and schedule constraints. Furthermore, such an antenna would be gain-limited at a frequency higher than S-Band, which was the frequency at which spacecraft hardware could be implemented. Thanks to advances in technology, the diameter of the DSN's largest antennas was extended to 70 m, the gain limit has been extended to a frequency higher than X-Band, and complementary technology has been incorporated in the spacecraft design.

These changes in the planetary program and expanded responsibilities and technology improvements suggest several ideas. The growing list of spacecraft requiring ground support implies that either more antennas are needed, or a change in the ground support strategy is required. Many of the missions in the planning stage are near-Earth and have communications requirements far less demanding than the deep space missions. Supporting this class of missions with 70-m class apertures would constitute over-design of the communications link.

On the other hand, the deep space missions that are being planned are even more constrained by cost, mass, and power than they were in the past. If reasonable data rates are to be supported from these distant spacecraft, the link capability must be sustained by large G/T capability on the ground. An array offers the flexibility to assemble an aperture that is tailored to the mission requirement.

The strategy of providing continuous communications with a deep space mission has proved to be highly successful in the past. It is clear that it will be very expensive to follow this strategy in the future because it requires an active uplink for every spacecraft all the time, and the cost of providing this uplink nearly doubles the electronics cost for the antenna system. The uplink is needed to command the spacecraft and provide two-way Doppler measurements that are used to navigate. While commanding is a relatively infrequent need, the quality of navigation depends strongly on the quantity of two-way Doppler data and its spread over time. With the advent of ultrastable oscillators on the spacecraft, it may be possible to utilize one-way Doppler or to supplement the Doppler data with other data types in order to navigate in deep space. If true, there would no longer be the need for one uplink for every downlink. Uplinks could be time multiplexed and the DSN would enjoy a considerable savings in capital investment, maintenance, and operations cost.

Another motivation for this study stems from the contrast between two observations. The first observation, taken from the technical literature, suggests that the cost of large antennas is proportional to antenna diameter D raised to some power γ, where $2 < \gamma < 3$, with a most likely value of 2.5. The second observation comes from the fact that the cost of electronics (for some measure of functionality) is decreasing with time. Taken together, these observations would indicate that the optimum diameter for an array element should decrease with time.

In order to quantify these observations, consider that the total system cost for an array C_T, is the sum of the m subsystem costs C_i;

$$C_T = \sum_{i=1}^{m} C_i$$

where the antenna subsystem cost is merely one of the terms in the sum and the other terms represents such subsystems as the radio frequency amplifiers, digital electronics, etc. The cost for each subsystem can be separately modeled, and in general, each term (including the antenna subsystem) will contain a nonrecurring cost (NRC_i) and a recurring cost (RC_i) per antenna element. The NRC_i represents the setup, design, and management required for any large project, while RC_i represents the production cost per unit, and N_e represents the total number of elements in the array. For the ith subsystem

$$C_i = NRC_i + N_e \cdot RC_i$$

We will denote the antenna subsystem as i = 1 and assume that its recurring cost can be modeled as a power law function of the antenna diameter D_e such that

$$C_1 = NRC_1 + N_e \cdot \beta \cdot D_e^{\gamma}$$

where β and γ are constants. The total system cost is then

$$C_T = N_e \cdot \beta \cdot D_e^{\gamma} + \sum_{1}^{m} NRC_i + N_e \cdot \sum_{2}^{m} RC_i$$

In general, while the NRC_i and RC_i, are functions of the size of the total array, they can be assumed not to be functions of the antenna diameter. The number of elements in the array N_e depends on both the effective diameter of the aperture that is to be synthesized and the diameter of the individual antennas, i.e., it takes four -m paraboloids to synthesize the aperture of a 2-m paraboloid. If we are given the size of the aperture to be synthesized, then $N_e = k(D_e)^{-2}$, where k is some constant. Taking the derivative with respect to D_e, substituting for N_e, and solving for the value of the diameter that minimizes the total cost, yields

$$(D_e)_{min} = \left[\frac{2 \cdot \sum RC_i}{\beta(\gamma - 2)} \right]^{1/\gamma} \qquad (1\text{-}1)$$

We see that for $\gamma \leq 2$, there is no real solution, which implies that the minimum cost is a single aperture whose diameter was previously specified. However, for $\gamma < 2$, there is a distinct diameter that minimizes the total system cost. As technology changes, particularly in the area of high-speed digital signal processing, the recurring cost term in the above equation might be expected to decrease and the optimum diameter for an array element would decrease with time.

An additional consideration is overall system reliability. A single large antenna represents a potential single point of failure, whereas individual antennas in an array can fail with the result that performance is gradually degraded and does not go immediately to zero. With each antenna in an array providing a small quantized value of G/T together with the flexibility to combine any subset of an array, a communications link could be tailored to the data rate requirements and capabilities of a particular spacecraft. An array can be assembled of just a few elements for a near-Earth spacecraft with a low data rate, or of all elements for a distant spacecraft in trouble. The aggregate G/T would be determined by the combination of the most demanding link requirement and schedule loading.

However, the prospect of building new antennas for the DSN and arraying them on a regular basis raises a new set of questions. Perhaps the first, and certainly the most timely, of these questions is, Is there an optimum diameter for the elements of the array? This is the question that this study attempts to address, but to do so requires optimization of the total system cost and performance. One cannot replace a single large antenna with an array without first considering the performance and cost of the electronics needed to process the outputs of array elements.

1.3 UPLINK ARRAYING

Consider two identical parabolic antennas, pointed at the same area of the sky, each transmitting a power P, and driven by a coherent source. The far field is an interference pattern consisting of fringes, i.e., alternating bands of constructive and destructive coherence. Where there is destructive interference, the voltage from each antenna is completely out of phase and there is no power. Where there is constructive interference, the voltage from each antenna adds in-phase to produce 2 times the individual pattern voltage, or an effective power density of 4 times the individual radiated power. Thus, if a 70-m aperture having a 20-kW uplink is synthesized using four 35-m apertures (each has 0.25 of the gain of a 70-m), then 5-kW transmitters on each 35-m antenna are needed plus the ability to control the phase of the uplink in order to ensure coherence in exactly the direction we desire. If the synthesis utilized 500 3-m antennas, then a 40-W transmitter on each of the small antennas would be required. Thus, there is no savings in the uplink power requirement.

Superficially, the prospect of uplink arraying may appear to be economically attractive. The cost of a transmitting amplifier is not a linear function of the power rating. At low power ratings, amplifying elements can be radiatively cooled, thereby eliminating the circulating water systems needed for high-power elements. This is a savings in capital investment as well as maintenance and reliability. However, power conversion efficiency is likely to be lower for low power amplifiers, so the total electric bill will be somewhat higher. In addition, the capital investment savings are offset by the increased cost of the microwave components needed to protect the downlink low-noise amplifier (LNA), which can also incur a penalty in receive system temperature, and increase the number of small antennas needed to synthesize the receive aperture.

The technological problem in uplink arraying is phase control. The signal from each radiating element must be in phase at the receiver. Phase differences arise due to: (1) the geometry between radiating elements and receiver, (2) instrumental effects between transmit elements, and (3) the propagation medium. The instrumental phase offset arises from differences in the phase delay of separate electronic components and signal paths between radiating elements. These instrumental effects can be minimized by using a homogeneous array of identical elements with identical signal

paths so that differences cancel to first order. It may well be possible that these phase delays in the transmit configuration can be made very stable and can be calibrated as is possible in the receive-only configuration, but this remains to be demonstrated.

Note that just as in the case of a receive-only array, maintaining coherence becomes more difficult as the distance between the antennas increases. However, for compact arrays the geometrical portion of the phase difference can be calculated with high accuracy, as demonstrated by arrays like the VLA. Furthermore, in the receive-only array there is the possibility of correcting for phase errors in real time by correlating the signal from each antenna against another or against the sum of all antenna signals, i.e., self-coherence. In the transmitting array case, the "correct" instrumental phase for each antenna must be known absolutely (through the transmit electronics) and another correction added for the fluctuating phase changes due to the propagation medium as derived from the downlink signal. In the case of a spacecraft emergency when the downlink signal might be nonexistent, any doubt at all in regard to uplink coherence of the arrayed transmit beam would simply compound an already difficult situation.

It could be argued that the spacecraft signal acquisition problem could be reduced or eliminated by design and/or strategy changes. For instance, the fringes from the transmit array could be swept at a controlled rate across the point in the sky where the spacecraft it believed to be located. In principle, the spacecraft radio could be designed to respond to an RF signal that is amplitude modulated at the predetermined sweep rate. This necessitates close coordination with spacecraft designers.

In summary, we see that the potential decrease in transmitter cost per antenna must be balanced against the technological risk of maintaining uplink coherence. A very limited estimate of the cost savings for a transmit array done here suggests that it would be small to nonexistent. The technological risk cannot be quantified. Therefore, it was decided to limit this study to the receive-only array.

1.4 REQUIREMENTS AND GOALS

- *Synthesize a ground communications capability with a G/T ratio equivalent up to 3 times the current DSN 70-m antenna capability.*

If four 70-m antennas (the existing 70-m plus 3 new synthesized apertures) were arrayed, they would provide 6 dB more link capability than currently exists. This additional capability could be accomplished with 3 additional 70-m antennas, or the equivalent synthesized G/T from an array of smaller antennas. If the DSN had 6 dB more G/T at X-band, this X-Band capability would be

competitive with what is expected to be gained by going to Ka-band on a single 70-m antenna. This additional 6-dB link capability would service the Galileo S-Band mission and avoid the problems and expense involved in arraying with non-DSN antennas. With sufficient G/T on the ground, both the DSN and future missions could postpone Ka-band development, and thereby save development resources.

• *Plan for a single array at Goldstone with the option of duplicating the capability at the overseas complexes.*

If the DSN were ever to build an array of small antennas, it would most likely be at Goldstone first as a feasibility demonstration. There would be an option to duplicate the design overseas and expand it to whatever aggregate G/T is ultimately required by future missions. In order to constrain this design study, the following additional general requirements and goals were adopted:

• *The total cost for comparable G/T should be substantially less than equivalent 70-m parabolic antennas.*

It seems unlikely that the DSN will be able to garner the facilities funding to construct new 70-m paraboloid antennas. The existing 70-m network is almost 30 years old, and inevitably maintenance costs continue to increase while the time available for spacecraft support is decreasing. There is a reluctance by mission planners to design a mission that is critically dependent on 70-m support. According to Brunstein [1990], a 70-m beam waveguide antenna is estimated to cost $106M in 1990 dollars (not including electronics), which would be a difficult fit in an already overextended NASA facilities budget. If the cost of collecting area can be reduced by a factor of 1/2 to 1/5th, then funding might be more forthcoming.

• *Simultaneous S- and X-Band receive.*

Since all existing deep space spacecraft are either S- or X-Band (or both), even the Pioneers 10 and 11 and Voyagers could be serviced for many years into the future.

• *Listen-only (no transmit capability) for the smaller apertures, to be arrayed with a single 34-m antenna having up- and downlink capability.*

Current technology makes it possible to transmit high power from a single antenna (e.g., up to 1 megawatt). For instance, an 80-kW transmitter from a 34-m antenna in the DSN would be the functional equivalent of a 70-m antenna with 20-kW uplink capability. This suggests a ground configuration of a single parabolic antenna for uplink purposes in conjunction with an array of smaller antennas that provide a much larger collecting area to receive the weak spacecraft signal.

The array is then to be viewed as a supplement to existing DSN capabilities, not as a replacement. Single antennas will continue to provide uplink service while the new aperture will provide greatly increased downlink capability.

- *Sidereal tracking for all sources above 10° elevation.*

Spacecraft that are too far away to be serviced by TDRSS will appear to move in the plane of the sky but their angular rates are nearly that of the "fixed" stars, i.e., the sidereal rate. A 10° elevation limit is comparable to existing DSN antenna limits. Pointing and wind specifications were taken directly from DSN Document 810-5 [1991].

- *The synthesized aperture must be capable of operating as independent subapertures or as a single unit.*

Some future missions that are currently under discussion include multiple rovers or orbiters around or on the Moon and Mars. A substantial payoff can be gained in reduced spacecraft cost by keeping the communications capabilities of these rovers as simple and low-power as possible. In order to do this, the Earth-based part of the link must be highly capable. It would be desirable to transmit with the simplest, lowest possible power transmitter from the Martian surface. This calls for high transmit power and large effective collecting area on Earth. An array of antennas would provide important scheduling flexibility for this kind of scenario and provide backup capability to a Mars orbiting relay.

- *Each subaperture as well as the total aperture must be capable of arraying with existing DSN antennas in real-time.*

By operating as independent smaller apertures (i.e., roughly equivalent to a 34-m antenna), all or part of the array can be concentrated either on a single weak source (e.g., Galileo) or assigned independent targets.

1.5 THE APPROACH USED IN THE STUDY

"Never make forecasts, especially about the future."
- Samuel Goldwyn

The team started with a very conventional array design, estimated performance and costs, then redesigned based on what appeared to be performance or cost drivers. Each team member assumed primary responsibility for an area or subsystem in the following categories:

- Antennas subsystem (Tom Cwik)
- RF/IF subsystem (George Resch)
- Signal distribution (Ron Logan)
- Correlator/Combiner (Dave Rogstad)
- Monitor & Control (Bob Miller)
- Availability & reliability (Vahraz Jamnejad)

In practice, these areas were so cross-linked that all team members participated in all design areas. As the design progressed, it was necessary to expand the requirements and the functional block diagrams in successive levels of detail. This process continued to the point where it became possible to model both performance and cost of each subsystem.

It was realized early in the design process that the team was severely handicapped in regard to estimating cost for the antenna structures and it was decided to tender two small contracts to commercial antenna builders in order to establish cost estimates for these subsystems. Appendix A is a portion of the statement of work that was used to solicit this supporting study. Two companies responded and produced both performance and cost estimates for antenna elements ranging from 3 to 35 m in diameter.

In order to reduce the uncertainty of cost estimates, a ground rule of using "off-the-shelf" technology was adopted, i.e., it was decided that the design should not depend on something that had to be discovered or developed. The final section of this report lists those areas where additional development of new technology has the potential to either increase performance or decrease array cost.

2.0 ARRAY SPECIFICATIONS

The gain of an antenna divided by its system temperature (G/T) is one of the parameters that determines how much data can be sent over a communications link. Our goal is to determine if there is an optimum antenna diameter that minimizes the total system cost for an array. In order to calculate this cost we must first know how many elements are required to achieve the given level of G/T performance. Secondly, we must recognize the bounds on performance achievable with current technology and attempt to parameterize both performance and cost in a way that can be related to antenna diameter. Finally, we must understand how the overall reliability and availability of an array is related to cost and how it compares to a single large aperture.

2.1 THE NUMBER OF ANTENNAS NEEDED FOR A GIVEN G/T

The gain G, of an antenna is given in terms of its effective collecting area A_e, at an operating wavelength λ, as

$$G = \frac{4\pi}{\lambda^2} \cdot A_e \tag{2-1}$$

The effective collecting area can be written as the product of the physical aperture area A_p times a factor η, that is termed the aperture efficiency, i.e., $\eta < 1$. If we let N_{70} be the number of 70-m antennas that we wish to synthesize, then for an array of smaller antennas having the equivalent G/T, we can write:

$$\left(\frac{G}{T}\right)_{ary} = \frac{N_{70}}{L_C}\left(\frac{G}{T}\right)_{70}$$

where L_C is the average combining loss and is an expression of the fact that the output of the individual antennas can never be combined with perfect coherence. Assuming N_e identical array elements, having diameter D_e, aperture efficiency η_e, and total system temperature T_e, then

$$N_e \eta_e D_e^2 / T_e = N_{70}\left(\eta_{70} D_{70}^2 / T_{70}\right) / L_C$$

and the required number of elements in the array is

$$N_e = \frac{N_{70}}{L_C}\left(\frac{\eta_{70}}{\eta_e}\right) \cdot \left(\frac{T_e}{T_{70}}\right) \cdot \left(\frac{70}{D_e}\right)^2 \tag{2-2}$$

Table 2-1 summarizes the performance of the DSN 70-m antennas at S- and X-band that will be our benchmark.

If we take D_e as the independent variable, then we must specify both the performance and cost models for η_e, T_e, and L_C. If we further assume that maximum tolerable arraying loss is 0.2 dB, then using the values in Table 2-1 yields two equations, one for S-band and one for X-band.

$$N_e(S) = 208 \cdot N_{70}\left(\frac{T_e}{\eta_e}\right)\frac{1}{D_e^2} \tag{2-3}$$

$$N_e(X) = 168.6 \cdot N_{70}\left(\frac{T_e}{\eta_e}\right)\frac{1}{D_e^2} \tag{2-4}$$

TABLE 2-1: Summary of 70-m performance specifications.

	S-Band	X-Band
Antenna Gain (dB)	63.3	74.2
Aperture efficiency (45° Elev.)	0.75	0.69
Zenith System Temperature (K)	18.5	21.0

2.2 GAIN LIMITS FOR AN ANTENNA AND ARRAY

Equation (2-1) gives the relationship between the physical collecting area and gain of an aperture. Ruze [1952] pointed out that various mechanisms cause deviations in the reflector surface, which result in a systematic or random phase error. These errors can be mapped into the aperture plane and lead to a net loss of gain such that the relative gain is given by the expression

$$\frac{G}{G_0} = exp\left\{-\left(\frac{4\pi\sigma}{\lambda}\right)^2\right\} \tag{2-5}$$

where σ^2 is the variance of the phase error in the aperture plane. While Eq. (2-1) predicts that the gain of an antenna should increase as the square of the frequency, Eq. (2-5) predicts that when $(\sigma/\lambda)>1$, the gain drops rapidly. It is straightforward to show that the gain will be a maximum at a wavelength λ_{min}, which is approximately equal to 13 times the rms surface error σ. This point is

known as the gain limit of the antenna. Note that the concept of gain limit is equally valid for a synthesized aperture.

The phase error in the aperture plane is composed of several components; the surface "roughness" of the reflector(s), mechanical distortions from a strict parabolic shape, and the atmosphere. All of these components grow as D_e increases but at differing rates. In general it is easier (i.e., less expensive) to build a small antenna that has (and can keep) a very good surface accuracy than it is to build a large antenna with comparable accuracy. However, the large number of different technical approaches to reducing these errors makes for a complex cost estimation process. In order to simplify this process, we have restricted this study to "off-the-shelf" antenna technology.

One of the potential disadvantages of an array is due to the fact that its physical extent is always larger than the equivalent single antenna aperture that it synthesizes. As a result, phase errors due to atmospheric fluctuations, which grow as the distance between individual elements increases, can effectively gain limit the array.

2.3 SYSTEM TEMPERATURE

The performance numbers in Table 2-1 reflect large capital investments made over the years to improve collecting area efficiency and the use of state-of-the-art in low-noise amplifier (LNA) technology. The DSN 70-m antennas have very good gain performance at S-band and good gain performance at X-Band. Overall G/T performance is distinguished by the exceptionally low system noise temperatures, due to the use of traveling wave maser (TWM) amplifiers.

While TWMs have been procured from industry, they are not exactly an "off-the-shelf" item. In general, they are custom built in-house for the DSN. Mounted on the tipping structure of an antenna, they operate in a vacuum jacketed 4-K cryogenic environment that has a mean time between failures (MTBF) of approximately 2000 hr. Highly skilled technicians are required to maintain the entire package. The total cost of the entire TWM package is variously estimated to be between $400k to $1M each. The combination of high unit cost and high maintenance requirements makes these devices unsuited for a large array of small antennas.

An alternate LNA to the TWM is the new generation of transistor amplifiers, specifically High Electron Mobility Transistors (or HEMTs for short). Figure 2-1 illustrates the state of this technology in 1989. In this figure the effective noise temperature of an X-Band HEMT amplifier is plotted against the physical temperature of the device. It can be seen that the noise temperature of the amplifier varies almost linearly with the physical temperature. The data were fit with a straight line

(shown as the solid line) which indicates that the amplifier noise improves at the rate of 0.4 Kelvin per Kelvin or 0.44 in the region where the physical temperature is > 150K. If it were possible to derive a simple expression for the cost to cool these devices, the array design task would be considerably easier. Unfortunately, refrigerator technology is not that simple.

Figure 2-2 shows HEMT amplifier noise performance versus frequency for 3 common cooling configurations. The first is at room temperature, the second cooled to approximately –50 deg C with a Peltier effect cooler, and the third using a closed-cycle helium refrigerator capable of lowering the device temperature to 15 K. Note that cooling has the most benefit at the higher frequencies. It is also important to remember that this technology has been highly dynamic for the past several years. Like most areas of microelectronics, there have been rapid improvements in performance accompanied by reduced costs.

Table 2-2 lists the various noise contributions to the total system temperature we might expect for a HEMT RF package at both S- and X-bands. The atmospheric contribution comes from thermal noise generated by atmospheric gases and varies as the amount of atmosphere along the line-of-sight, i.e., as the secant of the zenith angle Z. The cosmic blackbody background is a constant 2.7 K. Spillover and scattering will depend on antenna (e.g., prime focus, Cassegrain, or BWG), feed, and support structure design.

Equations (2-2) and (2-3), taken together with the data in Table 2-2, indicate that the X-band requirements drive the size of the array, due to the higher estimated system temperatures. For instance, if we assume D_e = 3m, with an efficiency of 50%, then by using uncooled LNAs, we will need 4121 antennas and LNAs per 70-m aperture that is synthesized. The sensitivities of number to antenna temperature at the two frequencies are

$$\frac{dN_e(S)}{dT_e} = \frac{208 \cdot N_{70}}{\eta_e \cdot D_e^2}$$
$$\frac{dN_e(X)}{dT_e} = \frac{169 \cdot N_{70}}{\eta_e \cdot D_e^2} \qquad (2\text{-}6)$$

TABLE 2-2 Range of Total System Temperature

	2.3 GHz	8.4 GHz
Atmosphere (K)	2.0 sec(Z)	2.8 sec(Z)
Cosmic background	2.7	2.7
Spillover, scattering	4–8	4–8
Microwave Losses	4–12	4–16
subtotal	13–25	14–30
RECEIVER TEMPERATURE:		
Room temperature (290 K)	40	95
Peltier (210K)	33	70
Cryogenic (15K)	3–6	8–10
TOTAL (zenith)		
Room temperature	53–65	109-114
Peltier	46–58	85–98
Cryogenic (15 K)	16–25	22–38

While it may appear that a larger benefit accrues by improving the S-Band system temperature, in reality there is no benefit if the minimum array size is dictated by X-Band requirements. Using the above example of a 3-m antenna to synthesize one 70-m aperture then suggests that reducing the system by just one Kelvin could save 37–38 antennas in the array.

It is clear that the higher expected system temperatures at X-Band will set the number of elements in the array. Figure 2-3 plots N_e as a function of element diameter for the three different zenith system temperatures, assuming an aperture efficiency of 50% for each array element at the X-Band frequency. It is obvious that the number of elements gets very large for a small element diameter.

2.4 RELIABILITY AND AVAILABILITY

In Equations (2-3) and (2-4), we calculated the number of array elements required to synthesize a given G/T. However, the specification of a deep space communications link requires knowledge of the availability of the link components, one of which is the reliability of the ground aperture or array elements. If we were to operate an array whose size was dictated by Eq. (2-3) or (2-4) with no link margin, we would find that increasing the array size beyond some number N_{MAX}, leads to the interesting conclusion that the total data return is decreased!

In order to clarify this assertion, consider the following simplified argument. Define the availability of a system A_T to be the percentage of time that the system is operable for scheduled support. Thus, the downtime required for maintenance is not counted. We should keep in mind that the overall availability is a product of all subsystem availabilities, although for the remainder of this discussion, we will focus on the antenna availability. The total data return D_T, from a deep space mission can be written in terms of the system availability A_T, and the integral of the data rate

$$D_T = A_T \int DR(t) \cdot dt$$

where the integral is taken over the interesting portion of the mission. Suppose that the data rate DR(t), is adjusted to the highest level that can be supported by the total ground aperture used to receive the signal. If we use an array on the ground of N elements, each having availability p, and the total signal from the array is near the detection threshold, then the total data return can be written

$$D_T = N \cdot p^N \cdot f(t)$$

where f(t) is some function of time and includes all of the factors that enter into link performance (e.g., distance, antenna gain, duration of an encounter, etc.), and p^N is the availability of the entire array. Very often the f(t) cannot be increased and the total data return can only be increased by increasing the ground array. For instance, in a planetary encounter f(t) is limited either by the duration of the encounter or by how much data can be stored on-board the spacecraft. Since $p < 1$, we see that D_T has a maximum value at the value of N given by

$$N_{MAX} = \frac{-1}{log(p)}$$

A graph of N_{MAX} as a function of the individual array element availability p is shown in Fig. 2-4 and we see for an array whose size is greater than N_{MAX} that the data return drops precipitously. This result stems directly from our assumption that the data rate would be increased to take advantage of all the ground aperture—that is how it is done with a single antenna. In fact, use of an array requires that we consider antenna availability in a different way than we do for a single antenna. In a link with a single antenna, the antenna is a single point of failure. In an array, the concept of availability must be merged with that of link margin.

Consider an array of n+m elements where n are required for successful operation as discussed by Barlow and Heidtman [1984] and Jamnejad, Cwik, and Resch [1993]. The availability for each element is assumed to be equal to, but independent of the availability of the other elements. No correlation is assumed among the failure rate or timing of different elements. Then the

probability that at least n–m elements are operating successfully at any given time can be calculated as follows: The probability that all the elements are operating successfully, as was given above, is

$$P_0 = p^n$$

and probability that n–1 elements are operating successfully is equal to:

$$P_1 = n\,(1-p)\,p^{n-1}$$

since this is the sum of n conditional probabilities for the case when one element is not functioning but the rest are. The probability that n–2 elements are operating successfully is then given by:

$$P_2 = [n\,(n-1)/2]\,(p-1)^2\,p^{n-2}$$

This can be repeated until the case when only n–m elements are operating, for which case we have

$$P_{n-m} = C(n,m)\,(p-1)^m\,p^{n-m}$$

in which

$$C(n,m) = n!\,/\,[(n-m)!\,m!] \qquad (2\text{-}7)$$

is the number of combinations of m elements taken from a pool of n elements, and the ! sign designates the factorial of a number.

The total probability of success for the array is then the sum of all the above cases

$$P = \sum_{k=0}^{m} C(n+m,k)(1-p)^k p^{n+m-k} \qquad (2\text{-}8)$$

which is also a form of the cumulative Bernoulli or binomial probability distribution function. Note that we are comparing array elements having the same overall G/T, or assuming that T is more or less constant for the array, for the array elements of equal G, or equivalently, equal collecting aperture. Thus, for a total collecting aperture area of A, the individual element aperture of an array of n elements can be written as

$$A_n = A\,/\,n.$$

By adding m marginal elements of aperture A_n, the incremental increase in the collecting aperture is $m A_n$ and the percentage increase in the collecting area is given as

$$m A_n / n A_n = m / n.$$

Therefore, in order to make a comparative assessment of the various arrays' performance, the number of marginal elements are given as a percentage of the minimum required array elements. In Fig. 2-5, the array availability is plotted as a function of the number of extra elements that are devoted to margin. The number of extra elements is expressed as a percentage of the minimum number of array elements, for three array sizes, and for a fixed element availability of $p = 0.9$. From the above considerations, the following interesting observations can be made.

- The availability of the array can be increased by increasing the number of marginal elements.

- The array availability starts with a value much below the element availability, but increases rapidly and surpasses the element availability for a margin of less than about 30 percent or 1 dB.

- The rate of increase is much faster for arrays with a larger number of elements, even though the availability starts with a much smaller value.

- At some point as the margin level increases, all the arrays with a different number of elements reach the same availability level, beyond which a given margin results in higher availability for larger arrays than for smaller arrays.

- For larger arrays the margin can be increased more gradually, since each additional element constitutes a smaller fraction of the total array. For an element availability of 0.9, for example, the minimum availability of a 2-element array is 0.81, which increases to 0.972 by the addition of one element, which is the smallest increment and constitutes a 50% increase in the collecting area or a 1.76-dB margin. In contrast, for a 10-element array with the same element availability, the minimum array availability is 0.349, but by the addition of 3 elements (a 30% increase or a 1.1-dB margin), an array availability of 0.966 is achieved.

- Typically, for a given margin or percentage increase in the collecting aperture, a higher array availability is achieved in arrays with a larger number of elements.

This demonstrates some of the advantages of large array of smaller apertures in comparison with a small (few elements) array, in terms of providing a more graceful way of increasing the

performance margin, and conversely, a more graceful degradation in case of element failure. Furthermore, the fact that for a given margin or percentage increase in the collecting aperture, a higher array availability is achieved in arrays with a larger number of elements, can be used in trading off element reliability in larger arrays for cost, while still maintaining the same overall reliability as that of an array with a smaller number of elements with higher individual reliability. Interestingly enough, the smaller elements used in larger arrays typically have a much larger reliability than their larger counterparts to begin with, since they are less complex and easier to maintain.

3.0 ARRAYING CONCEPTS

Technology provides a variety of solutions to the telemetry arraying problem. We have not attempted to determine the "optimum" solution for the DSN in this regard—that would be the subject of a separate study. In order to simplify the cost and performance modeling, we adopt one technique—termed full-spectrum combining, that is the most general solution for all of the various DSN responsibilities and offers the best performance in the lowest *snr* (signal-to-noise ratio) situations [Mileant and Hinedi, 1990].

The major telemetry-combining techniques are briefly outlined in order to provide context for the choice. Some of the problems involved with full-spectrum combining are discussed, particularly in regard to those involving small antennas. It should be noted that although the DSN does not have experience with this technique, the radio astronomy community does. However, there are three major differences between what drives the DSN and the radio astronomical communities in this area. First, the DSN knows that the spacecraft of interest is a point source and there is no need to resolve it. Second, sensitivity is at a premium and single-bit quantization is not worth the loss in sensitivity it entails. Third, there is a continuing requirement to have the data in near real-time in order to monitor the health and safety of the spacecraft, which implies that tape recording and mailing the data is an unacceptable operations scenario.

3.1 ARRAYING TECHNIQUES

There are four basic signal-processing schemes that can be employed to combine the output of separate antennas that are observing a spacecraft-type signal. These schemes have come to be known as: (1) symbol stream combining (SSC), (2) baseband combining (BC), (3) carrier arraying (CA), and (4) full-spectrum combining (FSC). Mileant and Hinedi [1990] have analyzed the performance of these techniques and have discussed the complexity in regard to the reception of spacecraft signals. Their analysis will merely be summarized here. It should be noted that the first three of these schemes (SSC, BC, and CA) work *only* with a signal that has well-defined modulation characteristics. They utilize the fact that the signal source has a unique spectral characteristic and process accordingly. The fourth scheme (FSC), works equally well with radio sources whose output is noiselike.

All of the arraying techniques fall in the general category of signal processing. The overall *snr* is set by the capture area of the antenna and the thermal noise generated by the first amplifier. In the current DSN signal-flow diagram, the low-noise amplifier is followed by open-loop downconverters (2 stages) that heterodyne the portion of spectrum occupied by the spacecraft signal to a frequency that can be easily digitized. Digital signal-processing techniques are then employed,

and ultimately an estimate is made of the data bits impressed on the carrier at the spacecraft. The data are then delivered to the project that operates the spacecraft. Although the front end of the signal-flow diagram is identical for all of the arraying techniques and the ultimate goal is the same, the details of implementation vary, and this results in very different capital investment and operations costs. These differences make it extremely difficult to unambiguously determine the "best" arraying technique. The general characterization of these techniques is as follows:

Symbol Stream Combining (SSC) - The block diagram is shown in Fig. 3-1. The signal from each antenna is used to track the carrier, subcarrier, and perform symbol synchronization. Once symbol synchronization is achieved, it is a relatively straightforward matter to delay one data stream in order to align the symbols in time. The symbols are then combined with the appropriate weights to form an estimate of a "soft" symbol, i.e., the raw telemetry data, before the decision is made as to whether a given bit is +1 or −1.

The two primary advantages of this technique are that combining loss is negligible and data are transmitted to some central combining site at the symbol rate. The symbol rate is some multiple of the data rate, which for most deep space missions is relatively modest. The rate at which data are communicated to a central site is an important cost consideration since most deep space projects want their data in real time. In addition, there are no stringent requirements on instrumental phase stability.

The disadvantages of SSC stem from the requirement that a carrier, subcarrier, and symbol-tracking device must be provided for each antenna. Given that the cost per unit of complexity for digital electronics is rapidly decreasing with time, it may well be possible to build a "receiver on a chip" for just a few dollars, so the cost impact may be negligible. However, the performance is another matter. The fact that all of the tracking loops must be locked implies that the combination of signal strength and integration time puts you in the strong *snr* regime. For small antennas with inherently low signal strength, the implied integration time (i.e., narrow loop bandwidths) becomes impossibly large and the technique is impractical.

Baseband Combining (BC) - The block diagram is shown in Fig. 3-2. In BC, the signal from each antenna is carrier locked. The output of the carrier loop is at a baseband frequency and consists of the subcarrier harmonics. The baseband signal is digitized, delayed, weighted, and then combined. The combined signal is used to achieve subcarrier lock and symbol demodulation.

In effect, the carrier signal from the spacecraft is used as a phase reference so that locking to the carrier eliminates the radio-frequency phase differences between antennas imposed by the propagation medium. The information bandwidth containing the subcarrier and its harmonics is relatively narrow and can be heterodyned to baseband. The low baseband frequency then imposes

instrumental stability requirements that are relatively easy to compensate for. The baseband data that must be transmitted to a central combining site contain all of the significant subcarrier harmonics and can therefore be more of a cost consideration than SSC.

The disadvantage of this technique is that carrier lock is required on the signal from each individual antenna. As the antenna diameter decreases, the carrier *snr* is reduced and must be compensated for by either longer integration time or having the spacecraft increase the amount of power in the carrier. Halving the carrier *snr* implies four times more integration time (or equivalently a narrower bandwidth in the phase-locked tracking loop), which is sometimes possible but cannot be carried out indefinitely because of lack of signal stability either due to the transmitter, receiver, or propagation medium. If the spacecraft is programmed to increase the carrier power there is less power available for the data, and the data rate must be reduced.

Carrier Arraying (CA) - The block diagram is shown in Fig. 3-3. In carrier arraying, the individual carrier tracking loops on each array element are "coupled" in order to enhance the received carrier *snr* and thereby decrease the "radio" loss due to imperfect carrier lock on a single antenna [Butman, et. al., 1981].

In effect, all of the carrier tracking devices are used to arrive at a "global" estimate of the best carrier synchronization. Alternatively, a single large antenna can provide carrier lock information to a number of smaller antennas. The actual combining can then be done either at an intermediate frequency or at baseband with the attendant advantages and disadvantages of each. However, carrier lock information must be transmitted to a central site and the global solution must be transmitted back to each antenna. For antennas separated by a large distance the carrier lock information must be corrected for different geometries.

Full Spectrum Combining (FSC) - The block diagram is shown in Fig. 3-4 and has been analyzed by Rogstad [1991]. In FSC the signals from each antenna are heterodyned to baseband, sampled, and transmitted to the combining site where they are combined. To ensure coherence, the signals must be delayed and phase adjusted prior to combining. An estimate of the correct delay and phase is normally accomplished by correlating the signal streams.

The primary advantage of FSC is that it can utilize the spectral characteristics of the signal source but does not crucially depend on them, i.e., the received spectrum can be filtered if the spectral characteristics are known, or accepted in total if the spectrum is unknown or noiselike. FSC can be used when the carrier is too weak to track, or is not possible to track with a single antenna. In this case, the gross relative delays and phases between antennas are determined a priori from geometry calculations. Then the residual relative delays and phases are determined by cross-

correlation of the signal arriving at each antenna. These delays and phases are used to correct the signal from each antenna and the signals are then combined.

The main disadvantage with FSC arises when the signal spectrum is unknown or noiselike. The entire signal bandwidth must then be transmitted to the combining site. If the transmission is analog, then the link must have high phase stability and low dispersion set by the requirement to maintain phase coherence at the radio frequency. If the link is digital, it must have relatively large bandwidth (assuming multibit digitization). Depending on the compactness of the array and the cost to install fiber-optic cabling, this may not be a disadvantage.

3.2 COHERENCE

In general, the wave front of an electromagnetic signal from a distant source arrives at each element of an array at a different time. Some fraction of the energy contained in the wave front is captured by the collecting area of each antenna. The captured energy generates a voltage that is amplified and guided to a point where combining takes place. This voltage, as a function of time, is simply a phasor and the process of combining can then be thought of as an exercise in phasor alignment.

Suppose that we use two antennas to track a radio source. If we use $\vec{\mathbf{B}}_\lambda$ to denote the vector baseline between them (measured in wavelengths) and $\hat{\mathbf{s}}$ to denote the unit vector in the direction of the source, then the phase difference between the signals received at these two antennas as a function of time can be written as [Thompson, Moran, and Swenson, 1986]

$$\phi(t) = 2\pi\vec{\mathbf{B}}_\lambda \bullet \hat{\mathbf{s}} + \phi_{inst} + \phi_{prop} \tag{3-1}$$

where the term ϕ_{inst} is the instrumental phase difference between the two signal paths and ϕ_{prop} is the phase difference due to the propagation medium. If we knew $\phi(t)$ exactly, it would be a relatively straightforward matter to apply it to the signal stream so that the combined signal from both antennas would be perfectly coherent.

Unfortunately, it is quite impossible to know $\phi(t)$ exactly. Both the baseline and the source position are measured quantities and have an associated measurement error. If these errors are small, and we can calibrate the instrumental phase, and the propagation-medium phase difference is small, then we can compute $\phi(t)$ and combine. This is called a priori combining. Obviously, if any of these quantities varies without our prior knowledge, then the combining will involve some loss of signal strength, as discussed in the next section. A priori combining places stringent limits on baseline and

source position knowledge as well as instrumental stability. Propagation medium errors are uncontrolled and set a limit on the size and/or operating frequency of the array.

The alternative to a priori combining is to estimate the phase difference between the antennas in real time and use this estimate to correct the phase of one of the antenna signals. This is termed self-coherence, and the phase estimate is derived by computing the complex cross correlation of the signals. Self-coherence reduces the sensitivity to systematic errors in baseline, source position, instrumental phase, and even fluctuations in phase due to the propagation medium. However, the phase estimate is a measurement whose accuracy is subject to the limits set by the snr.

3.3 ARRAYING LOSS

For an array of N_e identical elements, Ulvestad [1988] has shown that the average power from the combiner is

$$\langle P \rangle = N_e(N_e - 1)V^2 \left\langle exp\left(i\Delta\phi_{ij}\right)\right\rangle + N_e V^2$$

where the bracketed term is the expected phase between the ith and jth elements, and V is the voltage amplitude from a single element. Dewey [1992] derives a similar expression for a non-homogeneous array, but with weighting factors in the summation that are appropriate for array elements having various values of G/T. In order to simplify the discussion, we will consider only the case of array elements with identical G/T. For perfectly coherent combining $\Delta\phi_{ij} = 0$, the exponential term in the above equation is unity and the average power becomes

$$\langle P \rangle_{coh} = N_e^2 V^2 = P_{max}$$

The ratio of summed power from the combiner to the maximum possible power is simply

$$\frac{\langle P \rangle}{P_{max}} = \frac{N_e - 1}{N_e} exp\left[\frac{-\bar{\sigma}_{ik}^2}{2}\right] + \frac{1}{N_e} \qquad (3\text{-}2)$$

where it is assumed that the phase difference between the i and k elements is a Gaussian distributed random variable with variance $\bar{\sigma}_{ik}^2$. The effective combining loss between two identical array elements for various values of the phase difference $\Delta\phi$ is shown in Fig. 3-5.

The combining loss L_C, can then be defined as

$$L_C = 1 - \frac{\langle P \rangle}{P_{max}} \tag{3-3}$$

For large N, the loss rapidly approaches

$$L_C \approx exp\left[-\sigma_\phi^2/2\right] \quad \text{for } N >> 1$$

where σ_ϕ is the average phase difference between elements. Of course, the similarity of this expression with Ruze's formula in Eq. (2-5) is no accident. Both are derived from a model of combined phasors that suffer random Gaussian phase shifts. If the phase shifts are due to irregularities of a parabolic surface, then the phase shift is doubled due to reflection. Figure 3-6 shows the combining loss for the array for N_e from 2 to 1000 and three different values of σ_ϕ.

The implication of these calculations is that we should seek to keep the phase difference between array elements to less than 12° if we require combining loss to be less than 0.1 dB. This amount of phase error is equivalent to 0.047λ, or a physical distance of 0.6 cm at S-band and 0.17 cm at X-band. Typically, instrumentally induced phase errors are related to the temperature stability of various electronic components and cabling, while propagation effects occur randomly. Very often, instrumental stability problems are characterized by a diurnal phase variation. For a priori combining this means that (a) the instrumental phase shift should be determined at the start of an observation with precision better than 12° and (b) we cannot accumulate more than 12° of differential phase between elements in a worst-case (i.e., a priori combining) observation time of 12 hr. (42300 sec.). This sets a differential stability requirement on the instrumentation of

$$\frac{\Delta\phi}{\phi} \approx \frac{12}{360 \cdot 8.4 \cdot 10^9 \cdot 43200} \approx 10^{-16}$$

which is stringent but nevertheless achievable. It must be emphasized that this requirement is for **differential** stability, not absolute. For an array of identical elements, many components of the instrumental error budget will cancel because they are common among elements. The DSN regularly achieves a stability in its receive electronics on the order of a few parts in 10^{-15} and there is evidence [Armstrong and Scramek, 1982] that the Very Large Array (VLA) has instrumental differential stability on the order of a few parts in 10^{-17}. For most of the combining schemes that we will discuss, the differential phase between array elements is estimated in real time and used to correct and combine antenna outputs. In these schemes, the time scale over which phase stability is required is set by the integration time necessary to obtain adequate *snr* for phase estimation. This integration time is typically 1 to 100 sec, and the resulting differential phase-stability requirement stated above is reduced by two to four orders of magnitude.

However, as shown in Eq. (3-1), instrumental effects are not the only cause of differential phase errors between elements of an array. As the wavefront travels through different portions of the Earth's atmosphere before reception at the various array elements, it experiences differing degrees of phase retardation due to refractivity fluctuations in the atmosphere. The static portion of the atmosphere can be well-modeled so that the average phase ϕ_{prop} = constant, but the fluctuation along the different ray paths leads to a dispersion σ_ϕ. These fluctuations are dominated by water vapor in the troposphere (i.e., the lower ~ 2 km of the atmosphere).

The calculation of σ_{ik} due to atmospheric effects is given by Treuhaft and Lanyi [1987] who derived the structure function of delay fluctuations for two ray paths through the atmosphere when the ray paths are separated by a distance ρ (i.e., the baseline length). Figure 3-7 shows the standard deviation of the phase difference between array elements versus their separation due to atmospheric fluctuations for zenith ray paths. It was assumed that these fluctuations are described by Kolmagorov turbulence, whose strength is characterized by the parameter C_n, a scale height h, and the turbulence pattern that is transported by the wind while retaining its spatial distribution (i.e., the "frozen-flow" model).

One interpretation of Fig. 3-7 is that it represents an ensemble average. If there were an ensemble of antenna pairs, each with identical separations, observing a source at the zenith, and if we measured the instantaneous phase difference between them, then the scatter in this set of phases would be σ_{ik}. Alternatively, if we had just one antenna and measured the phase as a function of time, then the resulting time series would be characterized by σ_{ik}. The top axis in Fig. 3-7 illustrates the time axis assuming a wind speed of 10 m/s. In effect, it indicates that the phase of the signal as received at a single station, integrated for the period along the x-axis, would have a standard deviation as given along the y-axis.

The dashed line in Figure 3-7 is drawn at 12° of phase difference corresponding to approximately 0.1 dB of gain loss. For X-band zenith observations, this suggests a distance scale of 350 m and a time scale of 35 sec. The structure function is a function of both elevation and azimuth, and in the worst case the phase variance will increase approximately as the secant of the elevation angle. For a minimum elevation angle of 10°, the secant represents a factor of approximately 6, the critical linear scale becomes 145 m, and the integration scale is reduced to 15 sec. An array of fully steerable antennas is necessarily larger than the single aperture it synthesizes. Further, the smaller the array element is, the longer the required integration time is for a given target. Therefore, an array will suffer more gain degradation as a function of elevation angle than the corresponding single aperture.

In order to quantify further the atmospheric effects on an array, additional information must be specified. We need to know the cumulative probability distribution of the turbulence parameter

C_n and the spatial distribution of array elements. The quantity C_n can vary from day to night, season to season, and is site-dependent. Knowledge of the probability of these variations would allow us to calculate the average gain loss or gain-versus-elevation angle profile. The spatial distribution of array elements is important because the quantity required in Eq. (3-2) is the average phase error, $\overline{\sigma}_{ik}$. An array of N_e elements contains $N_e(N_e-1)/2$ independent baselines so that the computation of the average phase error depends on the array geometry, i.e., $\overline{\sigma}_{ik}$ is a weighted average. The weighting factors for the σ_{ik} are obtained from the transfer function of the array [Christiansen and Hogbom, 1985], which represents a map of all spacings contained in the array and their relative weights. Thus, the inner spacings of a compact array are weighted more heavily that the fewer large spacings.

It should be noted that Edwards [1990] has demonstrated that this level of residual error can be obtained on baselines as long as 20 km at X-band using a 26-m and a 34-m antenna. This suggests that phase errors due to both instrumental and propagation effects are tolerable for telemetry-arraying purposes.

3.4 ARRAY CALIBRATION

Whether the array is combined solely on the basis of a priori information or the elements are self-cohering, there is a need for accurate baseline calibration. Typically, baseline calibration is done after initial installation and repeated whenever a major component in the signal path is moved or replaced. In the case of a priori combining there is the additional need for instrumental phase calibration, i.e., generally it must be repeated on a time scale that is short compared to the time rate of change of ϕ_{inst}.

Phase Calibration:

The precision of a phase measurement is given by

$$\sigma_\phi = 1/snr \quad \text{(radians)}$$

where *snr* is the signal to noise ratio. Thompson et. al. [1986] derives the $snr = \mathcal{R}$ for an unpolarized source as

$$\mathcal{R} = \frac{S}{k}\left[\frac{A_{ei}A_{ej}}{T_{Si}T_{Sj}} \cdot \frac{\Delta f \tau}{2}\right]^{1/2}$$

where A_{ei} is the effective collecting area of the ith antenna, T_{si} is the total system temperature of the ith antenna; τ is the integration time (= $1/\Delta f_{LF}$) of the lowpass filter; Δf is the intermediate frequency bandwidth, k is Boltzmann's constant; and S is the flux density of the radio source.

An *snr* of 5 ensures reliable signal detection and provides a phase measurement precision of $\Delta\phi \sim 11°$, i.e., below the 0.1-dB loss criterion. Figure 3-8 illustrates a calculation of the minimum integration time needed to achieve this *snr*-versus-antenna diameter for 2 cases. The interferometer in both cases consists of two elements, each having T_S = 85K (e.g., Peltier cooled X-band LNA), an IF bandwidth of 16 MHz, and a source strength of 1 Jy. In the first case, the two elements are assumed to be equal in diameter, and in the second case, an element of diameter d is paired with an aperture having an effective diameter of 70 m. Since the antenna diameter, system temperature, and bandwidth are set by design specifications, the only way to increase the *snr* is to lengthen the integration time, or use stronger sources.

Patniak et al. [1992] lists 800 compact sources whose positions have been measured with an *rms* accuracy of 12 milliarc seconds (mas) at X-band for the declination range $75° < \delta < 35°$. Figure 3-9 shows this data extrapolated to the solid angle of the celestial sphere observable from Goldstone (e.g., within a 24-hr period). It also shows the number of sources one can expect to find that have a strength greater than the value listed along the x-axis of the graph. Thus, we would expect to find approximately 167 radio sources having S > 1 Jy, 49 with S > 2 Jy, etc. A similar catalog is not readily available for S-band, however it should be noted that most of the sources in the X-band list are likely to be stronger at S-band.

The positional accuracy of these sources is more than sufficient for phase calibration. For a square array the largest baseline components are approximately 2 km or 6 x 10^6 wavelengths at X-band. The maximum systematic error in phase due to a 12-mas error in source position is less than 1.2° at X-band and less than 0.3° at S-band. We conclude that positional accuracy of the calibration sources is not a major factor in calibrating the instrumental phase.

However, the observation must be made with enough *snr* to provide a phase error < 10° and it would be preferable for the radio source used for calibration to be close to the source of interest to minimize array motion.

Baseline Calibration:

In practice, conventional surveying measurements cannot measure the vector baseline $\vec{\mathbf{B}}_\lambda$ with the accuracy required for a priori tracking of delay and phase. Instead, interferometric observations are used to derive a self-consistent set of baseline estimates. If we were to observe 4 sources having known positions, then in principle we could solve the resulting 4 simultaneous equations resulting from Eq. (3-1) for the baseline components X, Y, Z, and the instrumental phase

offset ϕ_{inst}, assuming that ϕ_{inst} is constant for the time it takes to make the 4 measurements. The error in the phase measurement is typically used to weight the data in a least-squares fitting procedure.

A high-quality baseline determination has two requirements: (1) observations along each baseline component, as much as possible, in order to minimize the geometric dilution of precision and (2) high-precision (i.e., large *snr*) phase data. In order to achieve the first goal, we can adopt a strategy of observing multiple sources at very different positions in the sky. Achievement of the second goal is limited by the *snr* considerations discussed previously. The initial calibration of the array might take many days of observing spaced over weeks in order to get good source geometry and to understand the instrumental phase stability.

Conclusions:

Summarizing the above considerations leads to the conclusion that an array of small antennas (i.e., $D_e < 10$ m), in which the elements are **individually correlated**, is impractical. The lack of strong radio sources implies impossibly long integration times to obtain sufficient *snr* for either instrumental phase calibration or baseline calibration. However, an array in which each element is correlated against the sum of all other elements appears to be quite feasible. A somewhat similar scheme was demonstrated in software at the VLA with telemetry signals during the Voyager encounter with Neptune, where the phases on all 351 baselines were used to solve for the 26 phase offsets between a reference antenna and the remaining elements of the array. Total power arraying is often done in radio astronomy experiments (e.g., using the summed VLA as one element in a VLBI experiment).

A scheme illustrating how the feedback could be implemented in hardware will be discussed in Section 4.5. The combined signal is fed back to be correlated against each individual element and the autocorrelation function of the signal from that element is subtracted. An interesting but unsolved problem is whether the process then converges to a fully coherent array and if so, how rapidly it would converge.

4.0 SUBSYSTEM COST MODELS

Several variations in the design were discussed during the study. Only the final version is presented here. The high-level block diagrams are shown to illustrate the functional partitioning of the system, the data flow, and the interfaces between subsystems. The detailed cost model for each subsystem is then discussed.

4.1 SYSTEM BLOCK DIAGRAMS

Figure 4.1-1 shows the overall block diagram of the array. Each antenna is equipped with a low-noise amplifier (LNA) that amplifies the radio frequency (RF) signal collected by the aperture. The system temperature is usually determined by the noise contribution of this LNA, with smaller contributions from the remaining elements of the electronics chain. There is at least one output, possibly several (depending on number of subarrays selected), that represent the coherently combined sum of all or some subset of array elements. This output consists of a digital data stream that would be routed to a DSN telemetry receiver for demodulation.

The block diagram of Fig. 4.1-1 also indicates that the RF signal from the LNA directly modulates a fiber-optic link which routes the signal to a central location. A more conventional design would include a downconverter on each antenna containing a local oscillator (LO), intermediate frequency (IF) amplifiers, and possibly bandpass filters. However, the diagram of Fig. 4.1-1 represents a considerable cost-and-complexity advantage. First, there is less equipment on the antenna, a particular advantage for very small antennas. Less equipment on the antenna also means there is less likelihood of equipment failures in the field, where repairs are more difficult and time-consuming.

Another advantage is that only one cable is required to return the signal, whereas a conventional approach requires a cable for the IF signal and a separate cable for a reference to phase-lock the local oscillator. Very often, the reference signal cable must be separately stabilized with the attendant penalty in cost and complexity. In the scheme shown here, we rely on the inherent stability of the buried fiber-optic cable to minimize unwanted instrumental phase drifts. One of the design aspects associated with the scheme shown in Fig. 4-1 is that 70 to 80 dB of RF gain is required to drive the modulator of the fiber-optic link, as compared to 30 to 40 dB of gain required for a more conventional scheme that would have a downconverter at each antenna.

Once the analog fiber-optic signals are brought to a central location, they are demodulated, and the resulting RF signal must be heterodyned with a coherent LO to some intermediate frequency. Design of the fixed LO distribution subsystem is simplified because of the proximity of all the signals. Also, thermal control, the main culprit of unwanted phase drifts, is less of a problem than

with the conventional design. If all mixers and IF amplifiers share the same environment and have similar phase-versus-temperature characteristics, then temperature effects tend to cancel in the common mode.

The heterodyne operation translates the RF bands 2.0 – 2.3 GHz and 8.1 – 8.5 GHz to an IF center frequency of 300 MHz. The signal is amplified again at IF and passed to the Correlator subsystem where it is downconverted to baseband using a tunable LO and filtered to limit the bandwidth to approximately 16 MHz. The correlator adjusts the delay using an a priori model of the geometry and then performs a complex cross-correlation to find the phase shift between the ith element and the rest of the array. This phase is then used to counter-rotate the phase of the signal from the ith element so that all elements are in-phase. Each signal is then passed to the combiner, which adds them with the appropriate weighting factor in groups corresponding to the subarray specification.

Each antenna is assumed to have its own pointing computer that understands the directives to TRACK, SLEW, etc. Operation of the array is coordinated by the Monitor and Control subsystem, which presents a "familiar" interface to the Signal Processing Center. In effect, the array would appear as one or more antennas in a link, or the subarrays could be present in different links, and accept the same set of commands and scheduling information that is currently used in the station Monitor and Control.

The output of the array consists of one or more (depending on the specified number of subarrays) data lines that are digital but could be converted to analog. As digital signals, a new interface to the Block V receiver would be required, but the cost has not been estimated in this study.

4.2 ANTENNA COST MODEL

The antenna system is an obvious and major component in the overall array cost model. As will be detailed, the antenna system will be divided into subsystems that include all mechanical and structural components, the foundation, and microwave optics (including the feed system), but does not include any electronic packages. To simplify the cost-estimation process within a limited time and budget, off-the-shelf technology was used for each subsystem. It was decided to contract to two companies specializing in antenna–ground station design and fabrication so that detailed antenna subsystem costs could be supplied and the estimated costs would not be speculative. These two companies are TIW Systems, Inc., Sunnyvale, CA (TIW), and Scientific Atlanta, Inc., Atlanta, GA (SA). The two companies have previously supplied JPL with antenna systems, and therefore they are familiar with the specific requirements and procedures of the DSN. The specific tasks that the contractors were to complete are as follows:

- For eight diameters ranging from 3 to 35 meters, production techniques will be investigated and a preferred design for each antenna subsystem will be specified.

- The design will include specifying antenna optics for each antenna size based on cost, manufacturability, and performance.

- Each subsystem will be further divided into nonrecurring and recurring costs.

- Because of the large number of antennas that could be fabricated (especially at the smaller diameters), it is expected that an economy of scale will be encountered. This cost study should outline breakpoints in production where costs drop for a given diameter as more antennas are fabricated.

- To assist in the probabilistic determination of the number of antennas needed to maintain a prescribed G/T margin, the cost estimates should outline antenna components which critically affect reliability, and detail the costs of critical components as a function of reliability.

Due to the limited time and budget of the contracts, the last three items were not examined in great detail. The costs in this section therefore do not reflect any reductions that may be gained by mass production of antenna systems specifically designed for this DSN array application. It is also noted that Scientific Atlanta has supplied antennas ranging from 2–21 m and presently manufactures antennas ranging in size from 3–18 m. TIW has supplied antennas ranging from 9–34 m.

4.2.1 ANTENNA SPECIFICATIONS

As outlined in Section 2.1, the number of antennas needed to synthesize the G/T of a 70-m aperture with an array is a function of the array element diameter and the system noise temperature. Since three LNA configurations were modeled, each having a different system noise temperature, there is a large spread in the number of antennas required. Shown in Table 4.2-1 is the range of the number of antennas needed for each of the eight diameters specified to the contractors. The column of minimum units corresponds to cooled amplifiers and enough antenna elements to comprise one station, while the maximum number of units corresponds to uncooled amplifiers and enough elements to comprise three stations. This range was specified to allow for economies of scale in production methods to surface, and for a complete parameterization of the antenna-amplifier system, based on system noise temperature and antenna diameter.

Common sense dictates that an array of inexpensive 3-m antennas using expensive cooled amplifiers, as well as expensive 35-m antennas using inexpensive uncooled amplifiers, should produce extremes in the cost model. These extremes would be expected to bound the cost model.

Note that the numbers in Table 4.2-1 were calculated on the assumption of perfect efficiency and are therefore slightly smaller than what would be calculated by using the equations in Section 2. However, they are sufficient to set the manufacturing scale for the contractors who supplied the detailed cost estimates.

Table 4.2-1. Minimum and Maximum Antenna Elements.

Diameter (m)	Units	
	Minimum	Maximum
3	545	27,000
5	196	10,000
10	49	2,500
15	22	1,100
20	12	615
25	8	394
30	5	274
35	4	201

The antenna optics are broken into two regimes. For small-diameter antennas, a frequency-selective subreflector is used to separate S-band—arranged as a prime focus system—from X-band, which is arranged in a Cassegrain system. For larger diameter antennas, both bands operate in a Cassegrain system, with the bands separated by either a dual-frequency (concentric) feed or a frequency-selective surface (FSS) diplexor. It was expected that the break would occur in the range of 10 – 20-m antenna diameters. This breakpoint option and frequency-combining method were left to the contractor. TIW arrived at designs which used prime-focus S-band designs, including an FSS subreflector for diameters up to and including 10 m and Cassegrain configurations with a dual-frequency feed for diameters of 15 m and larger. SA arrived at similar designs but with a breakpoint where the dual-frequency feed is used for diameters greater than 21 m.

To gain a better understanding of the antenna-system cost model, the antenna was broken into eight subsystems described as follows:

- Antenna Support Structure: The designs for all antenna sizes were conventional elevation-over-azimuth configurations. Due to the range of antenna sizes considered, modifications based on production, shipping, and assembly were made to arrive at a final design.
- Main Reflector Surface: Again, based on antenna diameter, different panel-production methods were used in the final design.
- Axis Drive: Includes actuators, drive gearboxes, and bearings.
- Position Control: Includes encoders, motors, cabling and controls.

- Feed System, including FSS: As noted above, different feed systems were used at the diameter breakpoints specified by the contractor.
- Foundation: No below-ground enclosure was supplied.
- Power Supply: Includes distribution on site.
- Shipping, Installation and Testing: Different strategies for installation and testing were used, based on antenna diameter.

Summaries of the designs, as well as the cost information, are contained in final reports supplied by the contractors.

4.2.2 PERFORMANCE REQUIREMENTS

The performance requirements specified to the contractors are those contained in DSN Document 810-5, Volume 1: Existing DSN Capabilities [1991]. The necessary specifications for this study are listed in Table 4.2-2.

4.2.3 THE ANTENNA COST MODEL

Traditionally, antenna cost models have followed a power law

$$C = \alpha + \beta \cdot D_e^{\gamma} \qquad (4.3\text{-}1)$$

where α represents a constant fixed cost, β is a constant, and D_e is the dish diameter. The exponent γ is the critical parameter in the cost model, which drives costs as the antenna size increases. This parameter has been previously estimated by examining costs of existing antennas and fitting the above power law to the data. One early estimate [Potter, Merrick and Ludwig, 1965] gave γ as 2.78, and this number has been widely quoted.

TABLE 4.2-2. Antenna Element Specifications.

Parameter	Specification
Operating Frequency	From S-Band to X-Band
Axis Coverage: Elevation Azimuth	 0° to 90° ±200°
Reflector Surface	Solid aluminum
Environments: Precision Operation: Wind Rain Temperature Normal Operation: Wind Rain Temperature Survival: Wind Seismic Hail Temperature Drive-to-Stow	 10 mph gusting to 12 mph 2 inches per hour 0°F to 115°F 30 mph gusting to 36 mph 2 inches per hour 0°F to 115°F 100 mph (stowed) 0.3 G horizontal and 0.15 G vertical Up to 1 inch diameter stones –20°F to 180°F 60 mph
Maximum Tracking Rates: Velocity Acceleration	 0.4°/sec 0.4°/sec^2
Maximum Slew Rates: Velocity Acceleration	 0.4°/sec 0.2°/sec^2
Site Location	Australia
Soil Conditions	3,000 psf bearing capacity at 3 feet below grade (no piles required)
Axis Configuration	Elevation over Azimuth
Pointing Accuracy: Precision Operation Normal Operation	 0.1 beamwidth 0.2 beamwidth
Surface Accuracy: Precision Operation Normal Operation	 0.030 inch RMS 0.035 inch RMS
Concrete Foundation	Minimum height (no building room required)

The constant fixed cost α, is taken to be the nonrecurring costs associated with engineering design, tooling, etc., for each antenna element. As noted earlier, limitations of this study did not allow an in-depth examination of nonrecurring costs, as well as economies of scale, which may lower incremental costs of the antennas—especially for the smaller diameters. Shown in Table 4.2-3 are estimates of nonrecurring costs supplied by the contractors. These numbers reflect nonrecurring costs for the total array of elements based on the minimum number of units in Table 4.2-1. The constant α in Eq. (4.3-1) would be the costs listed in the table prorated per element.

Table 4.2-3. Nonrecurring costs for antenna elements.

TIW		SA	
DIAMETER (m)	NONRECURRING $	DIAMETER (m)	NONRECURRING $
3	1,348,838	3	380,000
5	1,533,821	5	380,000
10	1,768,737	10	542,500
15	1,533,959	13.1	250,000
20	1,644,085	15.3	250,000
25	1,613,000	16.1	400,000
30	1,923,300	18.3	400,000
35	2,001,500	20.0	500,000
		21.0	550,000
		25.0	750,000
		30.0	350,000
		32.0	350,000
		35.0	1,000,000

Figure 4.2-1 shows the recurring cost estimates from the two contractors for the antenna elements as a function of diameter. SA supplied data for more diameters than specified because they have existing systems or cost data at 13, 16, 18, 21 and 32 meters. The SA data are not as smooth as the TIW–supplied cost data because of design variations at some diameters. Specifically, SA supplies an 18-m system where the structure, foundation, and shipping, installation, and test subsystems are optimized for cost.

Power law fits to the data are also shown on the plot. For both data sets, it is seen that the cost increases nearly as the diameter *squared*, counter to higher powers previously published. It is interesting to note that the Project Cyclops study [1971] came to the same conclusion for 25- –150-m antennas. The fact that antenna costs scale approximately as diameter squared profoundly affects the overall conclusions of this study.

4.2.3.1 ANTENNA SUBSYSTEM COSTS

Cost data for the eight antenna subsystems are presented in Figs. 4.2-2 to 4.2-9. Costs for specific subsystems at specific antenna diameters are plotted on the charts for both contractors. The cross and square symbols denote the points where data were supplied, and the solid and dashed lines are fits to the data. For some components, it is clear that the SA data do not fit the power law model well. As mentioned in the previous section, this is due to optimizations of certain diameters for cost reduction. Table 4-2.4 summarizes the constants β and γ for the subsystems. The line labeled "total" refers to the best-fit for the total antenna cost of Fig. 4-2.1.

Table 4.2-4. Summary of power law coefficients for the subsystems.

	TIW		SA	
SUBSYSTEM	β	γ	β	γ
SUPPORT	0.10	2.71	1.62	1.88
REFLECTOR	0.26	2.39	0.77	2.08
DRIVE	3.14	1.43	8.82	0.99
POSITIONER	12.94	0.73	12.22	0.44
FEED	10.75	1.06	0.43	1.65
FOUNDATION	0.20	2.13	0.31	1.89
POWER	2.68	0.72	0.95	0.65
SHP/INS/TST[a]	0.25	2.42	1.17	2.02
TOTAL	4.21	2.02	6.96	1.84

[a] Shipping/Installation/Testing

4.2.4 SUMMARY

For the purposes of the overall array cost model, the best-fit power law shown in Fig. 4.2-1 are sufficient to model the antenna system. The cost data (in K$) from the two contractors are remarkably similar over the range 3–35 m, even though there are marked differences in the estimated costs of components and the best-fitting power functions are different.

$$C_{TIW} = 4.21D^{2.02}, \qquad C_{SA} = 6.96D^{1.84}$$

For better local fits to the data, or for individual subsystem cost data, the individual models shown in Figs. 4.2-2 to 4.2-9 can be used. An antenna system cost model made up of the individual subsystems is then

$$C = C_{SUP} + C_{REF} + C_{AX} + C_{POS} + C_{FEED} + C_{FOUN} + C_{POW} + C_{SIT} \quad (K\$)$$

where the individual subsystem costs are given in the figures.

Figure 4.2-10 shows the percent of total cost for each of the eight subsystems for the TIW and SA data: Structure; reflector; and shipping, installation, and test subsystem costs increase with diameter size. Feed, position control, and power subsystem costs decrease, while foundation and axis drive costs are relatively constant. For 3-m antennas, the feed and position control subsystems contribute 57% of total cost in the TIW data and a similar percentage for nonshipping, installation, and test costs in the SA data. These are obvious areas for cost reductions for high-quantity production.

To extrapolate cost scaling for larger systems, the individual cost models were calculated for diameters up to 100 m. The costs were calculated based on the individual cost models for TIW data in Figs. 4.2-2 to 4.2-9, with power law fits made to the resulting extrapolated data. It was seen that when a power law was fit to data up to 50 m, the cost scaled as $D^{2.27}$; for fits to 70 m, the costs scaled as $D^{2.40}$; and for fits to 100 m, the costs scaled as $D^{2.50}$. As the diameter becomes large, the total antenna cost is dominated by the component having the largest exponent. For the TIW data, this is the support structure component and the exponent is 2.71. These costs are, of course, extrapolations to the small antenna diameter data and are speculative. However, this is the likely explanation why prior studies suggested exponents in the range 2.5–2.7.

4.3 RF, IF, AND LO COST MODEL

The radio frequency (RF), intermediate frequency (IF) and local oscillator (LO) subsystems all comprise analog devices. As indicated in Fig. 4-1, each antenna is equipped with a low-noise amplifier (LNA) that amplifies the RF signal collected by the aperture. The noise contribution of this LNA is usually the major component of the system temperature performance. Section 2 discussed three different LNA performance models. In this section we discuss their cost.

The block diagram of Fig. 4-1 also indicates that the RF signal from the LNA directly modulates a fiber-optic link that routes the signal to a central location. The advantages of this configuration were discussed in Section 4.1, and the cost will be calculated as part of the signal distribution subsystem. One of the design aspects associated with this scheme is that 70 to 80 dB of

RF gain is needed to drive the modulator of the fiber-optic link, as compared to 30 to 40 dB of gain needed for a more conventional scheme that would have a downconverter at each antenna. Once the RF signals are brought to central location they must be heterodyned with a coherent local oscillator to some intermediate frequency, amplified, and routed to the Correlator subsystem.

4.3.1 RF COST MODEL

From the discussion of performance in Section 2, we see that the number of required antennas in the array is directly proportional to the system noise temperature and the major component of the system noise is contributed by the noise temperature of the first RF amplifier, except in the cryogenic package. Three configurations were discussed: one in which the RF amplifier operated at ambient temperature, and two configurations in which the RF amplifier was cooled to a physical temperature well below ambient.

There are several different approaches that can be used to cool electronic components and assemblies to temperatures below the ambient environment. The discussion here will be limited to those techniques viewed as being commercially available for cooling microwave transistor amplifiers (FETs and HEMTs). Typically, the transistor is one of the least-expensive components of the subsystem. The cost is dominated by the packaging, which includes assembly and testing.

Stored cryogens (or coolants), such as liquid helium and liquid nitrogen, have been used for many decades. Use of liquid nitrogen usually offers the lowest cost method of cooling equipment to 78 K. Dewars suitable for cooling transistor amplifiers can be purchased for as little as $1,000 and have refill time intervals ranging from 1 day to 1 month. Liquid nitrogen is cheap (less than $1 per liter), available almost anywhere, and relatively easy to handle. While the capital investment for stored cryogenic cooling systems may be low, the life-cycle cost is high due to the need for proper servicing by appropriately trained and dedicated personnel. The Dewars also present mounting problems when located on the moving portion of an antenna (note that these problems can be avoided in a BWG antenna design). For these reasons, a Dewar-based cooling scheme was not considered in the cost model.

Peltier coolers offer a simple way to cool equipment to temperatures as low as 200 K. The cost of a Peltier cooling unit is expected to be less than $1000. It is important to note that cooled equipment must be packaged in a manner that excludes moisture and other condensibles. Vacuum insulation or other forms of insulation and a container with vacuum-tight microwave windows and power connectors are needed to thermally isolate and protect the cooled electronics from warm surfaces and contaminants. The low cost of the Peltier cooler may be offset by packaging costs that can easily range from $5k to $20k per package.

Gifford–McMahon cycle cryo-coolers are used extensively for many applications in industry and the scientific community. These are the most attractive commercially available coolers for HEMTs and FETs, with operating temperatures as low as 10 K. Complete closed-cycle cryogenic refrigerator (CCR) systems of this type are available at costs between $10k and $20k, depending on the model selected.

Again, as in the case of the Peltier cooler, the cost of the CCR is a small fraction of the cost of the cryo-cooled LNA package. The electronic equipment cost, the packaging cost, gas lines, and cables needed for antenna-mounted operation, monitor and control equipment, spare parts, documentation and testing costs can total $150k per package. The procurement of 30 to 50 HEMT/CCR systems might result in a lower price (perhaps somewhere between $75k to $100k per system).

For the three configurations used in our cost model, we assume a total RF gain of 75 dB at both S- and X-band. The unit cost for an uncooled configuration is taken as $15k, for a Peltier cooled configuration as $30k, and for the CCR configuration as $150k. It was assumed that the nonrecurring investment needed to develop and test these designs from a commercial source would be $200k, $400k, and $600k for the uncooled, Peltier cooled, and CCR packages, respectively.

4.3.2 LO AND IF COSTS

After the RF signal is routed to some central location and is demodulated from the fiber optics, it must be heterodyned to an IF frequency of approximately 300 MHz. The bandwidth could range from a few MHz to several hundred MHz, depending on the final requirements on the array. Even if the array were to be used only for telemetry, the bandwidths of the IF amplifiers might be larger than the frequency allocations for Deep Space Communications in order to reduce the instrumental calibration problems (e.g., see Section 3.4).

In the current architecture of the DSN, the RF signal is heterodyned on each antenna using a device called the "VLBI Downconverter." This device heterodynes four channels, two at S-band and two at X-band, to a 300-MHz IF center frequency with 100- to 500-MHz bandwidth. Thus, each device contains two local oscillators whose phase is locked to a 100-MHz reference signal and four IF amplifier chains. All these electronics are enclosed in an oven that is kept at a physical temperature higher than the ambient temperature is ever expected to reach. The box enclosing the downconverter is approximately 0.5 m^3 in volume, weighs almost 100 kg, and costs over $150k (i.e., $40k per channel) in single units. A large portion of the cost for this unit is due to the packaging and stems from the requirement that the unit be located on the antenna.

When the RF signals are all collocated, it would be more cost-effective to generate a single high-power LO signal and split it multiple times to power the mixers in individual channels. The mixer and IF amplifier could be greatly reduced in size, power consumption, and unit cost by using monolithic microwave integrated circuit (MMIC) technology, however the initial design cost would be high. A detailed cost estimate of this technology was not made during the study, we simply "guess-timated" a nonrecurring cost to be $1.5M and a recurring cost of $12.5k for the downconverter channel, the local oscillator, and the IF amplifier, plus any additional calibration equipment that might be needed.

4.4 SIGNAL DISTRIBUTION COST MODEL

The signal distribution and layout considerations pertaining to a telemetry receiving array differ from those of large antenna arrays used primarily for radio astronomy, since angular resolution of target position is not a primary design consideration. For the telemetry receiving array, the design goal is to maximize the gain of the array, which increases with the number and size of the elements in the array but does not depend critically on the physical dimensions of the array. The signal distribution scheme for a telemetry receiving array must therefore be a balance of several considerations: distribution system stability, optimal packing of elements, shadowing of adjacent elements, cable lengths and installation costs, land area required, and division of the array into subarrays. This section summarizes the findings of a study undertaken to determine the optimum design of the distribution system and layout. The results of this study are more fully documented in Logan [1993].

4.4.1 DESIGN CONSTRAINTS

For the array under consideration in this study, the following design constraints are assumed:

- The signal distribution links from the individual antenna elements to the correlator/combiner must have adequate phase stability over the integration times needed to support suppressed-carrier tracking of deep-space missions.

- No shadowing of adjacent antenna elements is permitted over the entire tracking range of 360° in azimuth, to 10° above horizontal.

- Minimum-length cable runs to the central correlator/combiner are desired.

• The whole array should be divisible into independent, identically shaped subarrays, so that the correlator/combiner hardware and software are not subarray-dependent.

• The least-costly cable installation method which preserves the stability of the signal should be employed.

4.4.2 SIGNAL DISTRIBUTION SYSTEM

All of the signals received by the individual antennas must be combined to yield a single output of the array or subarray. Since the G/T of the individual antennas prevents them from independently acquiring and locking to the weak spacecraft carrier signal, the correlator must integrate the combined output of all the antennas to achieve lock. Therefore, the primary performance requirement placed on the signal-distribution system links is to provide adequate phase stability for the transmitted signals throughout the integration time needed by the combiner/correlator to acquire and lock to the spacecraft carrier. The most stringent phase stability requirement is for carrier-suppressed signals, where the necessity of Costas-loop tracking increases the required integration time well beyond a symbol length.

For example, with the expected power levels from Galileo, calculations indicate that the tracking-loop integration time could be as long as hundreds of seconds. During this time, the phase of any signal input to the correlator should not drift by more than 1/10 of a cycle to avoid loss of coherence. These two requirements of the combiner/correlator therefore determine the stability requirements for the transmission links from the individual antennas to the combiner/correlator. In this study, we adopt the conventional design rule of requiring the differential (input-to-output) phase stability of each transmission link to be 10 times more stable than the transmitted signal phase-stability requirement. Therefore, the worst-case differential phase-stability requirement for each link is: no more than 1/100 of a cycle of phase drift (at X-band) during an integration interval. This corresponds to a differential phase-stability requirement for each link of approximately $\Delta\phi/\phi = 10^{-14}$ for a 100-second averaging time, and $\Delta\phi/\phi = 10^{-15}$ for a 1000-second averaging time. However, it can be shown [Logan and Maleki, 1994] that uncorrelated phase fluctuations of individual elements in an array are mitigated by a factor of N in the combined output. Therefore, this relaxes the phase stability required of an individual element by N.

Typically, temperature effects along and between cables are the largest source of differential phase changes. A 1-km cable length contains approximately 3×10^4 X-band wavelengths. If we assume a coefficient of thermal expansion of 10^{-5} parts per Kelvin, then the cables would have to be maintained within 30 mK during an integration interval in order to ensure no more than 0.01 cycle of phase drift. This level of stability has been observed at the Goldstone site at a depth of 1.5 m by Calhoun, Kuhnle, and Law [1993].

This stability requirement applies not only the transmission medium (i.e., coaxial cable, waveguide, or optical fiber), but also to the entire downlink electronics chain from antenna and subreflector to the combiner/correlator, including the low-noise amplifier (LNA), RF–IF downconverter, digitizer, etc. The choice of downlink architecture influences the type of transmission medium employed, so the transmission system and downlink electronics configuration are intimately related. Recent advances in fiber-optic analog signal transmission allow novel architecture to be employed which enhance downlink stability and reduce costs, as discussed by Logan, Lutes, and Maleki [1990] and Logan and Lutes [1992].

Four architectures were considered for the signal-processing and distribution system:

(1) Conventional RF–IF downconverter at antenna front-end, with coaxial cables used for LO and IF distribution.

(2) Conventional RF–IF downconverter at antenna front-end, with analog fiber-optic links used for the LO and IF distribution.

(3) RF–IF downconverter, digitization, and time-tagging at the antenna front-end, with analog fiber-optic link used for LO distribution and digital fiber-optic links used for sampled IF distribution.

(4) Transmission of the S- and X-band LNA outputs using analog fiber-optic links from antenna front-end. Conventional RF–IF downconverter and digitizer collocated with the combiner/correlator. No LO distribution to the antenna front-end is required.

The fourth option, RF fiber-optic transmission, was selected as the most stable and economical solution. The block diagram for this configuration is illustrated in Fig. 4.4-1. Analysis and demonstration at DSS 13 of this capability was documented by Yao, Lutes, Logan, and Maleki [1994].

Direct transmission of the RF output from the LNA over an analog fiber-optic link would probably provide the most direct method for meeting the stability requirements of any other option. A detailed design would likely utilize fiber-optic cable with a very low coefficient of thermal expansion for above-ground routes and buried single-mode fiber for the long routes between antennas and the control point. Burial at a depth of a meter would ensure differential thermal effects at the milli-Kelvin level or less. The direct transmission method also offers the attractive advantage of locating much of the downconverter chain in a well-controlled, centrally located environment in close proximity to the correlator and combiner hardware and the frequency standard. This improves the maintainability of the array and reduces the complexity and environmental control requirements for the front-end areas of the individual antennas. In fact, it is doubtful whether the 0.01 cycle of phase drift could be met if the downconverters were located on the antennas.

4.4.3 ARRAY LAYOUT AND CABLE ROUTING

The considerations for the layout of a telemetry-receiving array are different than for an astronomical array. The telemetry array under discussion should achieve a maximum gain-to-noise temperature ratio (G/T) at a minimum cost. Since G/T does not depend sensitively on the array layout, but the length of the cables in the signal-distribution system increases with the interelement spacing, it is desirable to utilize that layout scheme which provides for the lowest-cost cabling solution. These considerations were discussed in Section 4.2.1

To avoid shadowing of adjacent antenna elements, each antenna must occupy nonoverlapping circular areas A_{eff} of diameter $D_{eff} = D_e/\sin\alpha + D_{off}$, where D_e is the diameter of an individual antenna element, α is the minimum tracking elevation angle above horizontal, and D_{off} depends on the antenna mount design, as shown in Fig. 4.4-2. If the elements are arranged in a simple square or nearly square grid, we know from the discussion in Section 2 that the number of elements needed is a function of $(D_e)^{-2}$. Since the number of elements along one side of the square is approximately $\sqrt{N_e}$, and the length of the side is $(N_e-1)D_{eff}$, we see that the size of the array is practically independent of the element diameter. Instead, it depends on the constants in Eq. (2-2) and the minimum elevation angle. If we wanted to synthesize a single 70-m antenna with an array of four 35-m antennas having the same system temperature as the 70-m antenna, then the array would be approximately 335 m along the side if the minimum elevation is 6°. An array of 3-m antennas with 110-K system temperatures would be about 458 m along the side.

Although it is straightforward to estimate the signal-distribution costs for a square array, it is not the most cost-effective geometry. The most dense packing arrangement for these circular areas is the hexagonal-close-pack (hcp), as illustrated in Fig. 4.4-3, in which each circular element of diameter L_{eff} is surrounded by 6 identical elements. The hcp arrangement uses 86.6% of the area needed for a conventional square packing arrangement.

For a square array, it is obvious how to obtain identical square subarrays, but "it is a widespread source of irritation that hexagons put together do not quite make up a bigger hexagon" [Mandelbrot, 1977], i.e., it is not possible to construct identical hexagonal subarrays from the single-antenna hexagonal unit cells. However, a fractal geometrical construction, the Gosper snowflake [Gardner, 1976] retains the hcp arrangement while providing identical perfectly interlocking subarrays.

In Fig. 4.4-3, the seven elements arranged in hcp configuration represent a "first-order" Gosper snowflake. Higher-order Gosper snowflakes are obtained by recursive tiling of lower-order

snowflakes. Figure 4.4-4 illustrates a second-order Gosper snowflake, which is comprised of seven perfectly interlocking first-order snowflakes. Likewise, seven second-order Gosper snowflakes can interlock perfectly to form a third-order Gosper snowflake, as in Fig. 4.4-5. Second-order, third-order, and higher-order Gosper snowflakes retain this same shape. This "self-similarity" on all scales is a basic characteristic of fractal objects.

The Gosper snowflake configuration also provides for the possibility of nonoverlapping cabling to a central location, so that all cables may be installed via direct burial with a cable plow, as illustrated in Fig. 4.4-6 for the third-order snowflake. A detailed comparison of the cable lengths required for the Gosper snowflake and for a conventional square array [Logan, 1993] indicated that the Gosper snowflake layout is more economical than a square array. Also, the cable lengths in the Gosper snowflake are naturally equalized, which places less burden on the correlator to compensate for the inevitably unequal cable lengths resulting from a square array layout. Although the fractal geometry for the array layout was not used in the cost estimation process, the preceding discussion illustrates the potential for cost savings in land, cabling, and trenching, which should be explored if the arraying concept is to be pursued.

4.4.4 COST MODEL

The total cost of the fiber optic distribution system as a function of the antenna element diameter is modeled using terms for each of the components of the system:

$$C_{FO}(D) = L_{cable}\, C_{cable} + L_{trench}\, C_{trench} + N_e\, C_{term} + N_e\, C_{splice} + N\, C_{conn}$$

where L_{cable} is the total length of fiber-optic cable needed in meters, C_{cable} is the cost per meter of the cable, L_{trench} is the total length of trench in meters, C_{trench} is the cost per meter for trenching, laying the cable, and burial, N_e is the number of antenna elements, C_{term} is the cost of terminal equipment for a single antenna, C_{splice} is the cost of splices for each antenna, and C_{conn} is the cost of connectors for each antenna. Each of these terms will be treated separately below.

Trenches

For the purposes of this model, we assume that the antennas are laid out in a regular square grid pattern, separated by distance $L_{min} = D_e/\sin\alpha$, where D_e is the diameter of the antennas, and α is the minimum elevation angle to be tracked above the horizon. The grid will have sides of length $L_{side} = (N_e^{1/2} - 1)L_{min}$. Assume further that trenches are to be dug to route the cables, in a fashion similar to the Project Cyclops study [1971]. A central trench runs the length of the array vertically through the center, and horizontal trenches are dug for each row. There will be $N_e^{1/2} + 1$ trenches, each of length $N_e^{1/2} L_{min}$. The total trench length is thus $L_{trench} = (N_e + N_e^{1/2}) L_{min}$.

The cables can be laid in the trench and buried at a uniform depth. Recently, a price quote of $180/meter was obtained for a DSN job between DSS 16 and G-86 for trenching and installation of two conduits with pull cables. We will use this number for the following estimates. It is emphasized that the power cables for the antennas can be laid in the same trench with the optical fiber cables, since the fiber is immune to electromagnetic interference.

Cable Costs

It appears that the total length of cable required to run individual cables in the trenches from each antenna to the center of this square array can be approximated by $L_{cable} = N_e^{3/2}/2\ L_{min}$. This expression holds better for large N_e (> 50), but will be used for the purposes of this first-order estimate. The cost of single-mode fiber-optic cable for a recent DSN job was found to be $0.23/fiber-meter. This is a relatively high price, probably because this was only a 4-fiber cable, and so is a conservative estimate. It is assumed that the cost of adding a few multimode fibers to the cable is negligible.

Cost of Terminal Equipment

Assuming no quantity discounts, the costs of the terminal equipment for a directly modulated semiconductor-laser system for both S- and X-band are dominated by the cost of the transmitters. Two scenarios are considered: (1) a "conventional" LO/IF system, in which a frequency reference is distributed to each antenna on one fiber, the signal is downconverted, and the IFs are sent back on separate fibers at 300 MHz, and (2) an "advanced" system, in which the RF signals are transmitted directly on fiber from the antennas to the control room at S- and X-band on separate fiber-optic links. It should be noted that the second scenario is conservative, and it is quite likely that both S-, and X-band signals could be transmitted on the same link.

Splices

Each cable must be stripped at both ends, and connectors spliced onto the cables at a breakout box. The cost of the breakout box is included in the terminal equipment "misc H/W" amount. Assume that the cost to strip a cable is C_{strip} = $12.50, based on 15 minutes of labor at $50.00/hr, and the cost to splice single-mode and multimode fiber is about $1/fiber, if ribbon-type cable is used. S single-mode fibers will be used for the RF signals and M multimode fibers will be used for monitor and control, per antenna. Thus, we have the following costs per antenna for stripping and splicing:

$$2\ C_{strip} + 2\ (S + M)\ C_{splice}$$

Connectors

Connectors must be spliced to the ends of the fiber for connection to the terminal equipment at the breakout boxes. For each antenna, the costs are

$2\,S\,C_{sm\text{-}conn} + 2\,M\,C_{mm\text{-}conn}$

where the cost of a high-quality, low-reflection single-mode connector pigtail is $C_{sm\text{-}conn}$ = \$60.00 (based on the cost of a patch cord, cut in half to provide two pigtails with connectors). Multimode connector cost is substantially less, $C_{mm\text{-}conn}$ = \$6.00.

Option 1: LO/IF System, one transmitter shared among 4 antennas for frequency distribution. Assumed NO quantity discounts.

COMPONENT	QUANTITY	COST (k\$)
FO Transmitter (Ortel CATV)	2.25	31.5
Optical Isolators	2.25	4.5
FO Receiver (Ortel CATV)	3	18
FO 1 x 4 Splitter	.25	.1
Misc. H/W		5
Assembly & Test		4
TOTAL FO terminal equipment cost per antenna:	$C_{term\text{-}LO}$ = \$ 63.1 k	

Option 2: RF S- and X-band System. Assumed NO quantity discounts.

COMPONENT	QUANTITY	COST (k\$)
FO Transmitter (Ortel DFB)	2	30
Optical Isolators	2	4
FO Receiver (Ortel)	2	6
S- X-band RF Preamp	2	4
Misc. H/W		5
Assembly & Test		4
TOTAL FO terminal equipment cost per antenna:	$C_{term\text{-}RF}$ = \$53k	

The total cost of the fiber-optic system for the square array can now be written as:

$$C_{FO}(D) = (N_e^{3/2}/2)(D_e/\sin\alpha)SC_{cable} + (N_e+N_e^{1/2})(D_e/\sin\alpha)C_{trench} + N_e\{C_{term} + 2C_{strip} + 2(S+M)C_{splice} + 2S\,C_{sm\text{-}conn} + 2MC_{mm\text{-}conn}\} \quad (4.4\text{-}1)$$

4.4.5 CONCLUSIONS

The layout and cabling problems of a large deep-space telemetry-receiving antenna array were investigated. Transmission of the RF signals from the antenna front-end areas using fiber-optic links offers the best phase stability and simplifies the front-end area, compared to other methods of signal distribution. It is concluded that the antenna elements should be arranged in the hexagonal-close-pack configuration, and that the subarrays should have the shape of a Gosper snowflake. This arrangement provides the most dense packing without shadowing, so it requires the least amount of land and the shortest cable runs. Also, the Gosper snowflake provides perfectly interlocking, identically shaped subarrays, and enables a cabling scheme that does not require any crossing of cable trenches. This greatly simplifies construction, since all cables may be installed with a tractor-pulled cable plow at a uniform depth.

4.5 CORRELATOR AND COMBINER COST MODEL

Normally, as a spacecraft travels farther away from Earth and the telemetry signal-to-noise ratio (*snr*) gets poorer, two system-parameter trade-offs come into play. First, the telemetry modulation index is usually increased so more transmitter power is moved from the carrier into the telemetry signal, thereby improving telemetry *snr*. This, of course, may result in a carrier signal that is significantly harder to acquire and track. The limit for this trade-off is full modulation where no carrier is present. In this case, the carrier signal must be acquired and tracked using a less-than-optimal Costas phase-lock-loop technique.

The second trade-off that comes into play is the reduction of the rate at which telemetry data are transmitted back to Earth, resulting in an improved *snr* per telemetry bit. This has the unfortunate consequence of also reducing the total amount of data that can be returned during the critical encounter-phase of a mission (e.g., the Galileo S-band mission). Although other combining schemes are possible, the full-spectrum combining scheme appears to be the most general in that it can operate in the lowest *snr* conditions and would work with natural radio sources as well as the modulated signals from spacecraft. For these reasons it was selected as the combining scheme to be costed in this design study.

4.5.1 CALIBRATION

For any large system to function consistently, continual self checking and calibration are required. For arraying of many small antennas, the most important and sensitive calibration will be

the relative phase between the various signal paths. Along with the relative delay between signal paths, the relative phase must be driven to zero before the various signals can be added coherently. Normally, considerable efforts are made to maintain good phase stability within the cost limitations of the budget. Calibration can then be done infrequently (e.g., once a day or before and after a pass). An even better approach, however, is to self-calibrate by using the source being observed, provided that it has the right characteristics and is strong enough.

For the application under consideration, the source is normally a spacecraft telemetry signal consisting of a carrier signal upon which a subcarrier and/or telemetry symbols have been impressed. If a carrier is present, it provides a nice CW signal for calibration. If suppressed carrier modulation is used, then "squaring" of the signal must be performed before a CW is available for use. Unfortunately, when signal reception is accomplished through the use of many small apertures, the signal strength for either of these approaches is weak, at best. If the carrier cannot be directly tracked, cross-correlation offers some advantages.

4.5.2 CORRELATION

A key processing component in the full-spectrum combining technique is cross-correlation. As seen in the overall block diagram of Fig. 3-4, the correlator is the device that provides the measurement and control of delay and phase for closing the correction loop.

The correlation process is exactly analogous to the squaring process in a Costas-loop tracking receiver. For weak signals, there is a "squaring" (or correlation) loss due to the multiplication of signal and noise. This must be overcome by proper filtering before correlation (hence the matched filter shown in Fig. 3-4) and lengthy integration (narrow-loop bandwidths) after correlation. In the single-antenna Costas-loop tracking, integration is limited by instabilities of signal phase. However, for correlation, many of these instabilities are reduced or eliminated by common mode rejection, and therefore longer integration time is possible.

One further step can be taken to overcome the problem of weak signals. Rather than simply correlate the signals from each small aperture a pair at a time, improvement is obtained if each aperture is correlated with the sum of all the others. This provides a gain of a factor of N–1 (N being the number of small apertures) in the correlation *snr*. It does, however, require that the sum of the apertures adds up coherently to start with. This can be accomplished either by calibrating ahead of time on a strong source, or by using some "bootstrap" technique. The design presented and costed below includes this capability to allow for the possibility of smaller apertures.

4.5.3 DESIGN

Figure 4.5-1 presents a block diagram of a full-spectrum correlator/combiner to be used in a small aperture array. It is assumed that multiple IF signals centered at 300 MHz arrive from many antennas, and that these need to be downconverted to baseband, corrected for delay and phase, and finally combined. The output will be fed into a normal receiver to accomplish symbol extraction.

Downconverter and Digitizer

The downconverter module shown in Fig. 4.5-2 consists of two parts: downconversion to near baseband where an IF of 64 MHz and about 120 MHz bandwidth is digitized at 256 MS/s (where MS/s = megasamples per second); this is followed by a second digital downconversion to 0 MHz IF, resulting in a bandwidth of ±8 MHz, or 16 MS/s sample rate, both I and Q (in-phase and quadrature-phase) components. This second downconversion is tunable over the 120 MHz in steps of 1 MHz.

Signal Corrector

An antenna module is shown in Fig. 4.5-3. In the first half of this module is found a delay line and a phase rotator. These are controlled by a microprocessor which calculates the settings of these devices, based on known instrumental and geometric models for the array. To the calculated values are added the residual delay and phase determined by the correlator.

It is expected that the model calculations should be able to provide delays accurate to a few nanoseconds, and phases to less than a millicycle. The residuals will be probably on the order of a microsecond in delay, and actually up to many hertz for the phase rate.

Correlator and Combiner

The correlator block in Fig. 4.5-3 consists of a matched filter that extracts the individual harmonics of the spacecraft telemetry out of the signal, one at a time, and cross-correlates them to obtain estimates of the delay and phase residuals. The correlation takes place between each antenna and the sum of all antennas.

The harmonic extraction is accomplished by separate downconverters for each harmonic followed by narrowband filters. These signals are then integrated over the length of a symbol (at several different symbol phases to provide a crude symbol synchronization), and then correlated. The result of this correlation is Fourier transformed over a long enough time interval to allow extraction of the residual delay and phase with good *snr*, and then the loop is closed with these residuals.

4.5.4 COST MODEL

Table 4.5-1 gives a summary of the hardware and software components that are necessary to accomplish the combining function, together with an estimate of their cost. The costs, as presented, do not include the economies that will occur in buying large quantities. This savings should be accounted for at a higher level.

4.5.5 CONCLUSIONS

Because of the potentially large number of antennas in the arrays under consideration, the most important cost is not the nonrecurring portion, but the recurring part. Any recurring cost that scales with the antenna number, or even more important, any part that would scale with the number of antenna pairs, will grow to dominate the cost of a large array. This is seen clearly when we realize that if the number of antennas is N, then the number of antenna pairs is $N(N-1)/2$. In developing the present design, by correlating each antenna against the sum of the others, all components that scale as the number of pairs have been eliminated. This feature was obtained at the sacrifice of requiring some precalibration before these correlations produced a significant output. However, the result is a relatively modest cost per antenna, as compared to the other system components.

TABLE 4.5-1: Correlator/Combiner Cost Estimation.

Recurring Costs -

Downconverter / Digitizer Chassis:

	#/ant.	$K	$K/ant.
Downconverter Module			
IF-IF D/C & Dig.	1	10.00	10.00
Digital Video D/C	1	10.00	10.00
Link	2	0.05	0.10
Controller Modules			
CPU	0.125	4.00	0.50
Memory	0.125	2.00	0.25
Ethernet	0.125	2.00	0.25
Cabinet/PwrSup	0.125	8.00	1.00
Correlator / Combiner Chassis:			
Antenna Module			
Delay Line	2	0.10	0.20
Phase Rotator	1	0.25	0.25
Correlator	1	0.50	0.50
Module Controller	1	0.50	0.50
PC Board	1	0.20	0.20
Links	4	0.05	0.20
Combiner Module			0.00
Adder	32	0.05	1.60
PC Board	0.0625	0.15	0.01
Link	32	0.05	1.60
Controller Modules			0.00
CPU	0.0625	6.00	0.38
Memory	0.0625	3.00	0.19
Ethernet	0.0625	3.00	0.19
Cabinet/PwrSup	0.0625	8.00	0.50
Assembly and Test	0.0625	10.00	0.63
Total Recurring (per Antenna)			**29.03**

TABLE 4.5-1: Correlator/Combiner Cost Estimation (continued).

Nonrecurring Costs -			
System Controller:			
Workstation			50.00
Network			20.00
	WY	$K (FY '92 $)	
Engineering:	20	134.00	2680.00
Total Nonrecurring			**2750.00**

4.6 MONITOR AND CONTROL COST MODEL

When this circuit learns your job,
what are you going to do?
- Herbert Marshall McLuhan

A top-level design for the Monitor and Control subsystem (M&C) is presented. It is argued that the monitor and control costs for an array depend weakly on the diameter of antenna elements. These costs are strongly dependent on the functional complexity and the number of different interface types, both external and internal. As the diameter of the "small" antennas increases, the decrease in the number of antennas required reduces the monitor and control complexity. Although antennas with larger diameters are more complex, this effect is offset by the fact that the overall system design includes a 34-m antenna. Thus, the monitor and control cost for the array decreases as antenna size increases.

The approach to producing a cost model for the M&C was as follows:

- Identify Constraints
- State Assumptions
- Identify Monitor and Control Functionality
- Produce a design with sufficient detail to model costs

Figure 4.6-1 shows control flow paths for the monitor and control subsystem. These flow paths are pertinent to the Monitor and Control function for the array, and should not be confused with the spacecraft telecommunications data flow. Boxes with plain lines contain functions dedicated to monitor and control. Boxes with dashed lines contain functions that are not dedicated to monitor and

control, but with which monitor and control must communicate. The remaining portion of this section details the steps that led to the monitor and control design and to the resultant cost model.

4.6.1 CONSTRAINTS

In order to minimize development costs, a constraint imposed on the entire task was to use existing, proven standards and technologies in producing the designs and resultant cost models. For Monitor and Control, this constraint means:

- Use Commercial Off-the-Shelf (COTS) software wherever possible
- Vendor supplied software and hardware must be nonproprietary, open architecture, and have a sufficient client base such that assistance, maintenance, and qualified personnel are available

Constraints are also imposed by the DSN. The draft version of document 820-1, DSN Functional Requirements and General Requirements and Policies, states that TCP/IP communication protocols shall be used throughout the Network.

Document 821-18, DSN Monitor and Control System Functional Requirements and Design [1994], prohibits an increase in the number of Complex personnel in operations as new subnets are added. Therefore, the array must be an integral part of the DSN, and not a special case requiring dedicated operations personnel.

4.6.2 ASSUMPTIONS

Given the rapid advances in computer-processing speed, memory size, disk space, etc., it is assumed that computers with sufficient "horsepower" exist such that performance limitations will not be an issue. This assumption is based on work done for the NOCC Upgrade Task. It will be shown that the data rates for NOCC-RT are 3–5 times greater than the rates expected for the array Monitor and Control.

Methods used in recent DSN implementations can be used for the array. Examples are: NOCC Upgrade and RTOP 73 at DSS 13. While the exact implementations may not be replicated for the array, it is assumed that a base software component is available for easy incorporation into the

design. The average cost of one line of code, fully tested and debugged, is assumed to be $58. This may vary somewhat, depending on the difficulty of the task.

In the cost model, any deviations from this assumption are noted. It is anticipated that more than one computer will be required for the array. A distributed architecture is assumed. The cabling costs to individual antennas for the purpose of monitor and control are not a part of this estimation because it is assumed that these costs are part of the Signal Distribution subsystem.

The array interfaces to the DSCC Monitor and Control Subsystem (DMC) will resemble those of standard microwave and antenna subsystems. To the DMC, each subarray will appear as an individual DSS. It is assumed that the array has various "canned" antenna types (e.g., 70-m, 34-m, 26-m), and that a "pseudo-DSS" is assigned to each possible subarray. That is, given the current task goals as stated in Section 1.4, there could be as many as:

20 26-m DSS IDs
12 34-m DSS IDs
3 70-m DSS IDs

The DMC will not assign individual antennas to a subarray. Instead, it will simply assign a DSS to a link, and the array Monitor and Control will interpret the link assignment and configure the equipment. The prerequisite scheduling must be done by the NSS in order to prevent conflicts.

In keeping with the philosophy of a centralized DSCC monitor and control, it is assumed that local control of the array will be used for calibration and maintenance purposes only. This implies that:

- DMC directives, whether from an operator or a station event list, will have overall array control
- the array will receive and act on antenna predicts
- the array will report status to the DMC

In the realm of software and distributed architecture, there is a difficulty associated with the handling of a single instance, e.g., the pointing of an antenna. There is an additional difficulty associated with the handling of multiple instances, e.g., the simultaneous pointing of several antennas. However, given proper software techniques, and within limits, the difficulty in handling N instances is less than N times the difficulty in handling one instance, for $N > 3$. In other words, controlling 10 antennas is not ten times more difficult than controlling 1 antenna.

4.6.3 MONITOR AND CONTROL FUNCTIONALITY

The following monitor and control functions are defined:

• Routing (Gateway) - In order to meet the requirement that the array is perceived by the DMC (and other Complex assemblies) as a set of standard antenna/microwave combinations, there must be a single physical interface between the array and the DMC.

• Command Interpreter/Event Scheduler - Directives are received from the DMC; responses to these directives are sent to the DMC. Commands from the DMC (e.g., link assignments) must be translated into control inputs for the array assemblies. Subsequent events are scheduled and monitored for completion.

• Facility Monitor and Control - The status, configuration, and performance of the array facility (e.g., program set health, LAN loads, disk utilization, program set initialization, etc.) require monitor and control.

• Control of Combiner/Correlator - The Combiner/Correlator requires control of calibration, pre-pass, pass, and post-pass sequences. Event notices from the C/C are logged.

• Control of Signal Distribution - The Signal Distribution Assembly requires control and the logging of event notices.

• Subarray Control - Each subarray requires control of calibration, pre-pass, pass, and post-pass sequences. Event notices from subarrays are logged.

• 34-Meter Antenna Control - The 34-meter antenna requires specific controls for the microwave, exciter, transmitter, etc., assemblies. The control of these assemblies is in conjunction with control of the calibration, pre-pass, pass, and post-pass sequences.

• "Small" Antenna Control - The individual antenna elements require control (e.g., pointing). A communications method with the antennas requires definition.

• Data Evaluation (Information Synthesis) - Low-level data from the individual antenna elements, subarrays, and other assemblies must be summarized in order to present hierarchical information to the operator

• Interprocessor communications - A means to communicate between the individual processors must be defined.

• Availability - The array Monitor and Control design must meet standard DSN availability requirements.

• Fault Recovery - The array Monitor and Control design must be devoid of single points of failure and must permit rapid recovery in case of a hardware malfunction.

4.6.4 FUNCTIONAL DESIGN

The functional design is presented in Fig. 4.6-1. One should view the boxed items as program sets rather than individual computers. Given the nature of a distributed architecture, there may be one, more than one, or perhaps all program sets, housed in a single computer. The design presented is deliberately traditional. There may be debate with regard to implementation methods, but the functions listed in Section 4.6-3 and the allocation to program sets and hardware that follow are fairly standard. The individual functions assigned to each program set or hardware device are:

Gateway

- Receive and validate inbound streams from DMC
- Route monitor and control data
- Send outbound streams to DMC
- Provide FTS, TELNET capability
- Provide network services (ARP, RIP, DNS, etc.)
- Act on inputs from the Network Manager

Facility Manager

- Monitor processors and LAN using SNMP or some other COTS package
- Provide software version validation
- Handle logging functions
- Provide centralized management of files
- Act on inputs from the Command Interpreter

Command Interpreter/Event Scheduler

- Validate directives from DMC
- Translate directives from the DMC into commands for the other the array assemblies (Correlator/Combiner, Signal Distribution Assembly, Subarray Controllers, 34-Meter Antenna)
- Send responses to the DMC (via gateway)

Data Evaluator (Information Synthesizer)

- Accept and process status, configuration, and performance data from all the array assemblies in real time
- Act on inputs from the Command Interpreter
- Act on inputs from the Network Manager
- Receive predicts, standards, and limits from DMC or access from internal data stores
- Flag parameter values which are out-of-tolerance or which do not match the commanded configuration
- Provide summary parameters
- Send the array status to DMC (via gateway)

Subarray Controller(s)

- Act on inputs from the Command Interpreter
- Receive predicts, standards, and limits from DMC or access from internal data stores
- Send commands to the individual antennas (Small Antenna Control)
- Receive feedback from the antennas
- Provide status to the Data Evaluator
- Act on inputs from the Network Manager

34-Meter Monitor and Control

- Act on inputs from the Command Interpreter
- Receive predicts, standards, and limits from DMC or access from internal data stores
- Monitor and control all assemblies associated with the 34-m antenna

Utility Software

- Experience has shown that about 15% of the software falls into the "utility" category

Ethernet LAN (or Fiber Optic)

- Provide interprocessor communication

Fiber Optic

- Provide communication between the Subarray Controller(s) and the individual antennas

Processors

- Provide necessary CPU, memory, and disk resources to execute the program sets with sufficient margin
- Via high MTBFs and redundancy, meet the availability requirements

4.6.5 COST MODEL

Before a cost model can be formed, it must be determined whether the functional design is sufficient to proceed. Given that this design was constructed by a party of one, imperfections are expected. However, it will become evident that the monitor and control costs are so weakly coupled with the diameter of the small antennas that even an imperfect design is sufficient.

Estimating software efforts is not an exact science. A very accurate estimate can be obtained by doing careful analysis and a detailed design. However, since analysis and design usually contribute to 40% of the software costs, investing this level of effort in an estimate is usually not cost-effective. At the other end of the spectrum, one can eyeball the job and base the cost estimate on experience, analogy, etc. The approach taken here is a hybrid of the two extremes. Sufficient analysis and design are performed to partition the task into pieces that are small enough to estimate either empirically or by analogy.

An assumption stated in Section 4.6.2 is that current computing capability is adequate to effect the design. This assumption will be validated after examining the cost model and the corresponding coefficients. It must also be shown that the architecture meets the availability and fault tolerance specifications.

The cost model is as follows:

Data Routing (C_{DR}) - Independent of the number of computers for a network this size

Facility Monitor and Control (C_{FAC}) - Independent of the number of computers for a network this size

External (operator or DMC) Control and Response (C_{OPS}) -Dependent on the number of operator directives (N_{OD}) and the cost per directive (C_{OD})

Command Interpreter/Event Scheduler (C_{CI}) - Dependent on interpretation of commands from the DMC, scheduling complexities, and responses to status as provided by the Data Evaluator

Combiner/Correlator Control (C_{CC}) - Dependent on the number of procedure calls (N_{PC}) from the Command Interpreter. The cost of each procedure call (C_{PC}) is dependent on the number of parameters per procedure (N_{PP}) and the cost per parameter (C_P). So

$$C_{CC} = \sum_{i}^{Npc} (C_{PC})_i = \sum_{i}^{Npc} (N_{pp})_i \cdot C_p$$

Signal Distribution Control (C_{SD}) - Same format as Combiner/Correlator

Subarray Control (C_{SAR}) - Same format as Combiner/Correlator

34-Meter Control (C_{34}) - Use numbers from RTOP 73 as basis

Small Antenna Control (C_A^{TOT}) - As expected, the cost model for this item is convoluted. One cannot produce a model based solely on the number of small antennas, because supporting twenty 3-meter antennas is much less of a task than supporting twenty 18-meter antennas. Complexity components which scale linearly for some antenna diameter regimes are not applicable in others. The result is a model which is best described as piecewise continuous. There does not exist a single analytical relation which covers the entire domain of small antenna diameters from 3 to 34 meters.

It is obvious that bigger antennas are more complex, and that the cost of supporting a single small antenna increases with the diameter of the antenna. It was assumed that the complexity of supporting a single small antenna increased proportionally with diameter. This term is C_{AC}. However, the array must support a 34-m antenna as its base station. Therefore, building 34-m "small" antennas, or small antennas in the same class as a 34-m antenna, incurs no additional cost with respect to the monitor and control of a single antenna. It was assumed that small antennas 18 m in diameter and larger were of the same class as a 34-m aperture, meaning that the incremental cost to support a single antenna of this class is zero. Also, antennas in the 9- to 18-m range were assumed to have a fair amount of commonalty with the larger antenna class. Finally, the smaller antennas (D < 9 m) were assumed to have some commonalty with the larger antennas. Specifically:

$$C_{AC} = 0 \qquad (D \geq 18m)$$
$$C_{AC} = (1.4 \cdot (D/18) - 0.4) \cdot C_{34} \qquad (9m \leq D < 18m)$$
$$C_{AC} = (D/18) \cdot C_{34} \cdot 0.7 \qquad (D < 9m)$$

The next contribution to C_A^{TOT} is C_{NP}, the cost due to the handling of N total parameters. The number of parameters is simply the number of antennas times the number of parameters per antenna. It is assumed, somewhat empirically, that the effort scales as the square root of the total number of parameters. Using the same rationale as in the preceding paragraph:

$$C_{NP} = C_P \cdot (34/D) \cdot N_P^{34} \cdot N_{34} \qquad (D \geq 18m)$$

$$C_{NP} = C_P \cdot 34 \cdot (18 \cdot D)^{-1/2} \cdot N_P^{34} \qquad (D < 18m)$$

where

C_P is the cost due to a single parameter

N_P^{34} is the number of parameters for the 34-m antenna

N_{34} is the number of 34-meter antennas for an equivalent 70-m G/T

The reason for this breakdown is as follows:

For $D \geq 21m$, the number of parameters per antenna is a constant; thus, the cost scales as the square root of the number of antennas, or in effect, as the diameter of the small antennas.

For $D < 21m$, since the number of parameters per antenna is proportional to D, and the total number of parameters is proportional to the number of antennas (inversely proportional to D^2), the cost effort is inversely proportional to $D^{1/2}$.

Finally, there is the cost simply due to the support of N small antennas: C_{NA}. Again, the cost is scaled as the square root of the level of effort, i.e., $N_A^{1/2}$, which is proportional to D.

$$C_{NA} = (D/34) \cdot C_{inc}$$

where C_{inc} is the incremental cost to support the number of 34-m antennas required to equal the performance of a single 70-m aperture. So,

$$C_A^{TOT} = C_{AC} + C_{NP} + C_{NA}$$

Data Evaluation -> Information Synthesis (C_{DE}) - Dependent on the number of processes/assemblies being evaluated (N_{AS}), the number of independent data items which contribute to each process (N_{DI}), and the cost per data item evaluated (C_{DI}). The part of this coefficient relating to small antennas has already been accounted for in C_A^{TOT}.

$$C_{DE} = \sum_{i}^{Nas} (N_{DI})_i \cdot C_{DI}$$

Status, Configuration, and Performance Displays (C_{SCP}) -Dependent on the number of assemblies (N_{AS}), the number of displays per assembly (N_{DS}), and the cost per display (C_{DS}). The part of this coefficient relating to small antennas has already been accounted for in C_A^{TOT}.

$$C_{SCP} = \sum_{i}^{Nas} (N_{DS})_i \cdot C_{DS}$$

Utility Software (C_{UT}) - Estimated as approximately 15% of the direct software effort.

Computer Processor Hardware (C_{HW} - Includes processors, disks, monitors, but not communications interfaces nor LANs) - Dependent on the amount of the array Monitor and Control software. The quantity of computer hardware required will be determined by comparing the amount of software required for the array versus the amount of software which currently runs in the NOCC-RT Sun SPARCs.

Communications Hardware (C_{COM} - Includes communications interfaces and LANs) - Dependent on the number of processors which must be interconnected within the array facility.

So, the total cost of monitor and control is:

$$C_{MC} = C_{DR} + C_{FAC} + C_{OPS} + C_{CI} + C_{CC} + C_{SD} + C_{SAR} + C_{34} + C_A{}^{TOT} + C_{DE} + C_{SCP} + C_{UT} + C_{HW} + C_{COM}$$

4.6.6 COST ESTIMATES

Given the cost model presented above, the costs for the array Monitor and Control are:

C_{DR} - $208,800 (3600 LOC)

C_{FAC} - $160,000 (3200 LOC @ $50 per LOC)

C_{OPS} - $203,000

The following directives are expected:

- Facility start-up
- Facility shutdown
- Program set init
- Program set abort
- Configure a subarray (pseudo-DSS) for a link
- Report status

- Accept predicts
- Perform calibration
- Six other miscellaneous directives

so N_{OD} = 14 and C_{OD} was estimated at $14,500. Note that the directive list does not include commands for the 34-m antenna assemblies, e.g., TXR, UWV, etc. This is included in the 34-m antenna specific costs.

C_{CI} - $829,400 (14,300 LOC)

A further breakdown follows:

- Interpretation of commands from DMC - 3300 LOC
- Response to status as presented by Data Evaluator -4500 LOC
- Scheduling of events - 6500 LOC

C_{CC} - $69,600

N_{PP} is estimated at 5

C_{PC} is estimated at $2,320

C_P is therefore $11,600

N_{PC} is estimated at 6

C_{SD} - $13,920

N_{PP} is estimated at 3

C_{PC} is estimated at $2,320

C_P is therefore $6,960

N_{PC} is estimated at 2

C_{SA} - $111,360

N_{PP} is estimated at 6

C_{PC} is estimated at $2,320

C_P is therefore $13,920

N_{PC} is estimated at 8

C_{34} - $870,000 (15,000 LOC)

The monitor and control effort for DSS 13 was on the order of 40,000 LOC. It is assumed that efforts involving other 34-m antennas are similar and approximately 62% of the code can be ported.

C_A^{TOT}

C_{AC} is determined from the formula presented in Section 4.E, given the estimate of C_{34} presented above.

C_{NP}

C_P = \$75 (approx. 1 work-hour)

N_P^{34} = 65 (derived by examining the current 34-m interfaces)

N_{34} = 4

C_{NA}

C_{inc} is estimated at \$20K

The estimates for the small antennas are (in \$K):

D	3	5	7	9	12	15	21	34
C_{AC}	54	90	126	162	144	90	0	0
C_{NP}	93	72	61	53	46	41	32	20
C_{NA}	226	136	97	76	57	45	32	20
C_A^{TOT}	373	298	284	291	247	176	64	40

C_{DE} - \$274,050 (4,725 LOC)

The estimated number of parameters evaluated for each assembly is:

7 parameters from the Correlator/Combiner

2 parameters from the Signal Distribution Assembly

2 parameters from the Subarray Controller

24 parameters from the 34-m antenna

The cost per parameter (C_{DIE}) is estimated at \$3,190. There is an additional cost of \$162,400 (2800 LOC) associated with providing the infrastructure necessary to support the parameter evaluations.

Status, Configuration, and Performance Displays (C_{SCP}) -Dependent on the number of processes/assemblies being evaluated (N_{AS}), the number of data items per process (N_{DI}), and the cost per data item (C_{DI})

C_{SCP} - \$158,000

The number of "custom" displays per function is estimated as:

Router	2
Scheduler	4
Correlator/Combiner	2
Subarray Control	3
Signal Distributor	1
34-m Antenna	6
Small Antennas	4
Hierarchical	3
	====
	25

Assuming 80 LOC per display (based on NOCC-RT), the cost is $100,000 @ $50 per LOC. There is an additional $58,000 (1k LOC) for supporting software.

C_{UT} - $464,000 (8,000 LOC)

C_{HW} - $120,000

Approximately 200,000 LOC reside in the 4 different processor types associated with NOCC-RT, i.e., on the average, each processor executes 50,000 LOC. The total estimated LOC for the array is approximately 62,000. To meet availability and redundancy requirements, two processors, plus a spare, are necessary. The estimated cost per processor is $40K.

Thus, the total cost ranges from $3.52M to $3.85M. For comparison, the estimated cost to do the monitor and control for the DSCC Galileo Telemetry Subsystem is on the order of $3M. This subsystem involves similar functions, and a like number of different assembly types, but not a large number of small antennas.

4.6.7 DESIGN VALIDATION

Is the design adequate with respect to CPU and I/O loading? One of the benefits of a distributed architecture is that if the software is properly designed and mated with the correct hardware architecture, CPU and I/O overloads can be solved simply by adding more hardware; the design is said to be "extensible." However, it will be demonstrated that the CPU and I/O loading anticipated in this design are not expected to tax the system.

CPU intensive operations are expected when the Command Interpreter and Scheduler receives a directive from the DMC to initiate a track. If, in the extreme case when the entire array is configured as twenty 26-m antennas, and an average track lasts 20 minutes, such a directive occurs on the average only once a minute. Subsequent scheduling operations involving precalibration,

track, and post-cal may cause short, intensive CPU loads, but these transients, again, pose no CPU loading problems.

The most sustained CPU loading is due to the Data Evaluation operation, that is, the collecting of data from all the array assemblies and the subsequent information synthesis. Suppose that 600 3-m antennas are required to effect a 70-m G/T, that each antenna reports 8 parameter values once every 5 seconds, and that each parameter requires 16 bits. This equates to approximately 15,000 bps. Using NOCC-RT as a comparison, a single SPARC 10 can process 75 kbps and maintain a 50% CPU margin. As one might expect, this process also involves the largest I/O component. Ethernet LANs can easily support 4 Mbps of primarily unidirectional traffic.

4.6.8 SUMMARY

A design and cost model for the array Monitor and Control has been presented. The design is based on current, proven software and hardware. The cost of supporting a "large number of little antennas" ranges from 1% to 9% of the total monitor and control cost.

4.7 AVAILABILITY COST MODEL

As discussed in Section 2, one aspect of performance in a communications link is availability, and like everything else it comes at some cost. In order to make a reasonable comparison of the costs for an array versus a single antenna, we must assume comparable availability for the two apertures. In Section 2 it was argued that the reliability or availability P_A, of an array is given by

$$P_A = \sum_{k=0}^{m} C(N_e + m, k) \cdot (1-p)^k \cdot p^{N_e+m-k} \qquad (2\text{-}8)$$

where N_e is the number of array elements needed to equal the G/T of some performance standard, p is the individual element availability, and m is the extra number of array elements that are used to increase the array availability. If we assume that the individual element availability is the same as the 70-m antenna, then $p = P_{70}$, and the above equation becomes

$$P_A \geq \sum_{k=0}^{m} \frac{(N_e + m)!}{(N_e + m - k)! \cdot k!} (1 - P_{70})^k \cdot (P_{70})^{N_e + m - k} \qquad (4.7\text{-}1)$$

which can be solved for m if N_e and P_{70} are specified.

The expressions for calculating N_e were given in Section 2.1 and a discussion of the relevant parameters that go into the determination of P_{70} is given in Appendix B. Based on this discussion we take $P_A = P_{70} = 0.992$ and solve Eq. (4.7-1) for m, given some value of N_e. Note that the value of N_e is always rounded up to the nearest whole integer. Figure 4.7-1 plots the value of m versus N_e for the range of array sizes needed to synthesize the G/T of a 70-m antenna at X-band, and an array availability equal to an individual element availability of 0.992.

In reality, it seems unlikely that one would construct an array with elements having the same availability as a single large antenna. It would seem worthwhile to investigate the cost of reliability and determine whether the investment should be toward making each array element more reliable or simply buying redundant elements. In addition, redundant elements would make it possible to make the array 100% available for scheduling, which is not feasible for a single aperture.

4.8 INTEGRATION, TESTING, AND CALIBRATION

Integration, testing, and calibration was not modeled in this study but was discussed in enough detail to understand that it would be an appreciable fraction of the total system cost. These activities occur at two levels, first in the field, and second at the signal-processing center (SPC), where it is presumed that all signals are brought to a common point and where the downconverters, local oscillators, correlator, combiner, and M&C computers are collocated.

The three items that are installed in the field are the antennas, LNAs, and the signal distribution system. The field installation and initial testing costs for these items are contained in the cost estimates for each subsystem respectively. Similarly, bench testing of the electronics components located at the SPC have been budgeted in the subsystem cost estimates. Once the individual components are in place they must be integrated and tested as a system. A list of some of the typical tasks that would be performed at this level include:

- Measure the individual antenna system temperature.
- Develop the individual antenna pointing model.
- Measure the individual antenna gain.

- Determine the instrumental phase delay to each array element and its stability.
- Determine each baseline.
- Measure the combiner loss.

When an organization builds large antennas occasionally, the first three steps on the above list can take a large amount of humanpower. If the G/T performance is critical, as it is in the DSN, then these tasks include not only measurement at the 0.1-K and 0.1-dB level but troubleshooting sources of spurious performance. The effort is usually measured in work years. If the time between building new antennas is longer than the time to test and calibrate an antenna, then the chances are that each antenna is treated individually. The tools and techniques may be redeveloped for each installation and the people doing the work may change, thereby diminishing the benefit of experience.

Clearly, it would be completely unaffordable to lavish a work year of effort per antenna on an array of 3000 elements. Equally clear is the fact that as the diameter of the array elements become smaller, some aspects of the test and calibration task become easier, e.g., the antenna pointing model. Construction of an array requires a far different approach to installation, calibration, and testing. The entire process must be extensively planned to automate repetitive tasks. This requires a substantial investment at the outset but may be recouped during the maintenance and operations phase.

4.9 MAINTENANCE AND OPERATION COST CONSIDERATIONS

The study by Brunstein [1990], which will be used as a reference for the cost of a 70-m antenna, did not include Maintenance and Operations (M&O). Therefore, M&O costs will not be included in the current cost model. However, a comparison of an array versus a single large antenna should include consideration of the life-cycle cost for each approach. Maintenance and Operations costs consume an increasing large percentage of the life-cycle cost as the expected lifetime of the array or single antenna is lengthened. There were no members of the Maintenance and Operations (M&O) organization on the design team, and therefore a cost model for M&O was not attempted. However, for the reader's convenience we summarize the salient points that were made in the LAAS study [Haglund, 1978] in Section V, written by J. T. Hatch and F. R. Maiocco and titled "M & O Cost Study" .

From the discussion in Section 1, it will be recalled that the LAAS study compared a single 100-m class antenna to an array of 30- to 38-m class antennas. The M&O portion of the study assumed what was termed "bent pipe" and "unattended" operation. These terms imply that the array

elements simply collect electromagnetic signals and deliver the arrayed signal to a Signal Processing Center (SPC) for telemetry or other processing. Furthermore, this is accomplished without human operators at each antenna or stationed at key pieces of equipment along the signal path. These assumptions are entirely consistent with the approach used in the present study.

The approach used in the LAAS study was to: (1) establish a maintenance policy, (2) analyze the maintenance tasks for each subsystem, (3) estimate workload and workforce requirements, and (4) estimate start-up and annual M&O costs. Since the architecture of the LAAS array that was studied was based on elements that could completely stand alone, the M&O cost elements were not completely overlapping with the array architecture in the present study. For instance, the LASS study assumed cryogenic LNAs (i.e., traveling wave maser amplifiers with 4-K cryogenics), a transmitter, exciter, and FTS subsystem on each antenna. Nevertheless, such other cost elements as documentation, training, system performance testing, support services, and the spectrum of common subsystems would be applicable to both studies.

The LAAS study also made a number of assumptions that appear consistent with the present study. These include:

- Major maintenance activities are scheduled as required and do not count as unscheduled outages for availability assessment.

- No time is spent on each array element repairing the LNA, the receiver, or the drive, other than that time required to remove and replace faulty equipment.

- All refurbishment, etc., is done at a maintenance facility after the operational spare is installed.

- Multiple apertures will permit improved utilization of workforce to perform scheduled preventive maintenance (PM).

- Operational reliability to be at least as good as the existing reliability if not better. All estimates to be based on DR data.

- Complex Maintenance and Integration (M&I) Team -
    - Centrally located.
    - Central repository for tools and spares.
    - Performs all PM, corrective maintenance (CM), engineering change order (ECO) implementations, and new equipment installations.

- Array configuration -
    - Maintenance crew scheduled 40 hr./wk (8 am – 5 pm local time).

- CM to be accomplished on next available day shift.
- PM to be accomplished on a scheduled basis.
- One or two array elements will be available to maintenance crew for PM that cannot normally be accomplished while tracking.

- Painting to be performed to keep the antennas aesthetically attractive.

The LAAS study also included two assumptions that **do not** seem consistent with the present study:

- System documentation, initial operational spares, and 180-day consumables will be supplied by engineering.

- Maintenance will be performed such that at the end of 30 years, the array will in general be ready for the next 30 years.

In the first case, the present study has not estimated spares or consumables, nor adopted a consistent philosophy in regard to the level of documentation. The second case appears at odds with the underlying thesis of this study—that changing technology drives down the optimum diameter of the array element. The discrepancy boils down to an extrapolation or "guess-timate" as to how fast technology is likely to change in the future. At some point in time, it becomes cost-effective to replace a piece of equipment rather than maintain it, and the estimate of this time determines the lifetime of the equipment and the M&O costs needed to sustain it.

Keeping in mind the similarities and dissimilarities between the LAAS study and the current study, let us consider the M&O cost estimates versus the number of array elements, as shown in Fig. 4.9-1, and versus antenna diameter, as shown in Fig. 4.9-2. The best linear regression line is for the cost versus number-of-elements plot and suggests a fixed M&O cost of \$1.5M/yr. plus \$203k/yr./antenna. If this expression is extrapolated to the largest array size that is envisioned (i.e., approximately 4000 3-m antennas), the yearly M&O will cost \$814M. This implies that it would cost more to maintain and operate the array every year than it took to build it in the first place. The only way around this dilemma is if the relation indicated in Fig. 4.9-1 is nonlinear, such that the cost of M&O decreases dramatically as N_e increases.

Clearly, any conclusions derived from an extrapolation of this expression outside the data range must be viewed with caution. Nevertheless, the preceding discussion suggests two things. First, a complete comparison of the cost of an array versus the cost of a single aperture must include M&O costs. Second, M&O cost considerations must be an integral part of the initial design for all subsystems. This latter point typically raises the design cost and initial capital investment. These

increased costs are only recovered gradually over the lifetime of the instrument, resulting in a funding dilemma that may be unacceptable to institutions focused on 1- to 5-year budgets.

In the discussion above regarding array availability, it was noted that the capital investment costs might be lowered by investing in less-reliable elements and accepting the fact that they would be replaced more frequently. A full analysis of the reliability vs. cost trade-off would include the implied M&O impact over the expected lifetime of the array. Any part that fails in the field will require a person to remove it and take it to a maintenance facility, a second person to repair it, and a third person to reinstall it in the field, and perhaps a fourth person to check it out. These repair people require an infrastructure of secretaries, managers, and supply clerks to provide supporting services. The sum total of this effort must then be multiplied by the lifetime to get the total M&O costs.

While it is possible to reduce the M&O task to many small steps and thereby estimate the workforce requirements, the total cost depends on how frequently the equipment fails. Failure statistics are more reliably arrived at empirically rather than theoretically, and for this reason the logical approach to building an array is to build a small one first and get the practical experience needed to estimate these costs.

5.0 TOTAL SYSTEM COST

The purpose of models is not to fit the data but to sharpen the questions.
- Samuel Karlin

The performance and cost estimates discussed previously for each subsystem were used to create three models. A separate cost model was created for three representative values of the system temperature. The calculations in each model are identical, but the results depend upon the number of antennas which in turn are determined by the assumed system temperature. Table 5-1 summarizes the tabular calculation for all three models using the TIW data for antenna costs and Fig. 5-1 shows the calculations graphically. The calculation represents the array cost to synthesize a single 70-m aperture having the same G/T and availability of one of the existing DSN 70-m antennas using parabolic apertures ranging from 3 to 35 m in diameter.

Performance Specification:

The performance is specified in the top four rows of the table. The top line lists the coefficients used to calculate the antenna aperture efficiency and could be used to model the efficiency as a function of diameter. In the particular model summarized in Table 5-1, the antenna efficiency is assumed to be a constant equal to 60% of the physical aperture. The second, third, and fourth rows list the three system temperatures that were used: 110 K, 85 K, and 30 K, corresponding to X-band zenith temperatures.

Starting on Line 5, the calculation proceeds by column with the diameter of the array element in this line. Line 6 is the calculation of antenna efficiency. Lines 7 through 12 calculate the number of antennas needed for each element diameter, for each system temperature and the additional number of antennas needed to raise the array availability to that of a single 70-m antenna. Given the aperture efficiency, system temperature, antenna diameter, and combining loss, the number of elements needed in the array can then be calculated according to Eq. (2-4). A combining loss of 0.2 dB was assumed, which increases the number of antennas in the array by 4.5% (but not the number of elements used for margin). The calculation of N_e was rounded up to an integer value. A separate calculation, as discussed in Section 4.7, was performed to estimate the additional elements that are necessary to ensure that the array availability is equal to or greater than the individual element availability.

Since the X-band specifications drive the maximum number of antennas, the S-band specifications have been neglected. In effect, at S-band the array would perform better than the equivalent 70-m aperture using model #1 and #2 and would have approximately comparable performance using model #3.

Cost Specification:

The three lower segments of Table 5-1 list the subsystem costs for each of the three system temperatures. Within each segment or cost model, the subsystem is listed by row and costs are listed under the column headed by N_e, the total number of array elements that was calculated in the upper part of the table. The nonrecurring cost (NRC) is listed in the second column of the table and is assumed to be independent of antenna diameter. As discussed in Section 4.2, an average value of the NRC was used for the antenna subsystem, even though the estimate supplied by the antenna contractors indicated some variation with diameter. In general the variations of this parameter are small compared to total antenna costs.

For antenna diameters of 15 m or less, the LNA costs for cooled configurations are doubled because of the previous assumption (*e.g.*, see Section 4.2) of a prime focus S-band and Cassegrain focus X-band configuration would imply physically separated LNAs. The signal distribution subsystem and M&C subsystem costs are not exactly a linear function of N_e, and were calculated separately. The remaining subsystem costs were modeled with a recurring cost times N_e, as discussed in Section 4.

The bottom row for each segment gives the subtotal of cost. Note that the units of the subtotal are in \$M whereas the entries are in \$k.

Learning Curve:

A quantity discount assumption was applied to all subsystems except the antenna costs, which were supposedly contained in the antenna contractors' cost estimates. The discount was assumed to vary as $\log_{10}(N_e)$. That is, we assumed that production-line learning would decrease total cost by 5% for each factor of 10 increase in number of units produced. Thus, there is no discount for 1 – 9 units, 5% discount for 10 – 99 units, 10% for 100 – 999 units, and 30% for 1000 – 9999 units.

Table 5-1: Array cost model using TIW antenna data.

Ant. aperture eff.=a+bD, where a=.6, b=0.0

Tsys1= 110 individual ant. avail= 0.992

Tsys2= 85 Elev(min)=8 deg.

Tsys3= 30 Freq.= X-Band

	Element Diam.=	3	5	10	15	20	25	30	35
	Aperture Eff.=	0.60	0.60	0.60	0.60	0.60	0.60	0.60	0.60
Tsys=110	**Ne1=**	3434	1236	309	137	77	49	34	25
	Ne1(avail.)=	41	18	7	4	3	3	2	2
Tsys=85	**Ne2=**	2654	955	239	106	60	38	27	19
	Ne2(avail.)=	33	15	6	4	3	2	2	2
Tsys=30	**Ne3=**	937	337	84	37	21	13	9	7
	Ne3(avail.)=	15	7	3	2	2	1	1	1

MODEL #1	NRC	RC	3475	1254	316	141	80	52	36	27
LNA1	200	15.00	43096	16096	4348	2088	1286	913	698	576
Cal./LO/IF	1500	12.50	37247	14747	4956	3073	2405	2094	1915	1813
Antenna	1671	4.21	136688	138541	141753	143567	145706	148676	148813	152389
C/C	2750	29.03	85769	33514	10777	6403	4851	4130	3714	3478
Sig Dist	1000		65447	40246	21705	15418	12234	10304	9012	8079
M&C	4275		4018	3951	3833	3744	3671	3607	3550	3497
Tst/Calib										
subtotal	11396	61	372	247	187	174	170	170	168	170

MODEL #2	NRC	RC	2687	970	245	110	63	40	29	21
LNA2	400	30.00	133977	49908	13344	3363	2120	1504	1206	988
Cal./LO/IF	1500	12.50	29328	11814	4197	2735	2217	1960	1836	1745
Antenna	1671	4.21	106071	107544	110279	112370	115098	114752	120202	118896
C/C	2750	29.03	67379	26704	9013	5617	4414	3818	3530	3319
Sig Dist	1000		50581	31610	17211	12325	9851	8357	7346	6627
M&C	4275		4018	3951	3833	3744	3671	3607	3550	3497
Tst/Calib										
subtotal	11596	76	391	232	158	140	137	134	138	135

MODEL #3	NRC	RC	952	344	87	39	23	14	10	8
LNA3	600	150.00	243665	90711	24169	5985	3815	2580	2025	1746
Cal./LO/IF	1500	12.50	11628	5255	2482	1949	1768	1665	1619	1595
Antenna	1671	4.21	38660	39217	40238	40919	43081	41249	42544	46328
C/C	2750	29.03	26271	11470	5031	3792	3372	3133	3026	2972
Sig Dist3	1000		18520	11931	6915	5211	4349	3827	3477	3226
M&C3	4275		4018	3951	3833	3744	3671	3607	3550	3497
Tst/Calib										
subtotal	11796	196	343	163	83	62	60	56	56	59

6.0 SUMMARY AND CONCLUSIONS

"There are some people who if they don't already know,
you can't tell them."

- Yogi Berra

Contrary to our initial supposition, the cost models illustrated in Fig. 5-1 indicate that there is no optimum antenna diameter in the 3- to 35-m range for an array that would synthesize a 70-m aperture. In this section, we discuss the reasons for this, the validity of the model, and what actions the DSN might consider next.

6.1 THE BOTTOM LINE

The lack of a well-defined minimum in the cost-versus-diameter curve is a direct result of the data illustrated in Fig. 4.2-1. This shows that the best-fit power law to the antenna cost data has an exponent of approximately 2 instead of 2.7, as suggested in previous studies. An exponent of 2 implies that the cost of the collecting area is independent of the antenna diameter and the total array cost must then increase as the number of antenna elements in the array. The reason for this stems directly from the functional behavior of the various cost components that make up the antenna subsystem. This same conclusion had been anticipated in the unpublished data of Stevens and McLaughlin [F. McLaughlin, JPL, 1993, private comm.].

When the antenna component costs were fit with a power law, several indicated exponents larger than 2, e.g., the support structure, reflector, foundation, shipping, installation, and testing. These are components that relate to the mass of material and reflect the fact that the antenna represents a volume, and these components dominate the cost for large antenna diameter. However, there are four antenna cost components whose functional behavior is more complex but nearly linear, e.g., the axis drives, positioner, feed, and power, and these components dominate the cost for small antenna diameter. The distribution of fractional cost among all 8 components versus the antenna diameter is shown in Fig. 4.2-10. The other subsystems in the cost model scale either directly or approximately as the number of array elements N_e. As a result, the cost of these subsystems does not determine the existence of a minimum in the curve but does determine the value of element diameter, if there is a minimum.

The discussion in Section 4.2.4 suggests that as the data for each cost component is extrapolated to larger diameters, the exponent of the power law that best fits the total antenna cost becomes larger than 2. With all of the clearness afforded by hindsight, it then seems safe to conclude that we should have modeled a larger range of antenna diameter. Had we done so, a minimum in the total system cost would probably have been found for a diameter > 30 m. Recall

that the conclusion of Potter, Merrick and Ludwig [1965] was that the optimum diameter for the array elements was approximately 65 m.

6.2 VALIDITY OF THE MODEL

Errors using inadequate data are much
less than those using no data at all.
- Charles Babbage

In Section 4 we discussed, but did not include in the cost model, several important elements of the total life-cycle cost of an array; installation, testing, calibration, maintenance, and operations. Potentially large costs involving land acquisition and site development were also left out of the model. The primary reason these cost elements were not included in the study is the time element—or lack thereof. Many of these costs scale as N_e and would not change the shape of the curves shown in Fig. 5-1. However, the facilities cost would likely scale as $(N_e)^2$ (i.e., proportional to area), and would possibly influence the shape of the curve.

6.3 WHAT NEXT?

It would be the height of folly— and self-defeating— to think
that things never heretofore done can be accomplished
without means never heretofore tried.
- Francis Bacon

Figure 6-1 illustrates how the fractional cost of each subsystem changes as a function of antenna diameter. We see that for a large diameter the antenna subsystem dominates the cost, whereas for small diameters the electronics dominate the cost. Although the power law function of the antenna cost is an approximation, it does represent some physical attribute of the subsystem component that it models, e.g., an exponent >2 relates to a volumetric term. Furthermore, it was noted that as the antenna cost data are extrapolated to larger diameter elements, the exponent of the best-fitting power law to the total antenna subsystem cost became larger than 2.

For the antenna components that were modeled as linear or piecewise linear functions, the physical attribute driving the cost is less clear. Also, as seen in Figs. 4.2-1 to 4.2-9, the disagreement between antenna suppliers is fairly large when measured as a percentage and grows with increasing antenna diameter.

If the basic thesis of this study is true—that advances in technology tend to drive the optimum diameter of the array elements toward a smaller diameter—then we may ask what are those areas of technology development that would most contribute to increasing performance and/or decreasing cost. By increasing the performance, the multiplier N_e in the cost model is reduced, and by decreasing the recurring cost, the product of N_e times RC_i is reduced. In addition to increasing performance and decreasing cost, there are areas of development essential to reduce the uncertainty of many aspects of performance and cost and, therefore, the risk to implementation. A (noncomprehensive) list of those areas of technology that impact the trade-off between cost and array element diameter would include the following:

• *Antenna Pointing/Drive Mechanisms* -

One of the elements that dominates the cost of small antennas is the pointing and drive system. To have an impact on the system cost model, the linear dependence of this cost element must be dramatically lowered for small antenna diameters. The requirement is to point with an accuracy of 1/10th of a beam width. The beam width is inversely proportional to the antenna diameter, so that meeting the requirement gets easier at small antenna diameters. An innovative design and component selection is needed in this area to provide an inexpensive solution to the problem of driving and pointing small antennas.

• *Feed Fabrication* -

There does not seem to be a technological problem involved with designing feeds for any of the antennas that were considered in this study. Rather, the problem seems to be to design a feed that is manufacturable in quantity for very low cost. The DSN is experienced in building things in small quantities and does not normally face this problem. It may be better to contract this aspect of the design if the array concept were to flower.

• *Signal Distribution* -

As argued in Section 4.4, the technology to directly modulate an FO link with the S- or X-band output of the LNA seems to be commercially available today. The benefits are fairly obvious—less equipment on the antenna (in the field) and concentration of functions in a central facility. Field maintenance and complexity are both reduced. Centralization of the downconverter and local oscillators would make it possible to miniaturize these components and achieve better overall system stability. What is necessary at this juncture is a convincing demonstration of this technology.

• *LNA/Cryogenics* -

The system temperature was modeled in three discrete steps because it did not seem feasible to assume that field-worthy systems were available at arbitrary physical temperatures. The derivative of the receiver temperature versus physical temperature curve is highest near room temperature, which suggests that low-cost cooling technology in this regime offers the most benefit. However, what is needed is an understanding of the life-cycle cost of the cooling technology— particularly the maintenance costs. As an example, consider that difference between Model #2 and #3 for a 35-m array element. The difference in total capital investment is a factor of two, which is also the difference in the LNA cost. However, it is certain that the M&O costs for cooled LNAs (Model #3) would be more than a factor of two larger than the Peltier cooled LNAs of Model #2. Over a thirty-year lifetime, this difference might exceed an order of magnitude for the LNA subsystem but would have to be balanced against the total M&O cost of an array of 17 elements versus an array of 7 elements.

• *Modular Down Converters* -

The planned DSN expansion of an additional 3 BWG antennas per complex (plus two inherited antennas at Goldstone), at potentially 3 operating frequencies (Ka-, X-, and S-band), and two orthogonal polarizations implies the need for up to 66 downconverters in the next few years. The current design uses all discrete components and contains 4 channels of downconverter electronics encased in an oven that is operated well above ambient temperature. There are 2 channels at X-band and 2 channels at S-band, each pair sharing a common local oscillator that is driven by a reference signal from the signal-processing center. This arrangement is packaged in a large bulky oven and is physically located in the antenna cone where space is at a very high premium. The variations of the physical temperature of the electronics is one of the prime factors in the overall stability of the unit.

Whether the downconverter is to remain on the antenna or located at a central processing center, it may be possible to achieve both cost and performance improvements by redesign of these devices using modern technology.

• *Correlator/Combiner* -

In Section 3 some of the problems involved with array calibration were discussed, and it was argued that the *snr* limitations could be minimized by using a scheme in which the combiner output was fed back and correlated against each individual element. This scheme should be analyzed and demonstrated with both telemetry signals and natural radio sources.

If the full-spectrum combiner approach is ever implemented in the DSN, then the signal spectrum must be filtered prior to correlation. This filter would have to be adaptive in the sense that

it would be a simple bandpass for sources whose spectrum is flat or unknown. In the case of spacecraft signals, the filter must be matched to the expected spectral power distribution within the a priori uncertainty on the frequency of that signal. Since the algorithms for doing this matched filter processing already exist in the Block V receiver, it seems logical to assume that some subset of the Block V design should be integrated in the design of the correlator and combiner in order to achieve maximum *snr* for the widest possible choice of signal source.

• *Atmospheric Issues*

In Section 3 some of the effects of atmospheric fluctuations on array gain were discussed and it was pointed out that these fluctuations lead to an effective gain loss for a telemetry array. For a given geometry, the gain loss depends on elevation angle and the strength of the turbulence. The turbulence strength is characterized by the parameter C_n, which is a statistical measure and also varies. For instance, very low values of C_n are possible during cold winter nights on the top of high mountains, whereas very high values of C_n can occur during a summer thunderstorm in the desert.

In effect, C_n is both site and season dependent, and like atmospheric attenuation or brightness temperature, it must be characterized in the form of a cumulative probability distribution (PDF) that is both site and season dependent. Knowing the baseline geometry and source elevation angle, the gain of an array can then be calculated with any desired degree of statistical certainty. These atmospheric effects are mostly negligible at S-band, noticeable at X-band on 10-km baselines, and appreciable at Ka-band. As the DSN evolves to an X-band and then Ka-band network of arrayed 34-m antennas, it becomes increasingly important to quantify atmospheric fluctuations.

A better understanding of the site and seasonal variations in atmospheric fluctuations should also influence the site selection of new antennas, but unfortunately the database needed to characterize these statistics does not exist. Like the statistics for attenuation and brightness temperature, the fluctuation statistics must be collected over a long period of time. In addition to the effects on array gain, atmospheric phase fluctuations will limit our ability to track a carrier signal on a single antenna and thereby impose another constraint on the design of a deep space communications link. Thus, the DSN should be interested in atmospheric fluctuations for several reasons. It is strongly recommended that compilation of this database be given a high priority.

Before I came here I was confused about this subject. Having listened to your lecture I am still confused. But on a higher level.

- Enrico Fermi

REFERENCES

Armstrong, J., and R. Scramek, "Observations of tropospheric phase scintillations at 5 GHz on vertical paths," *Rad. Sci.*, Vol. 17, #6, pp1579-1586, Nov.-Dec. 1982.

Barlow, R.E., and K. D. Heidtmann, "Computing *k-out-of-n* System Reliability," IEEE Trans. on Reliability, Vol. R-33, No. 4, October 1984.

Brown, D. W, W. D. Brundage, J. S. Ulvestad, S. S. Kent, and K. P. Bartos, "Interagency Telemetry Arraying for Voyager-Neptune Encounter," TDA Prog. Rept. 42-102, pp91-118, JPL, Pasadena, CA, Aug. 15, 1990.

Brunstein, S., "Comparison of implementation costs between a 70m BWG DSS and a DSS with an array of four 34m BWG antennas," IOM #3330-90-116 (internal document), JPL, Pasadena, CA, 4 Sep. 1990.

Butman, S. A., L. J. Deutsch, R. G. Lipes, and R. L. Miller, "Sideband-Aided Receiver Arraying," TDA Prog. Rept. 42-67, pp39-53, JPL, Pasadena, CA, Nov. 1981.

Calhoun, M., P. Kuhnle, and J. Law, "Environmental Effects on the Stability of Optical Fibers Used for Reference Frequency Distribution," presented at the 39th Ann. Meet. of the Inst. of Environmental Sci., Las Vegas, NV, May 2-7, 1993.

Christiansen, W. N., and J. A. Hogbom, Radio Telescopes, 2nd Ed. Cambridge Univ. Press, 1985.

Clark, B. G., "A continuous aperture approach to the VLA," VLA Report #2, 25 Jan. 1966, (available from the National Radio Astronomy Observatory, Charlottesville, VA).

Deep Space Network / Flight Project Interface Design Handbook, JPL Doc. 810-5, Rev. D, vI: Existing DSN Capabilities, vII: Proposed DSN Capabilities (internal document), JPL, Pasadena, CA, Sept. 15, 1991.

Dewey, R. J., "The Effects of Correlated Noise in Intra-Complex DSN Arrays for S-Band Galileo Telemetry Reception," TDA Prog. Rept. 42-111, pp129-152, JPL, Pasadena, CA, Jul.-Sep. 1992.

DSN Functional Requirements and General Requirements and Policies, JPL Doc. 820-1 (internal document; work in progress).

DSN Monitor and Control System Functional Requirements and Design (1994-2000), JPL Doc. 821-18, D-1164 (internal document), JPL, Pasadena, CA, February 15, 1994.

"DSN Performance Study: Telemetry Data Loss, January 1989 Through December 1992," Allied Signal Technical Services, Pasadena, California, February 20, 1993.

"DSN Performance Study: Telemetry Data Loss, January 1986 Through July 1990," Allied Signal Technical Services, Pasadena, California, October 1, 1990.

Edwards, C. D., "Development of Realtime Connected Element Interferometry at the Goldstone Deep Space Communications Complex," AIAA 90-2903, Aug., 1990.

Deep Space Network System Functional Requirements: General Requirements and Policies Through 1988, Vol. 1, Appendix C ("Functional Availability Definitions and Relationships"), JPL Doc. 820-20, Rev. A (internal document), JPL, Pasadena, CA, March 1, 1988.

Gardner, M., "Mathematical games," *Sci. Amer.*, v235, pp124-133, 1976.

Haglund, H. H., *et. al.*, "Large Advanced Antenna Station Status Report," JPL Internal Doc. 890-74 (internal document), JPL, Pasadena, CA, Aug. 1978.

Jamnejad, V., "Study of the Probabilistic Availability of an Array," JPL IOM 3327-92-069 (internal document), JPL, Pasadena, CA, October 9, 1992.

Jamnejad, V., T. Cwik, and G. Resch, "Cost and Reliability Study for a Large Array of Small Reflector Antennas for JPL/NASA Deep Space Network (DSN)," IEEE 1993 Aerospace Applications Conference Digest, February 1993.

Logan, R. T., G. F. Lutes, L. Maleki, "Microwave Analog Fiber-Optic Link for Use in the Deep Space Network," TDA Prog. Rept. 42-100, pp 21-33, JPL, Pasadena, CA, Feb. 15, 1990.

Logan, R. T., and G. F. Lutes, "High Stability Microwave Fiber Optic Systems: Demonstrations and Applications," Proc. 46th Ann. Symp. on Freq. Control, Hershey PA, May 27-29, 1992.

Logan, R. T., "Layout and Cabling Considerations for a Large Communications Antenna Array," TDA Prog. Rept. 42-114, pp 302-310, JPL, Pasadena, CA, Aug. 15, 1993.

Logan, R. T., and L. Maleki, "Effects of phase noise from lasers and other sources on photonic RF phased arrays," Proc. of SPIE O/E LASE 94, Optoelectronic Signal Processing for Phased-Array Antennas IV, Los Angeles, Jan. 26-27, 1994.

Mandelbrot, B., Fractal Geometry of Nature, Chap. 6, Freeman Co., NY, 1977.

McLaughlin, F., manager of program planning, TDA Planning Section (Section 410), private communication, Jet Propulsion Laboratory, Pasadena, California, June 1993.

Mileant, A. and S. Hinedi, "Overview of Arraying Techniques For Deep Space Communications," TDA Prog. Rept. 42-104, pp109-139, JPL, Pasadena, CA, Oct.-Dec. 1990.

Papoulis, A. , Probability, Random Variables, and Stochastic Processes, McGraw-Hill Book Company, 1965.

Patniak, A. R., I. W. Browne, P. N. Wilkinson, and J. M. Wroble, *Mon. Not. R. astr. Soc.*, 254, 655-675, 1992.

Potter, P. D., W. D. Merrick, and A. C. Ludwig, "Large Antenna Apertures and Arrays for Deep Space Communications," JPL Tech. Rept. No. 32-848, JPL, Pasadena, CA, Nov. 1, 1965

Project Cyclops, A Design Study for Detecting Extraterrestrial Life, CR 114445, NASA/Ames Research Center, Moffett Field, CA, 1971.

Rogstad, D. H., "Suppressed Carrier Full-Spectrum Combining," TDA Prog. Rept. 42-107, pp12-20, JPL, Pasadena, CA, Jul.-Sep. 1991.

Ruze, J., "Physical Limitations on Antenna," Tech. Rept. No. 248, Research Lab. of Electronics, Massachusetts Institute of Technology, ASTIA/AD 62351, Cambridge, Massachusetts, Oct. 1952.

Stevens, R., "Applications of Telemetry Arraying in the DSN," TDA Prog. Rept. 42-72, pp78-82, JPL, Pasadena, CA, Oct.-Dec. 1982.

Thompson, A. R., J. M. Moran, and G. W. Swenson Jr., Interferometry and Synthesis in Radio Astronomy, Wiley, New York, 1986.

Treuhaft, R. N., and G. E. Lanyi, "The effect of the dynamic wet troposphere on radio interferometric measurements," *Rad. Sci.*, v22, pp251-265, Mar. 1987.

Ulvestad, J. S., "Phasing the Antennas of the Very Large Array for Reception of Telemetry From Voyager 2 at Neptune Encounter," TDA Prog. Rept. 42-94, pp257-273, JPL, Pasadena, CA, Apr.-Jun. 1988.

Williams, D. R., "State-of-the-Art Cryogenically Cooled Amplifiers for Radio Astronomy," in The Radio Schmidt Telescope, Proc. of a Workshop held at Penticton, 1989 October 11-12, pp255-258, June 1991.

Yao, X. S., G. Lutes, R. T. Logan, Jr., and L. Maleki, "Field Demonstration of X-Band Photonic Antenna Remoting in the Deep Space Network," TDA Prog. Rept. 42-117, pp29-34, JPL, Pasadena, CA, Jan.-Mar. 1994.

Understanding is that penetrating quality of knowledge that grows from theory, practice, conviction, assertion, error, and humiliation.

-Anonymous

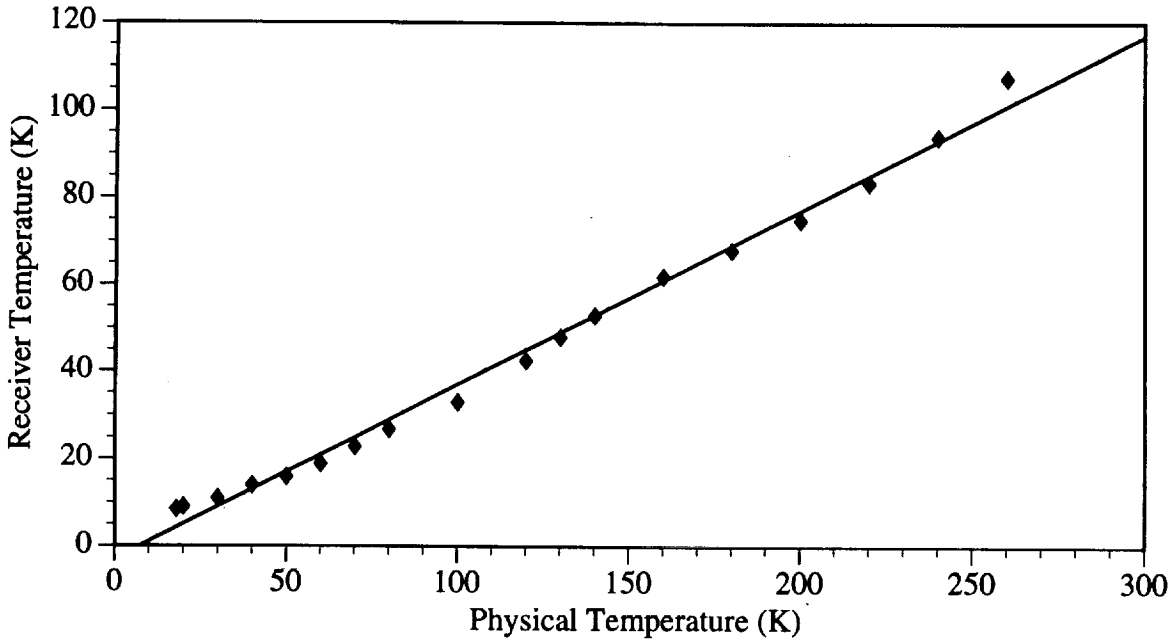

Figure 2-1. The cooling curve for an X-band high-electron mobility (HEMT) amplifier showing the amplifier's effective noise temperature versus its physical temperature together with the best linear fit, from Williams [1991] .

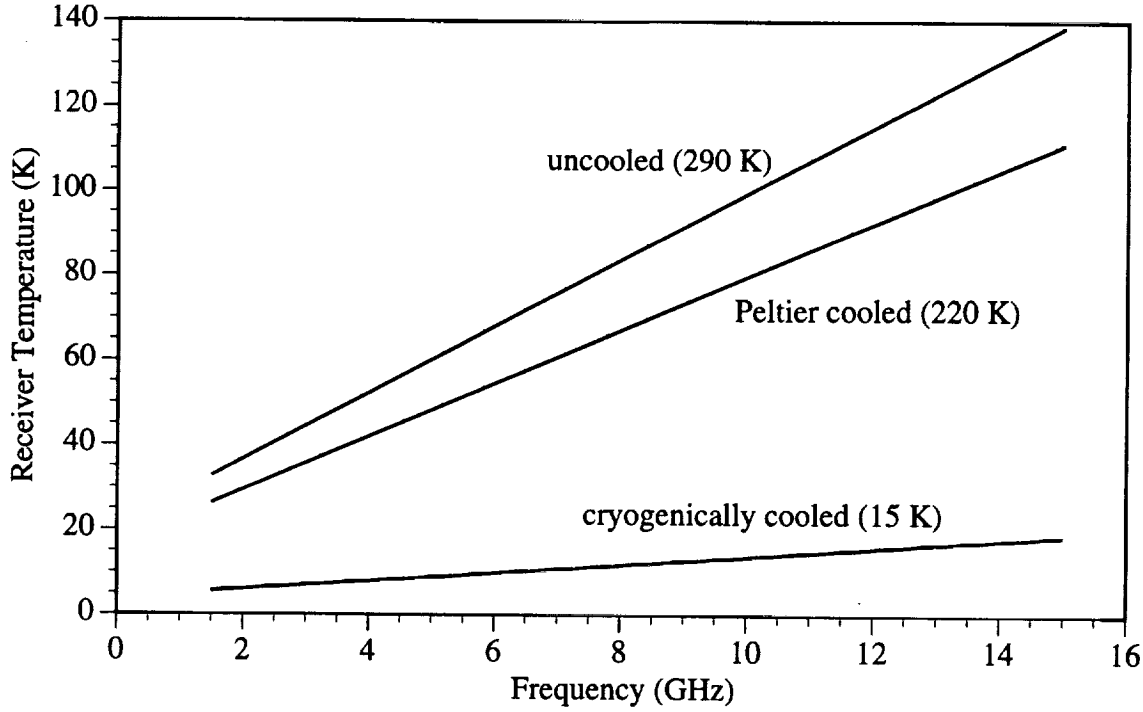

Figure 2-2. The HEMT amplifier noise performance versus frequency for 3 common cooling configurations, from Williams [1991].

C-2

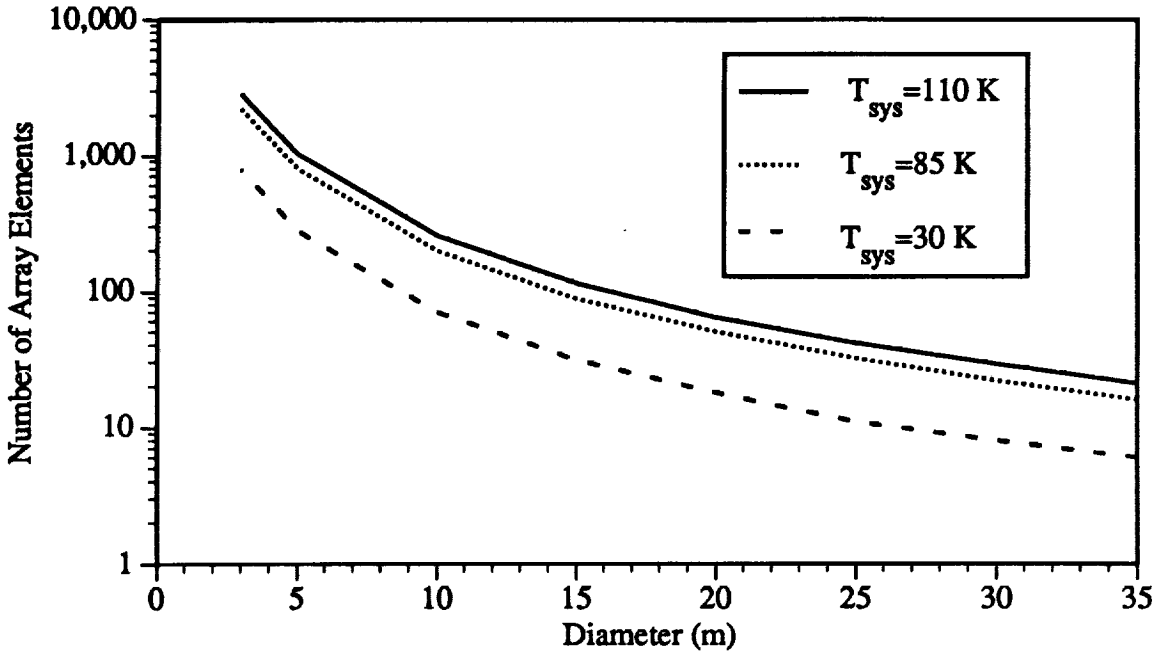

Figure 2-3. The number of array elements required to synthesize the G/T of a single 70-m aperture as a function of element diameter.

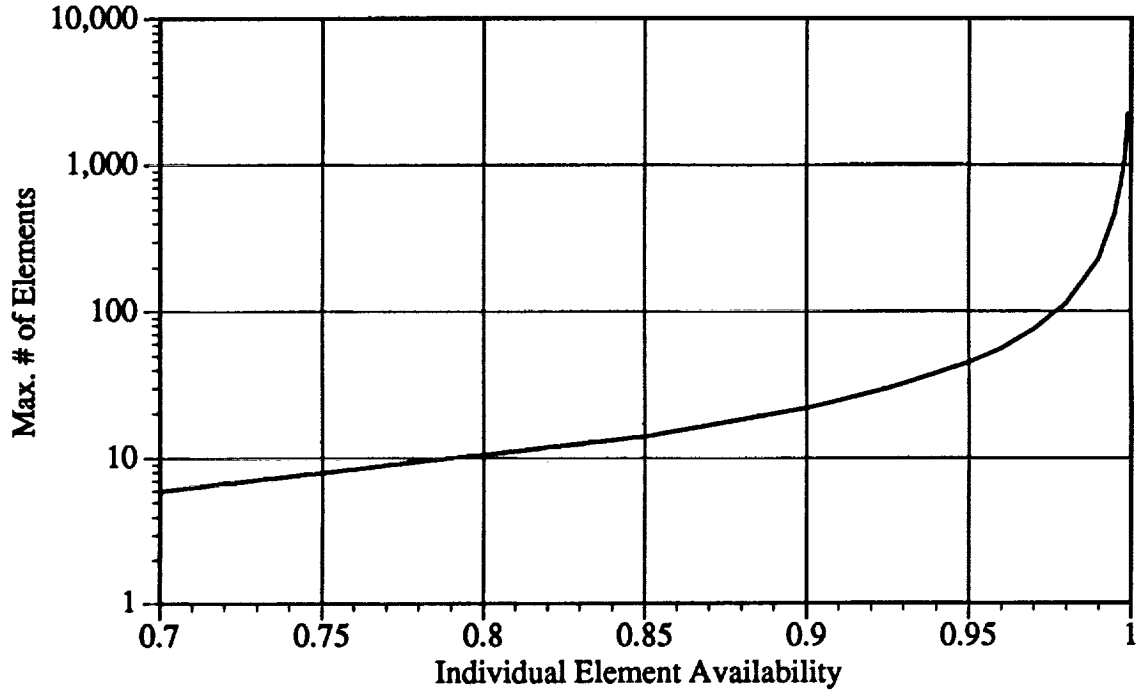

Figure 2-4. The number of elements in an array that provides maximum data rate (assuming no link margin) versus the individual element availability. Increasing the array beyond N_{max} would decrease the effective data rate because of element failures.

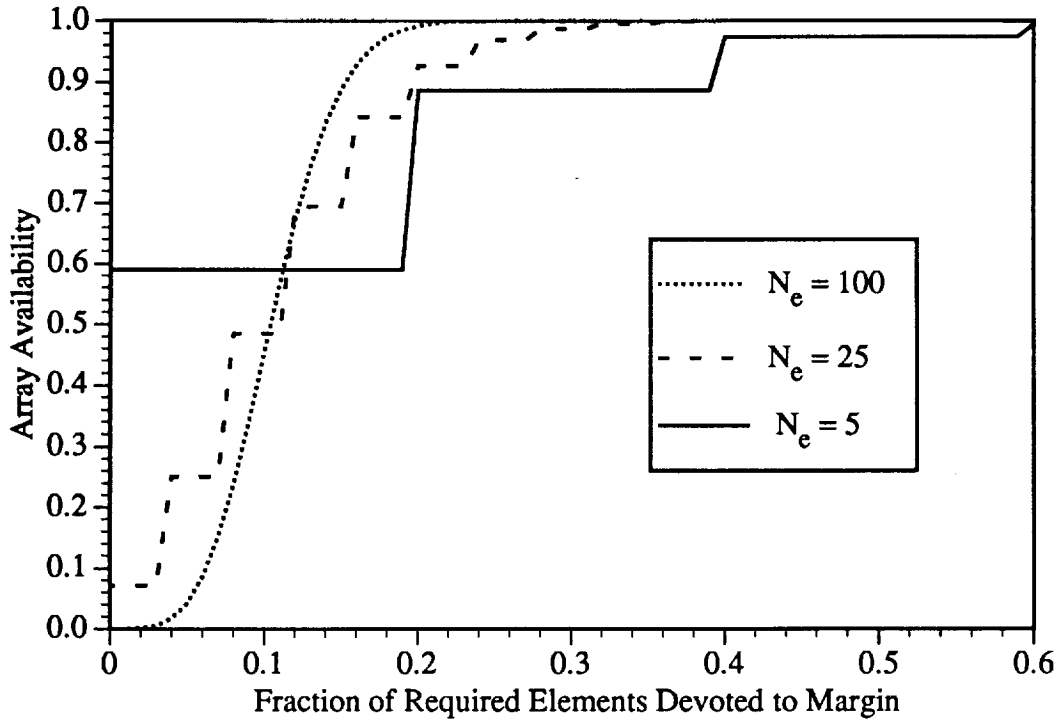

Figure 2-5. The array availability as a function of the number of additional elements devoted to margin, assuming an individual element availability of 0.9.

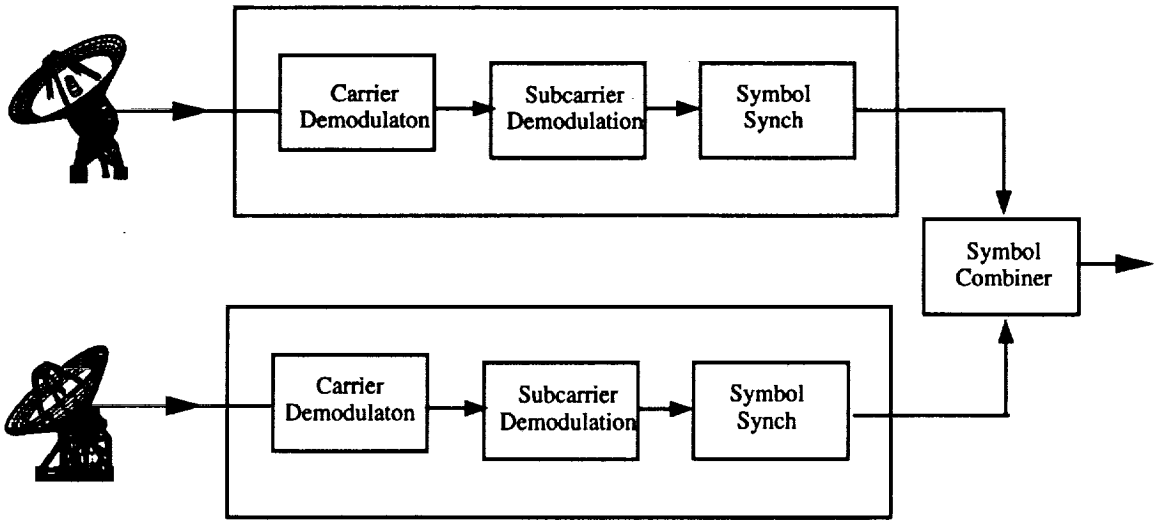

Figure 3-1. Block Diagram for Symbol Stream Combining.

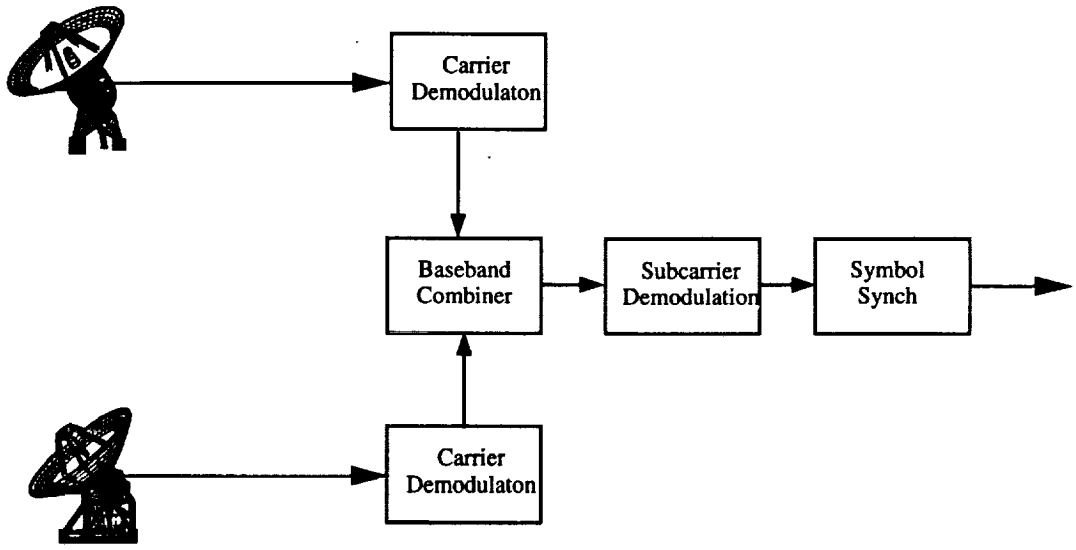

Figure 3-2. Block Diagram for Baseband Combining.

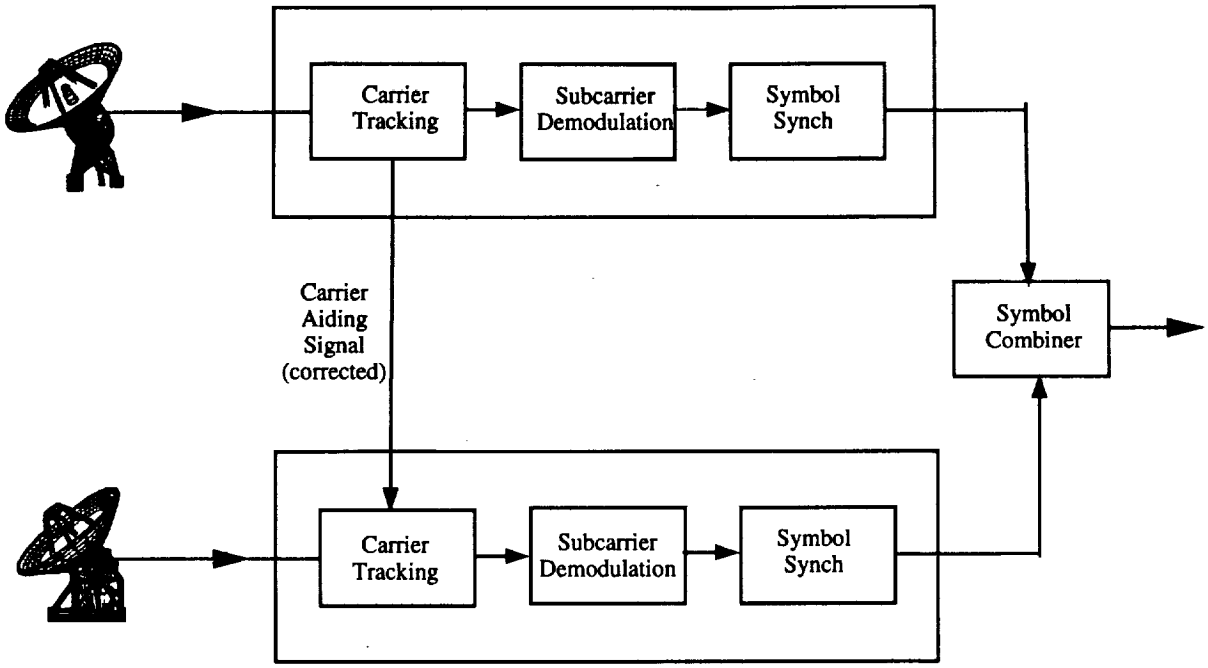

Figure 3-3. Block Diagram for Carrier Arraying.

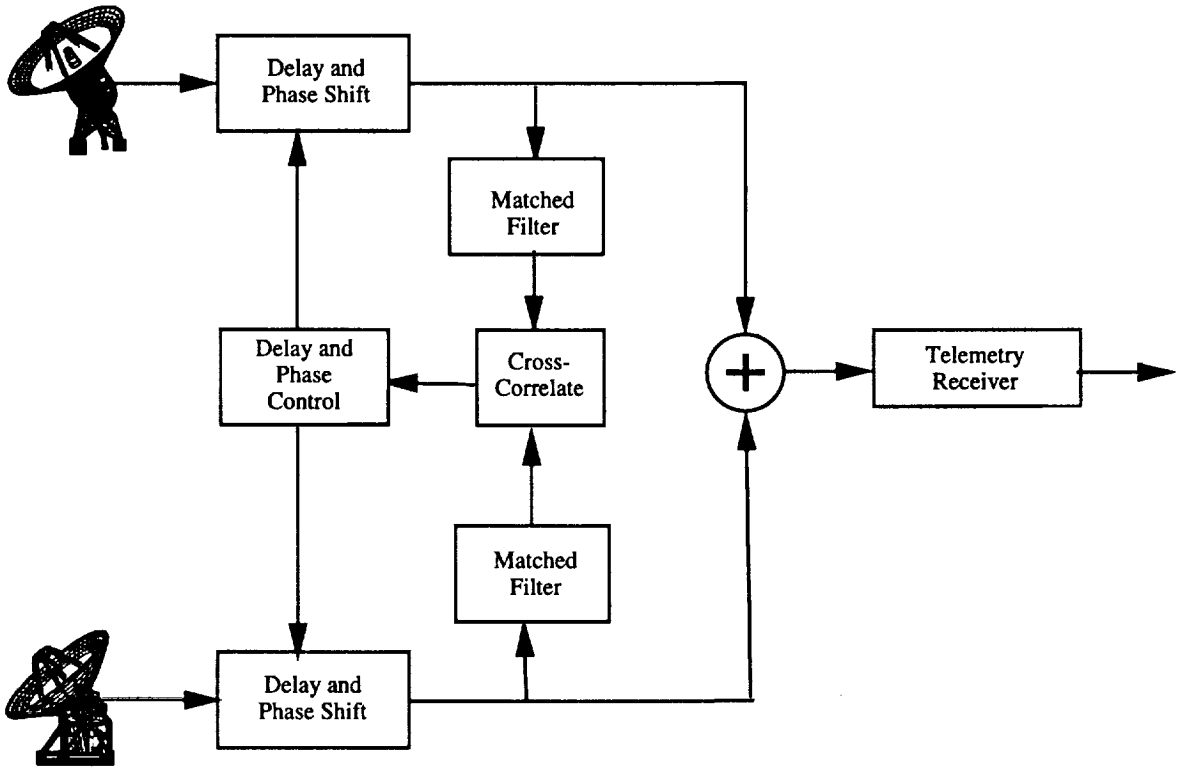

Figure 3-4. Block Diagram for Full Spectrum Combining.

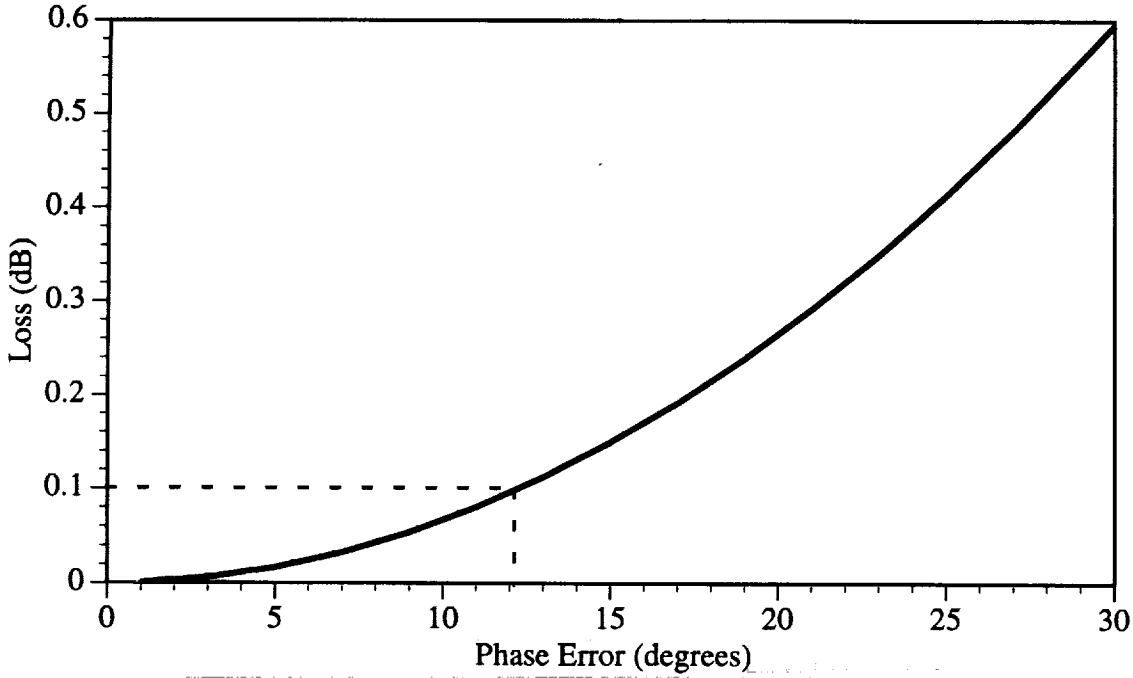

Figure 3-5. Combining loss for 2 array elements versus the phase difference between the elements.

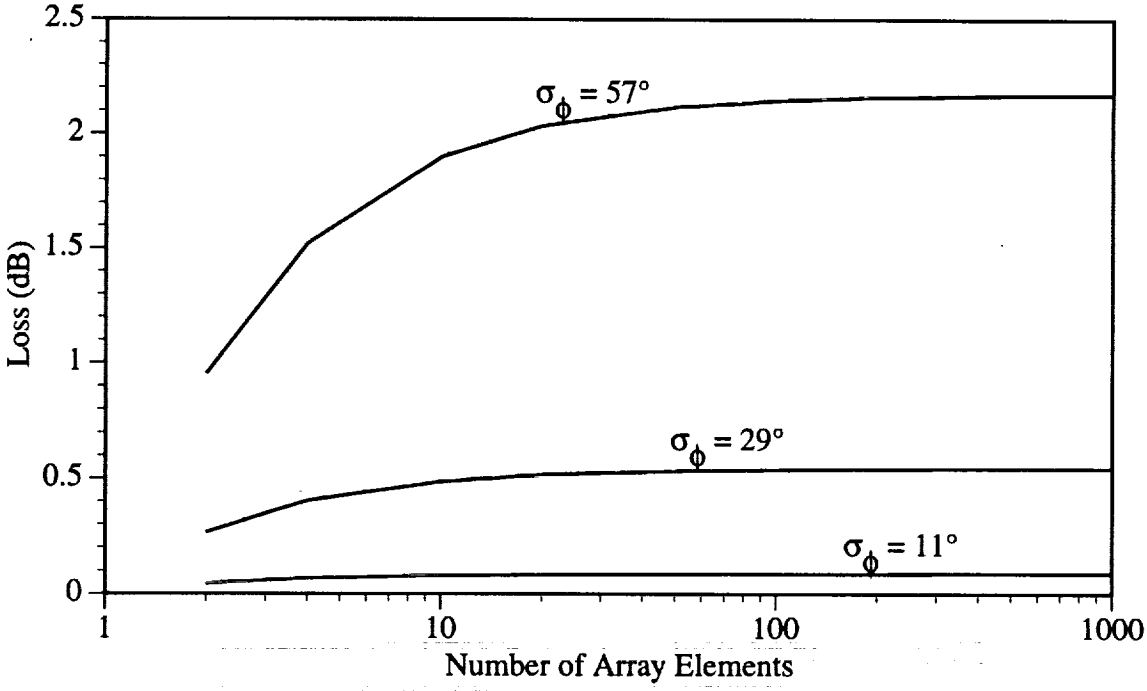

Figure 3-6. Combining loss for an array versus the number of array elements for three different values of average phase difference σ_ϕ.

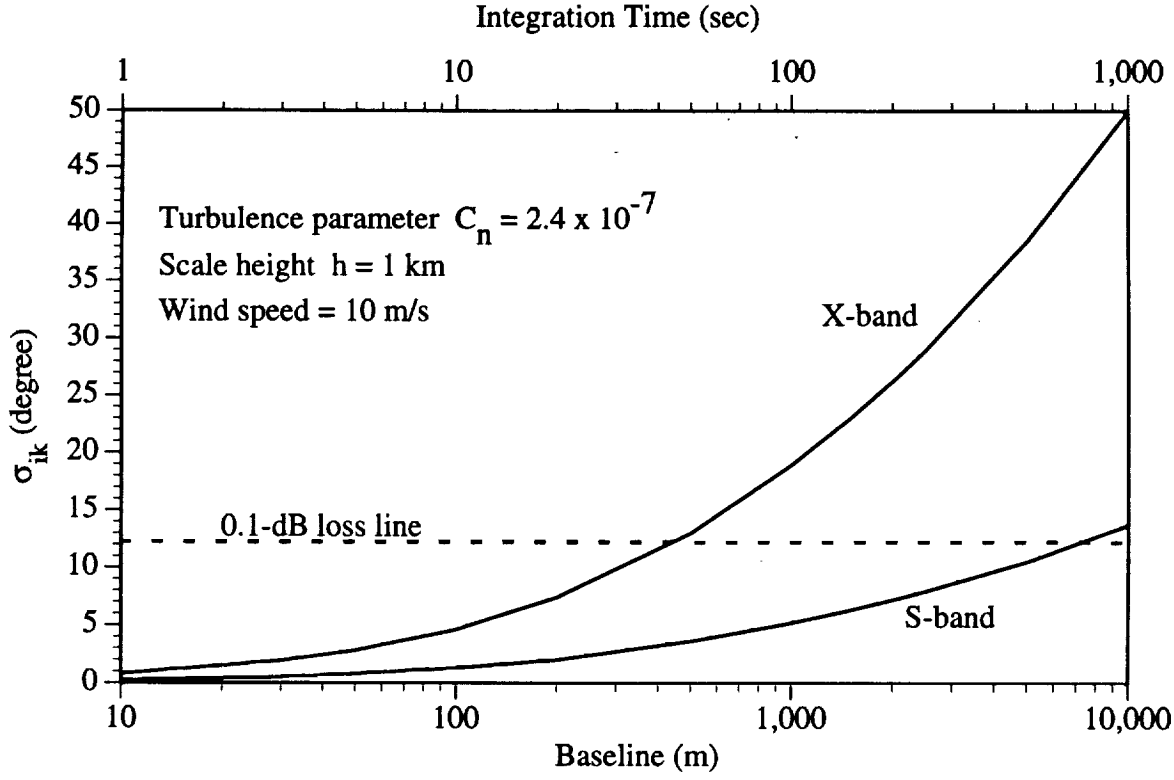

Figure 3-7. The standard deviation of the zenith phase difference between two array elements due to atmospheric fluctuation versus the baseline length. The bottom axis is the distance between the elements (i.e., the baseline) and the top axis is the integration time during which these fluctuations occur. A dashed line is drawn for 12° of phase error corresponding to 0.1 dB of gain loss.

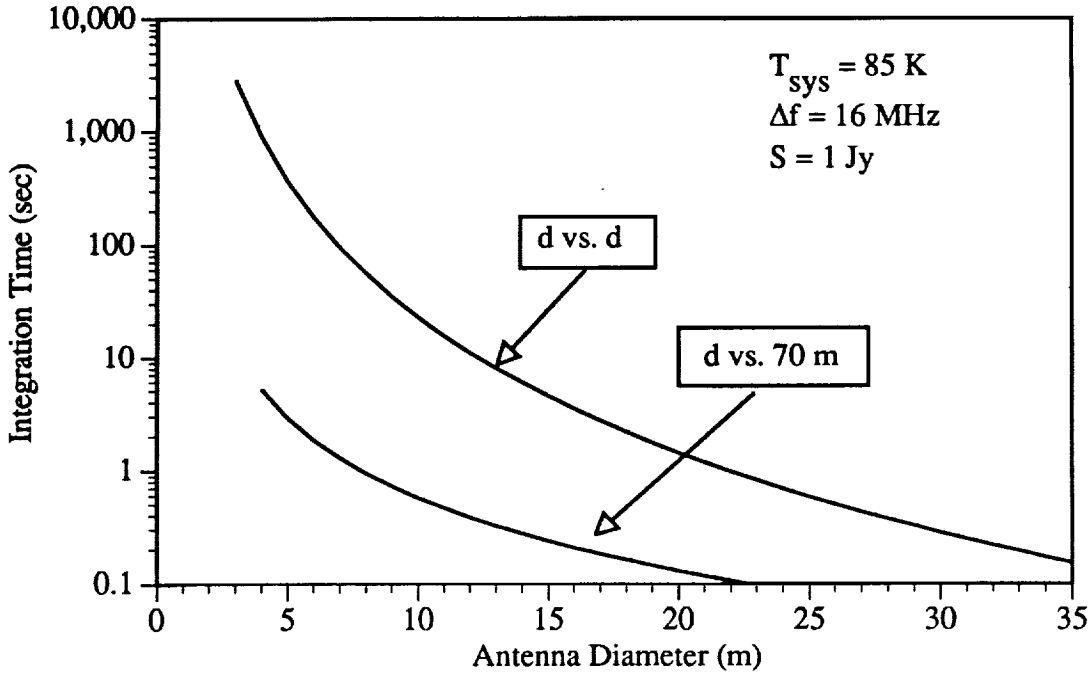

Figure 3-8. The integration time needed to achieve *snr* = 5 for two array elements vs. element diameter. In the first case both elements are assumed to have equal diameter (d vs. d) and in the second case one of the elements is assumed to be a 70-m antenna.

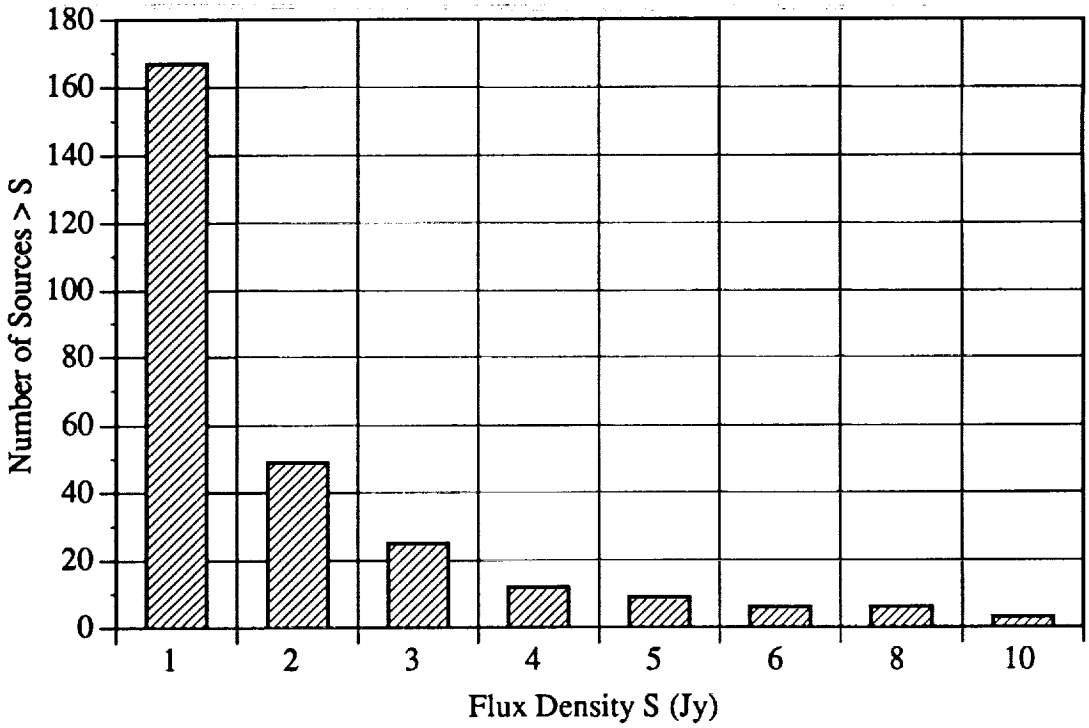

Figure 3-9. The number of compact radio sources visible from Goldstone greater than a given flux density (at X-band), from Patniak et al. [1992].

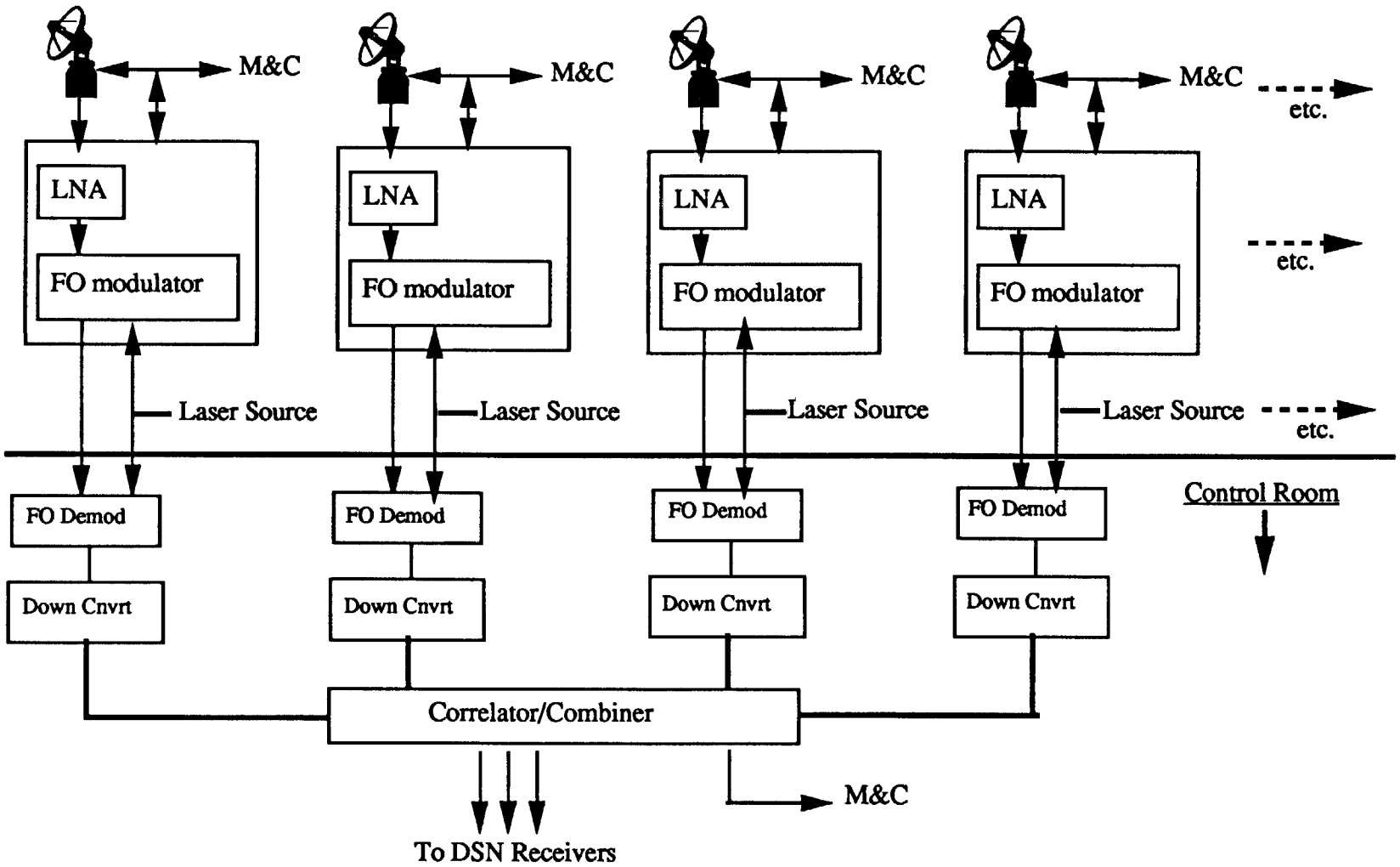

Figure 4.1-1. The system block diagram for a telemetry array.

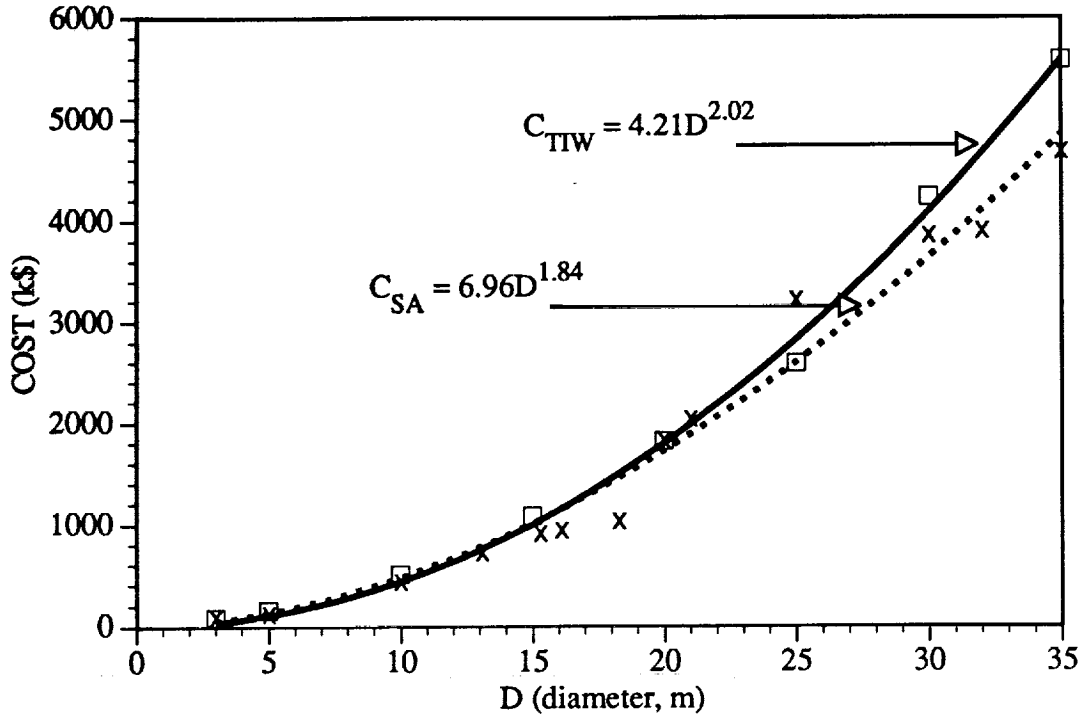

Figure 4.2-1. Recurring cost for an individual antenna versus antenna diameter and the best-fit power law function.

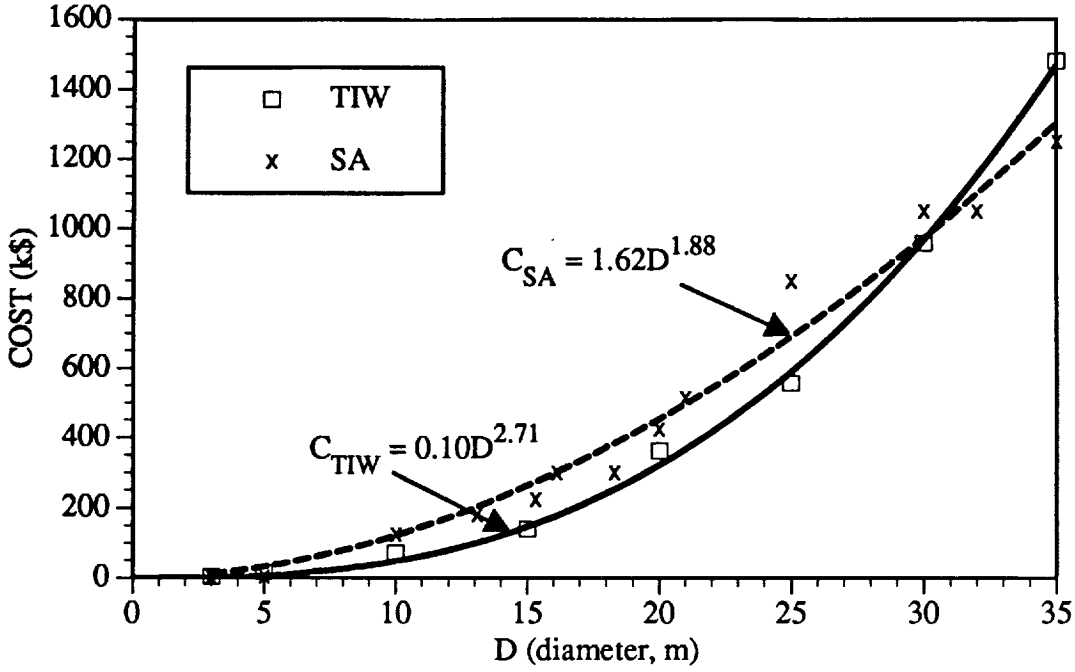

Figure 4.2-2. Cost and power law fit for the antenna support structure.

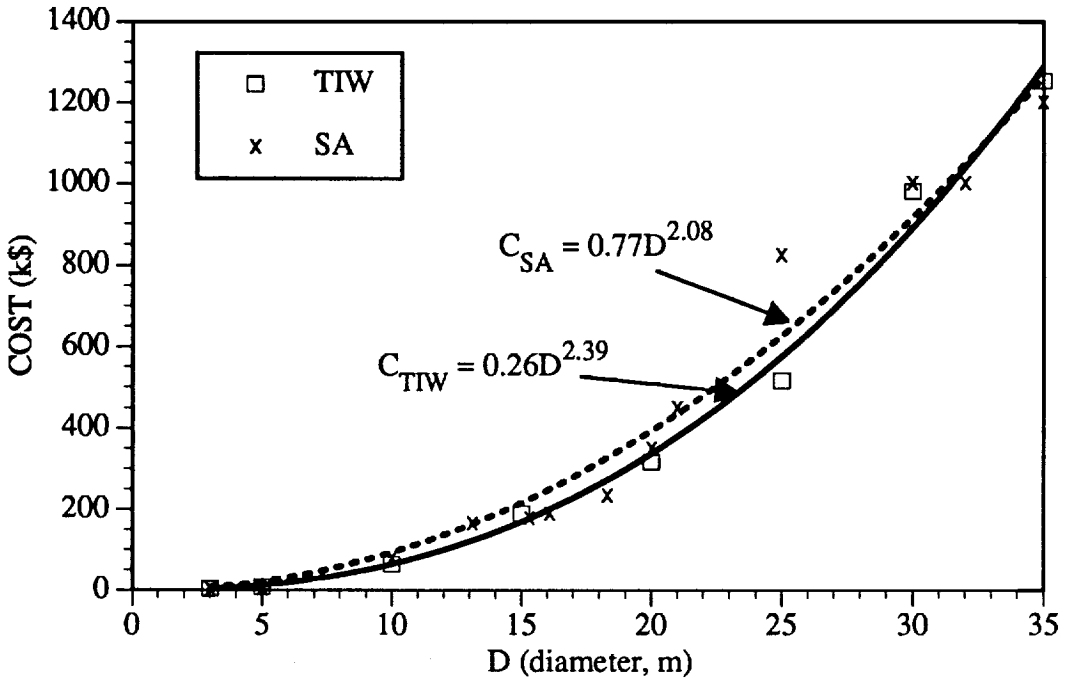

Figure 4.2-3. Cost and power law fit for the antenna reflector.

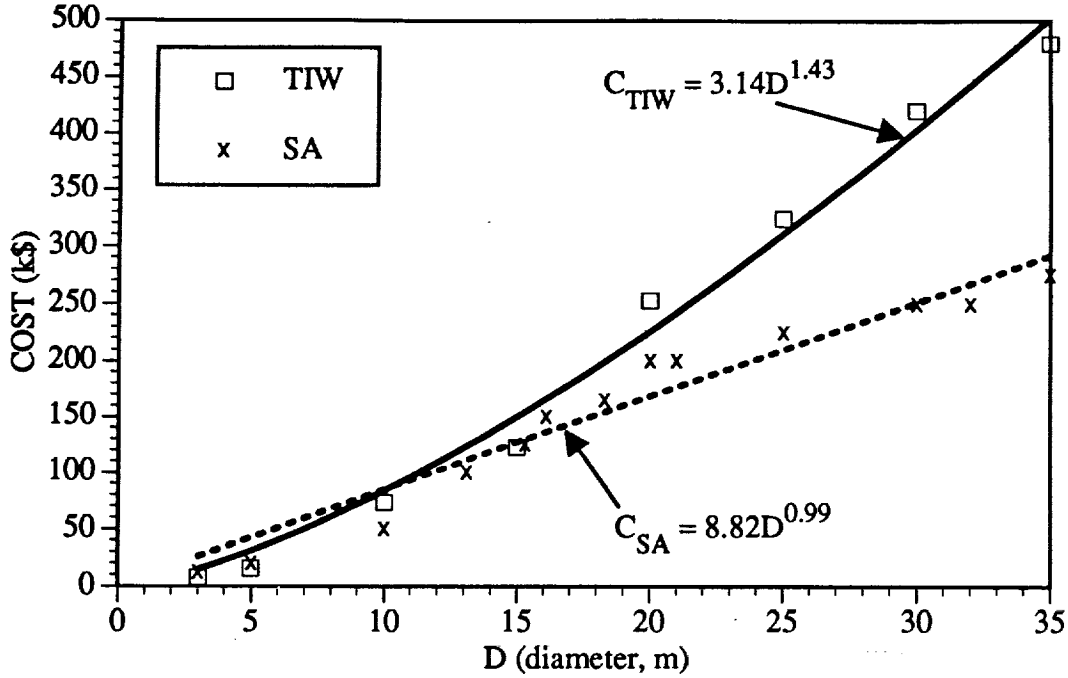

Figure 4.2-4. Cost and power law fit to the antenna axis drive data.

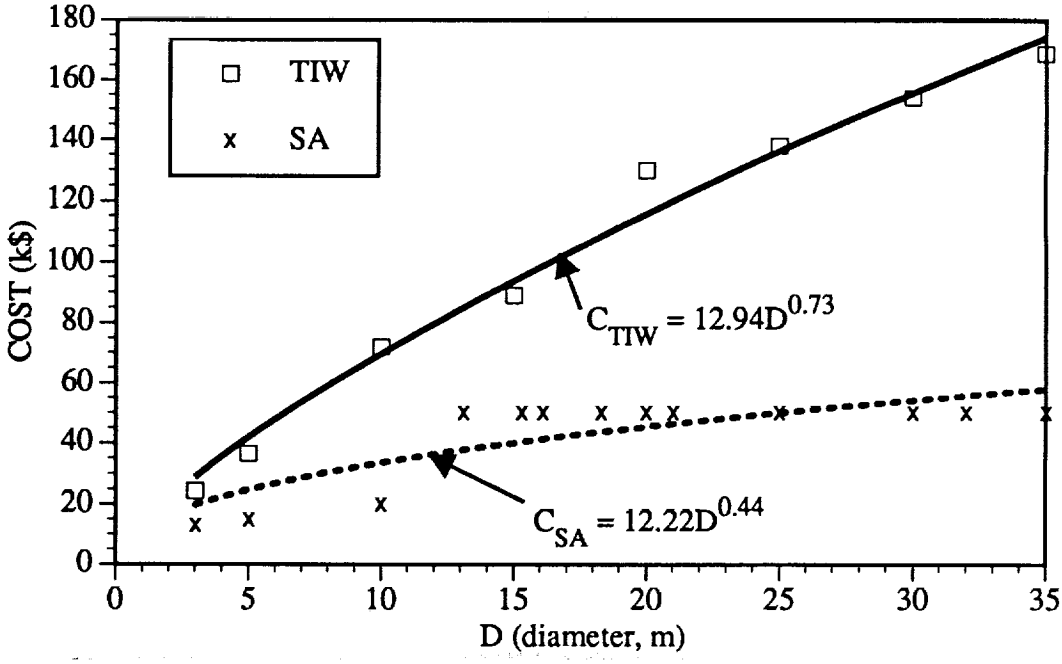

Figure 4.2-5. Cost and power law fit to the antenna position control data.

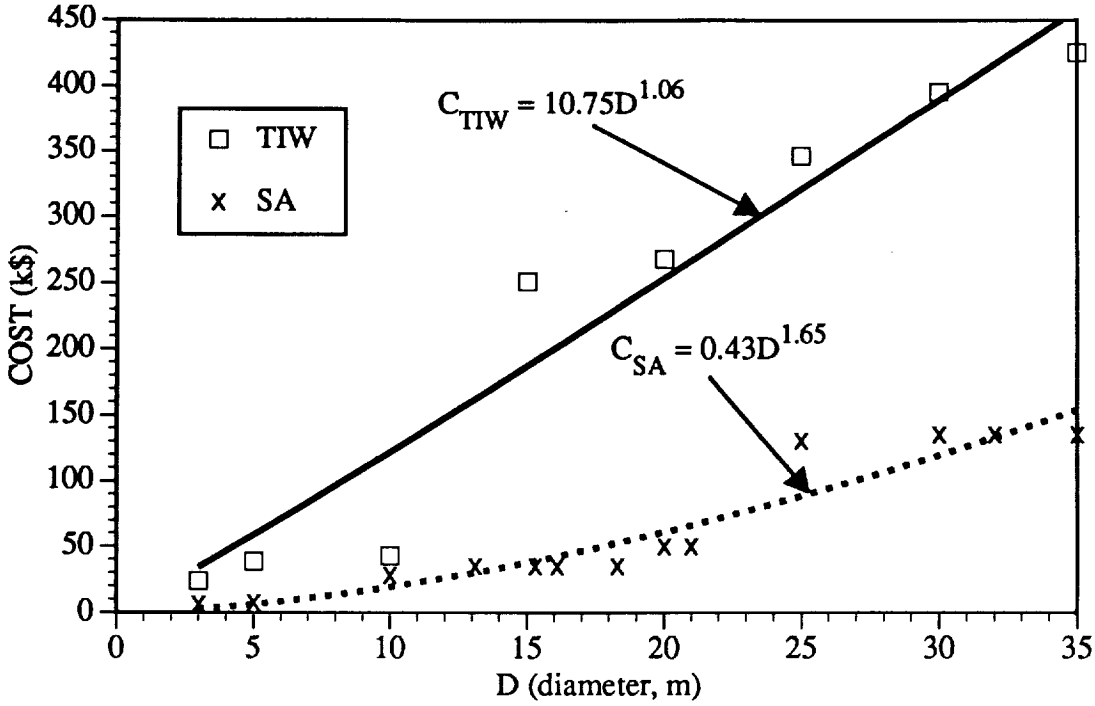

Figure 4.2-6. Cost and power law fit to the antenna feed data.

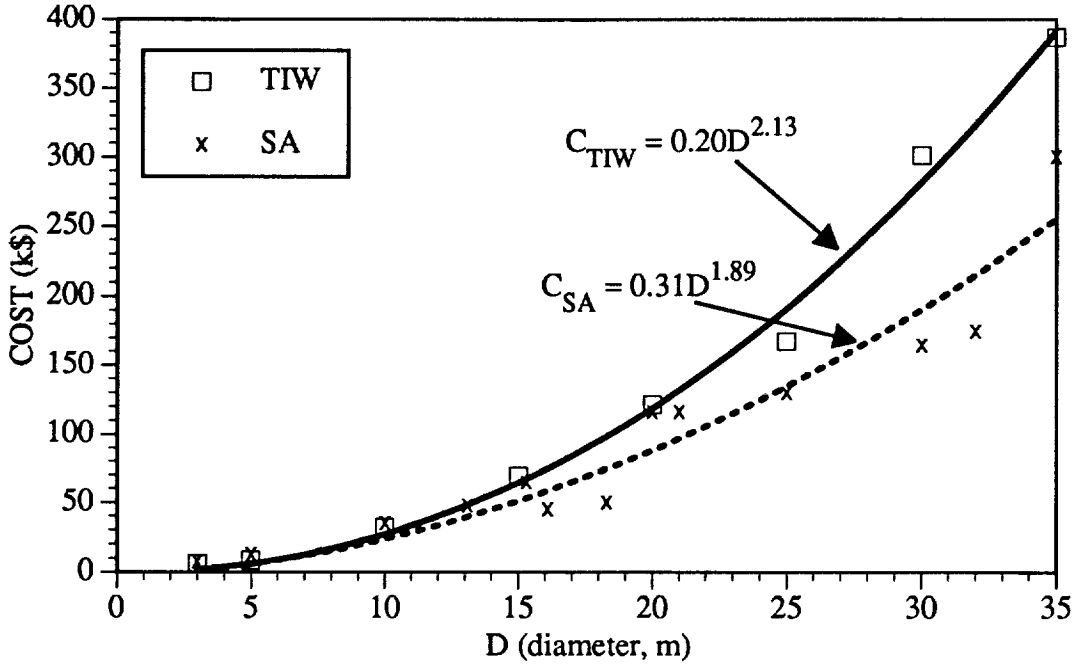

Figure 4.2-7. Cost and power law fit to the antenna foundation data.

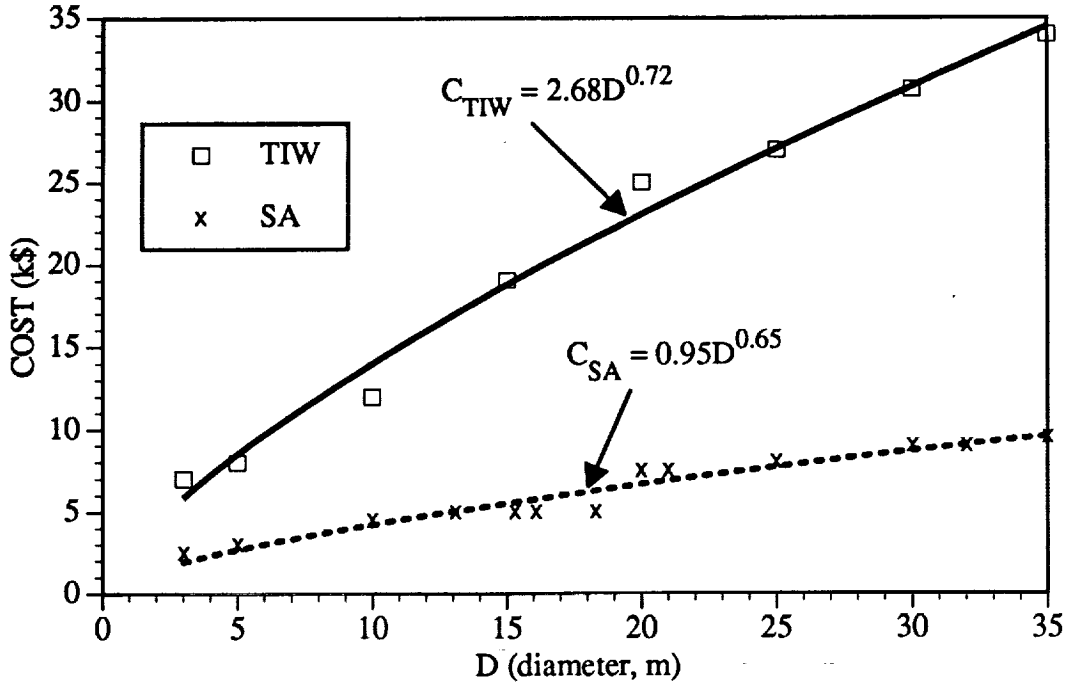

Figure 4.2-8. Cost and power law fit for the antenna power data.

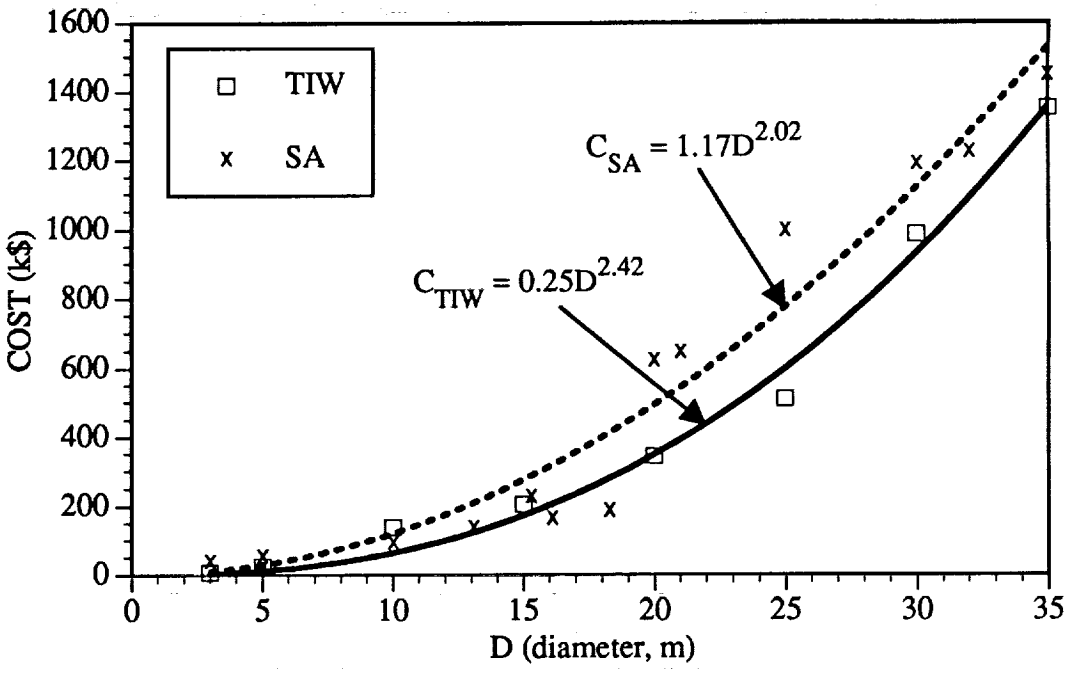

Figure 4.2-9. Cost and power law fit for the antenna shipping, installation, and testing data.

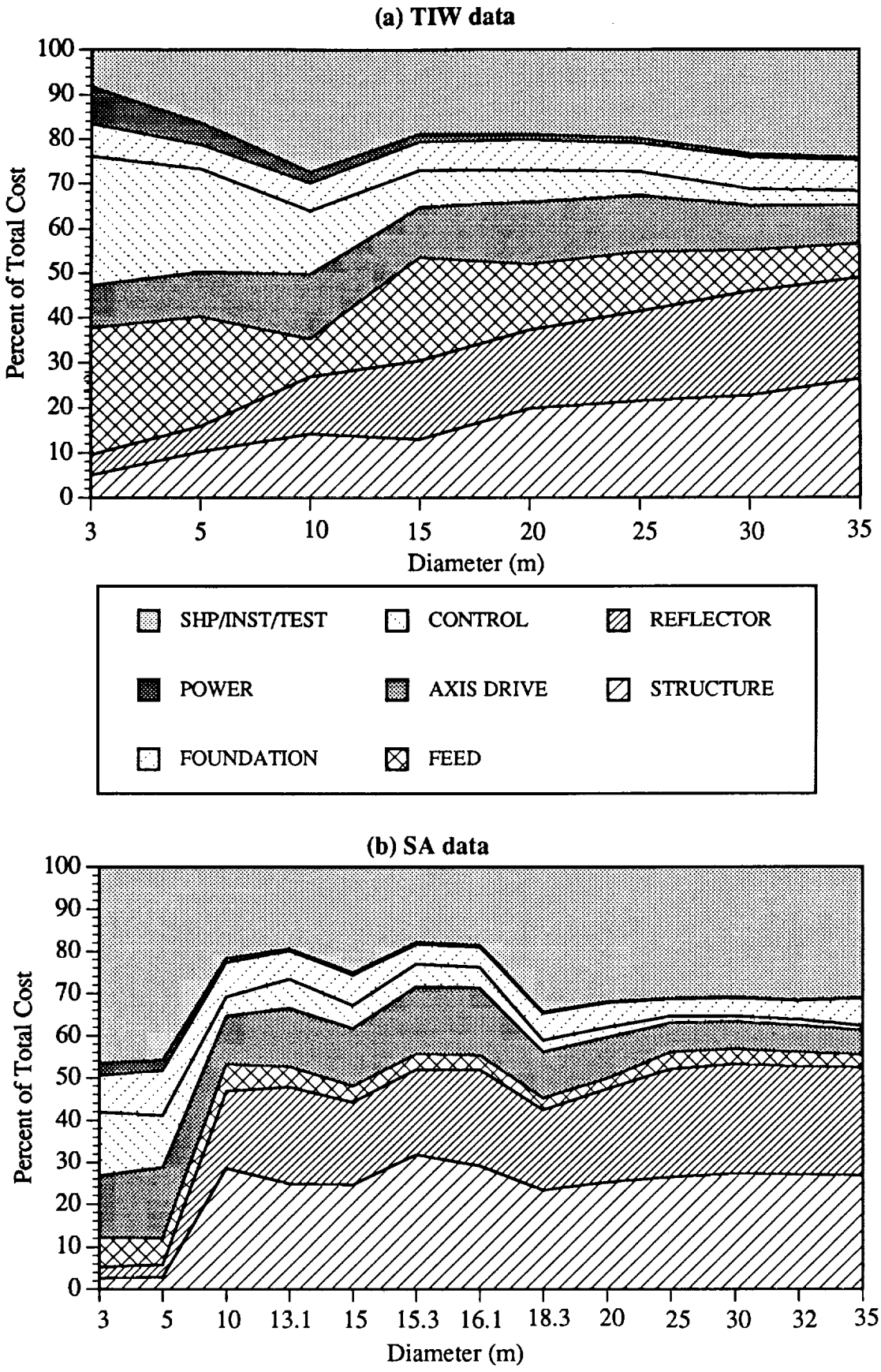

Figure 4.2-10. Cost breakdown by subsystem as a percentage of total antenna cost versus diameter for both TIW (a) and SA (b) data.

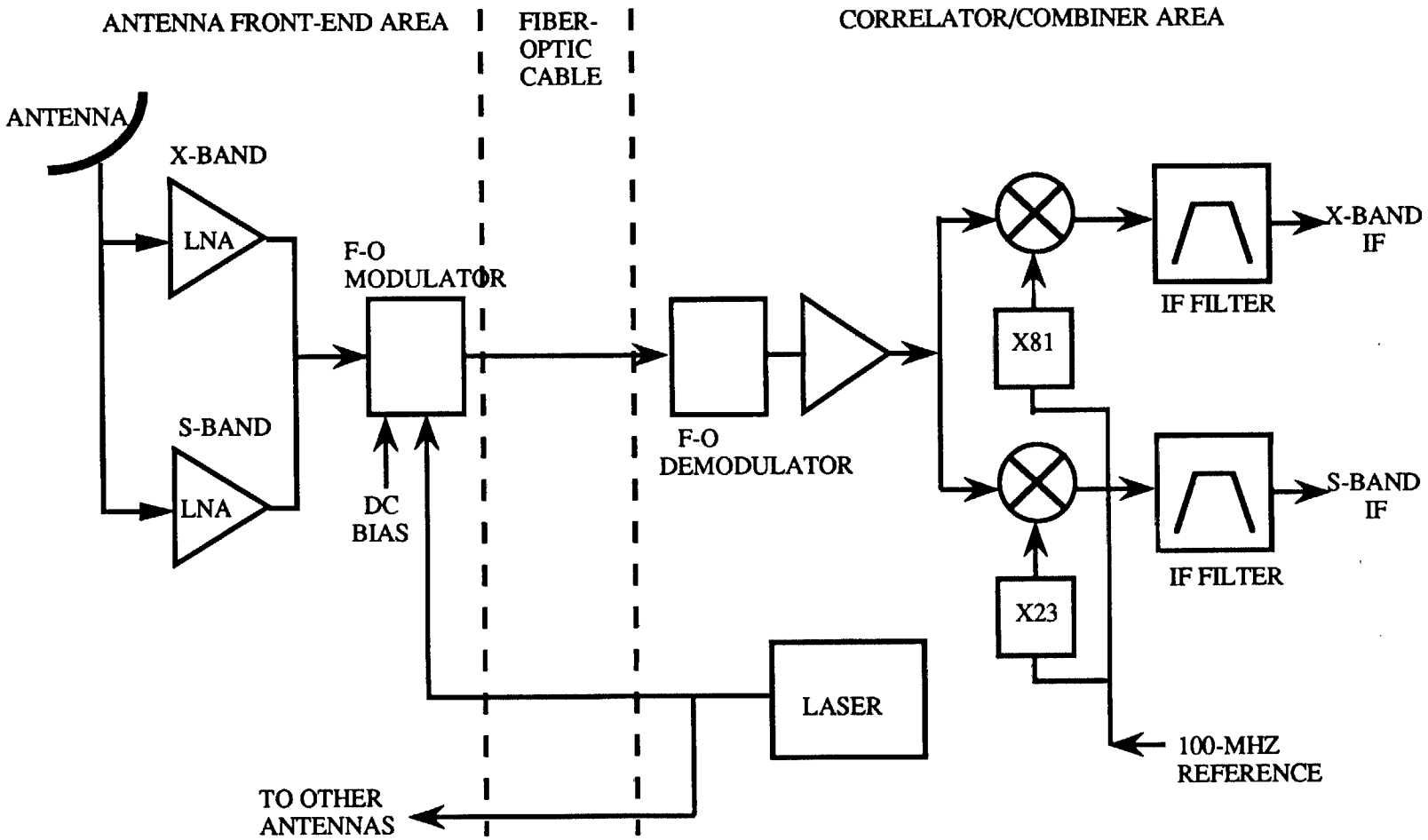

Figure 4.4-1. Architecture 4: The system block diagram showing direct RF transmission of the LNA output on analog fiber-optic link.

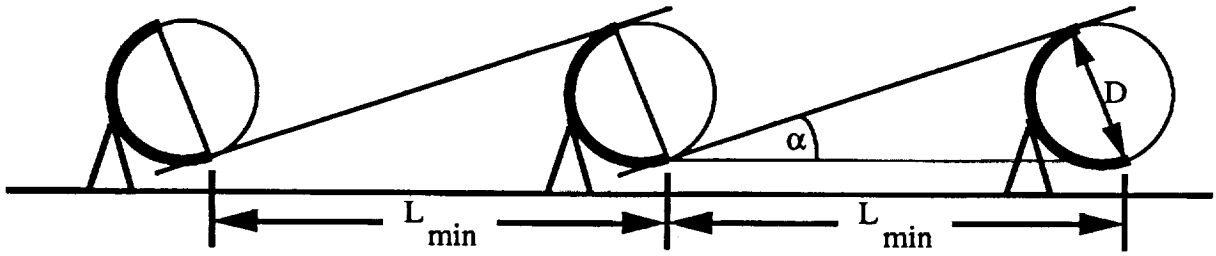

Figure 4.4-2. Geometry of the antenna shadowing constraint.

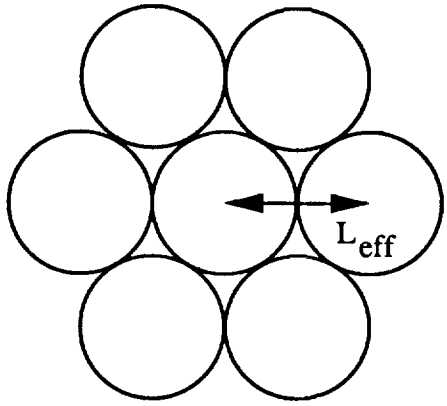

Fig. 4.4-3. The unit cell for the hexagonal close-pack array layout, often referred to as a first-order Gosper snowflake. The distance between centers L_{eff} is determined by the shadowing constraint.

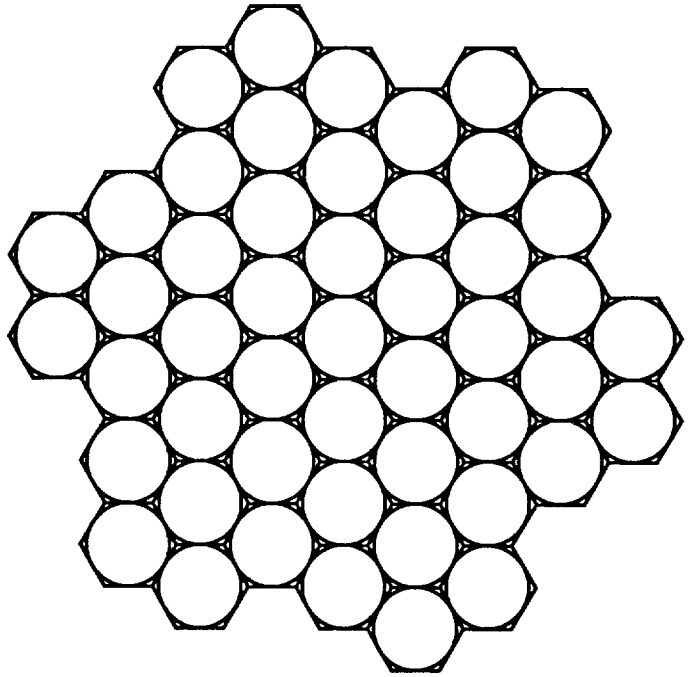

Figure 4.4-4. A second-order Gosper snowflake (49 elements) comprised of seven first-order snowflakes.

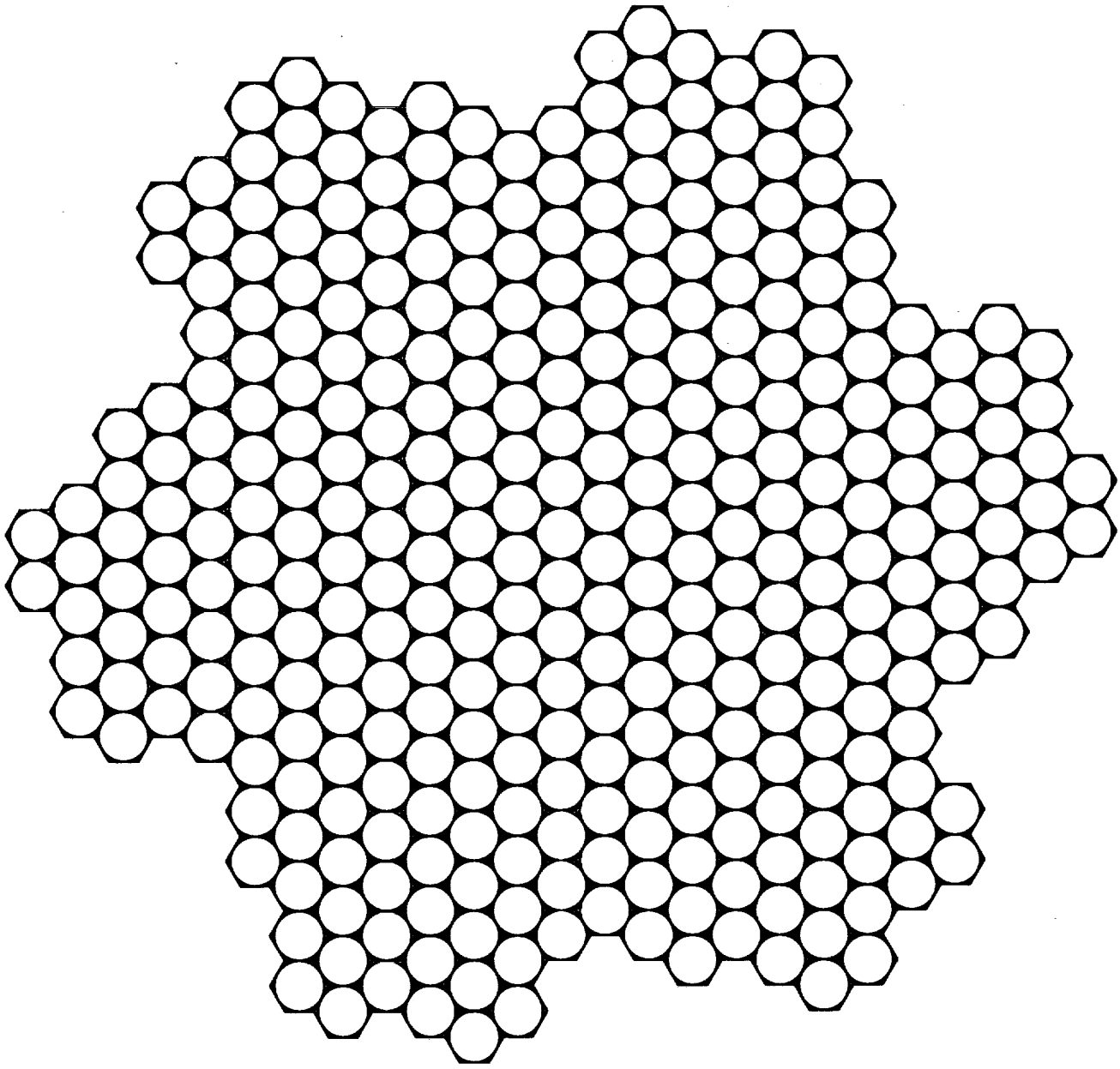

Figure 4.4-5. A third-order Gosper snowflake consisting of 343 elements.

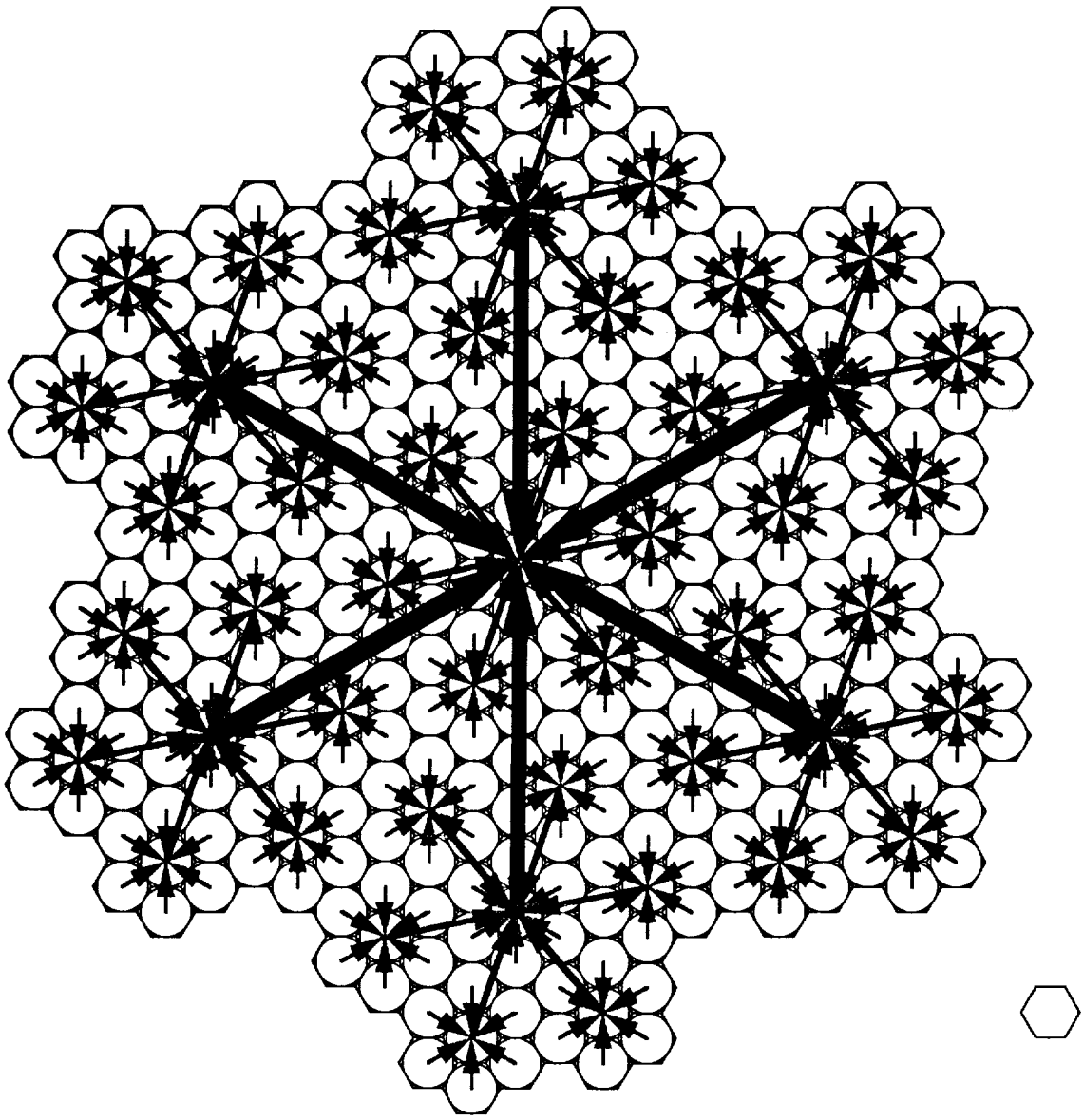

Figure 4.4-6. Cable routing for the third-order Gosper snowflake array geometry. Note that the interconnecting lines do not cross, indicating that direct cable burial is possible.

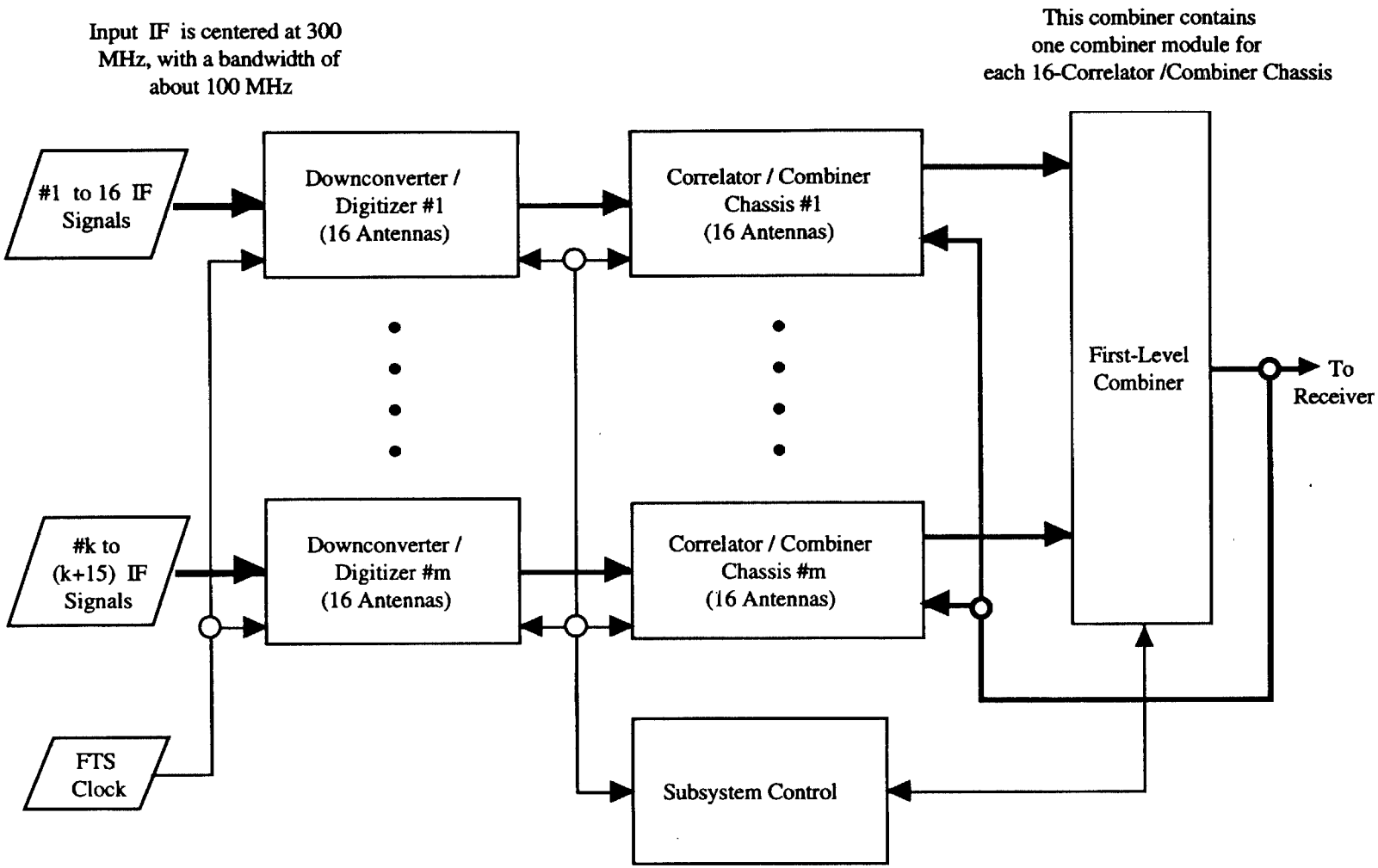

Figure 4.5-1. Block Diagram of the Correlator and Combiner Subsystem.

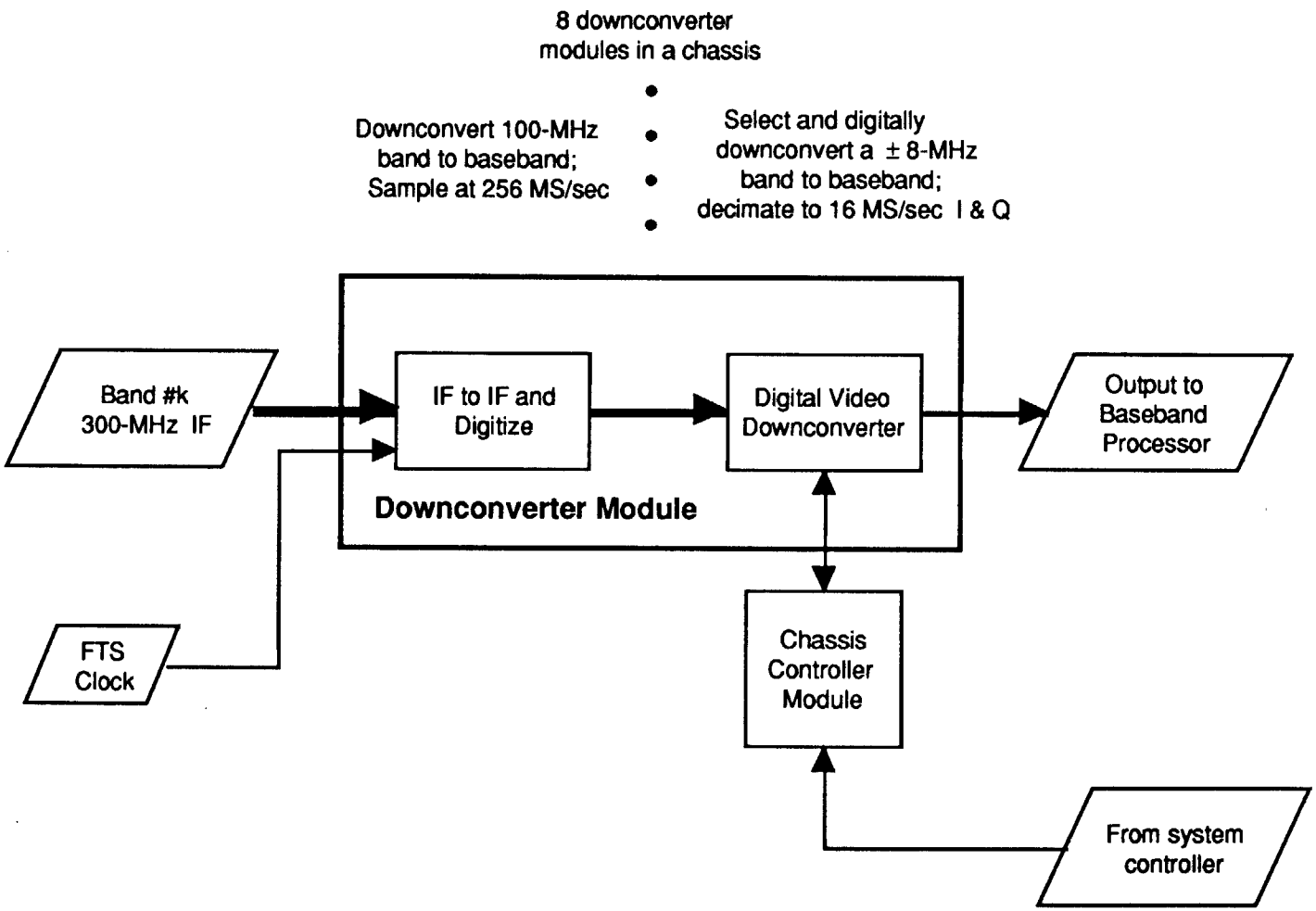

Figure 4.5-2. Block diagram of the downconverter module.

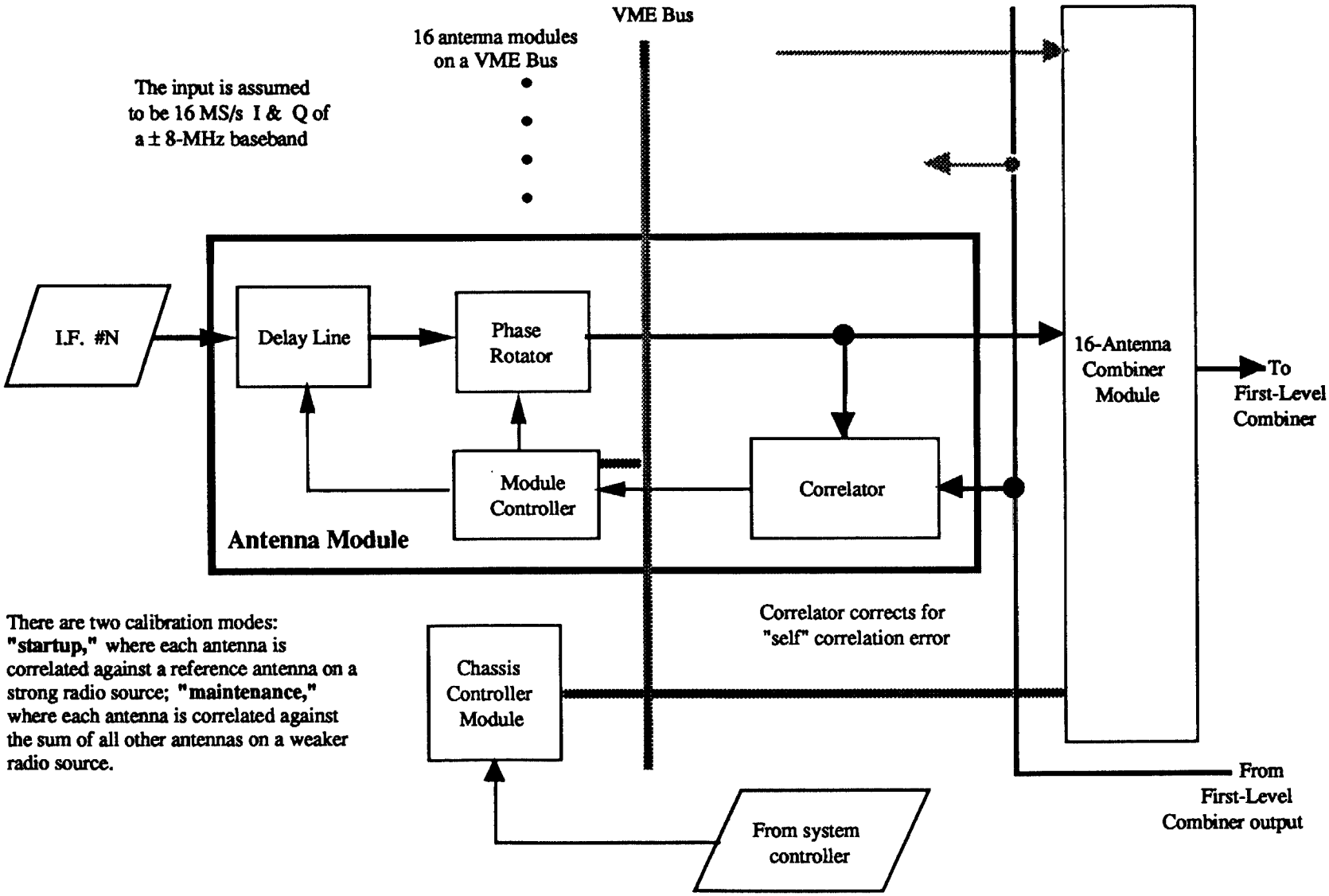

Figure 4.5-3. Block diagram of the correlator module per antenna.

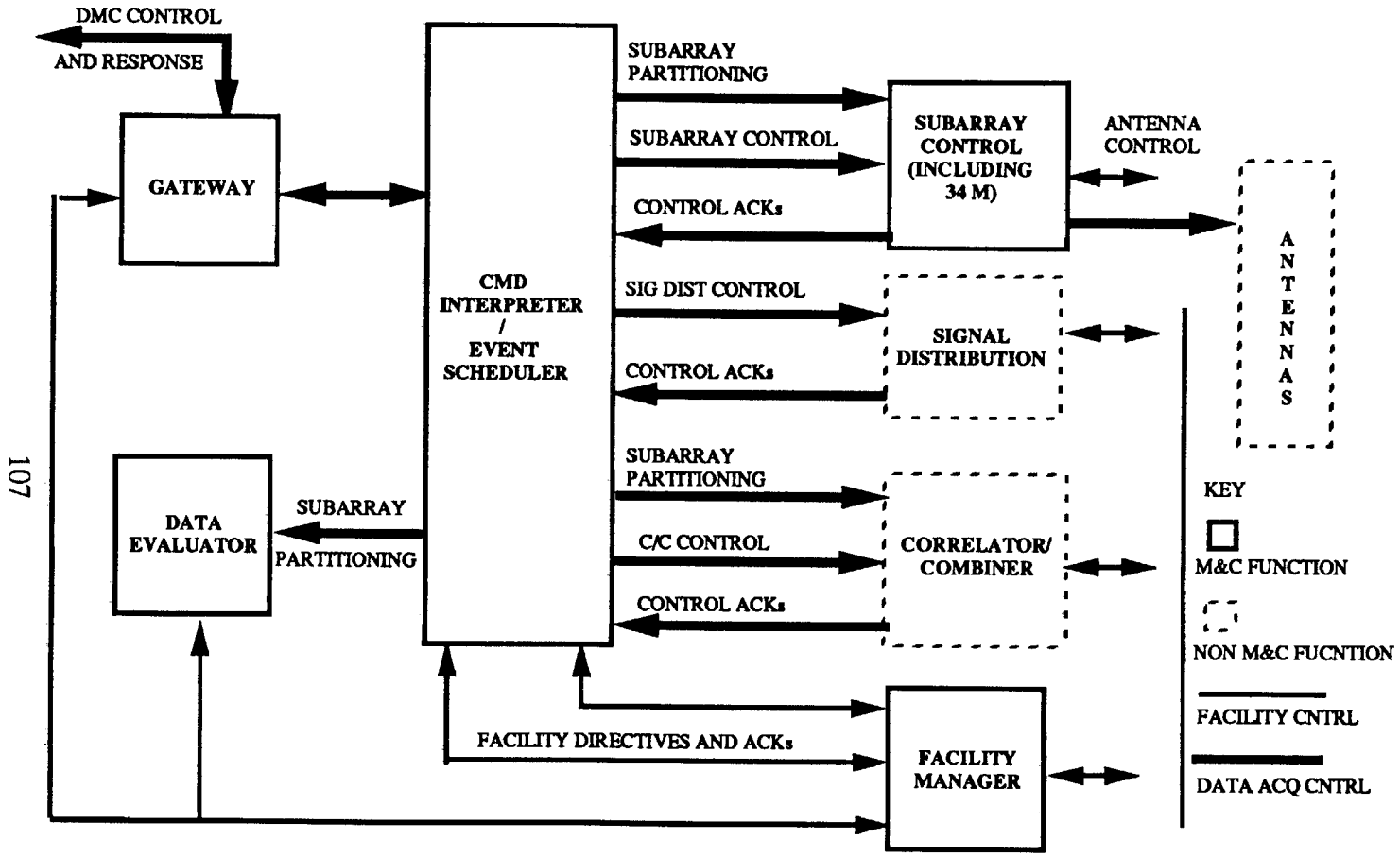

Figure 4.6-1. Control paths in the Monitor & Control subsystem.

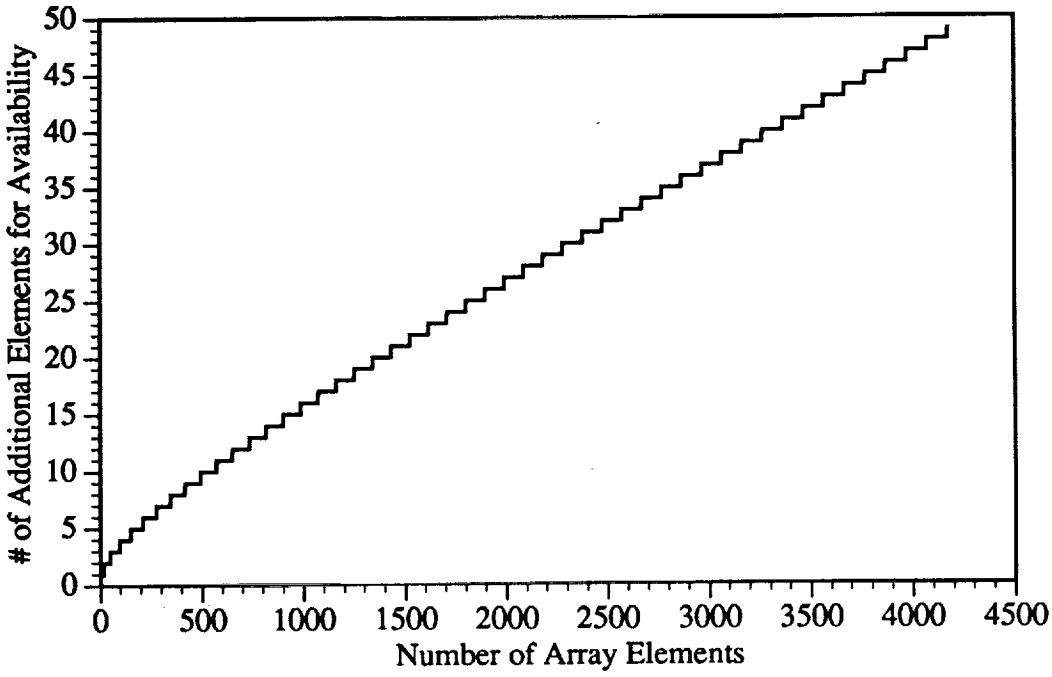

Figure 4.7-1. The number of extra array elements needed to make the array availability equal to or greater than the single element availability of p=0.992.

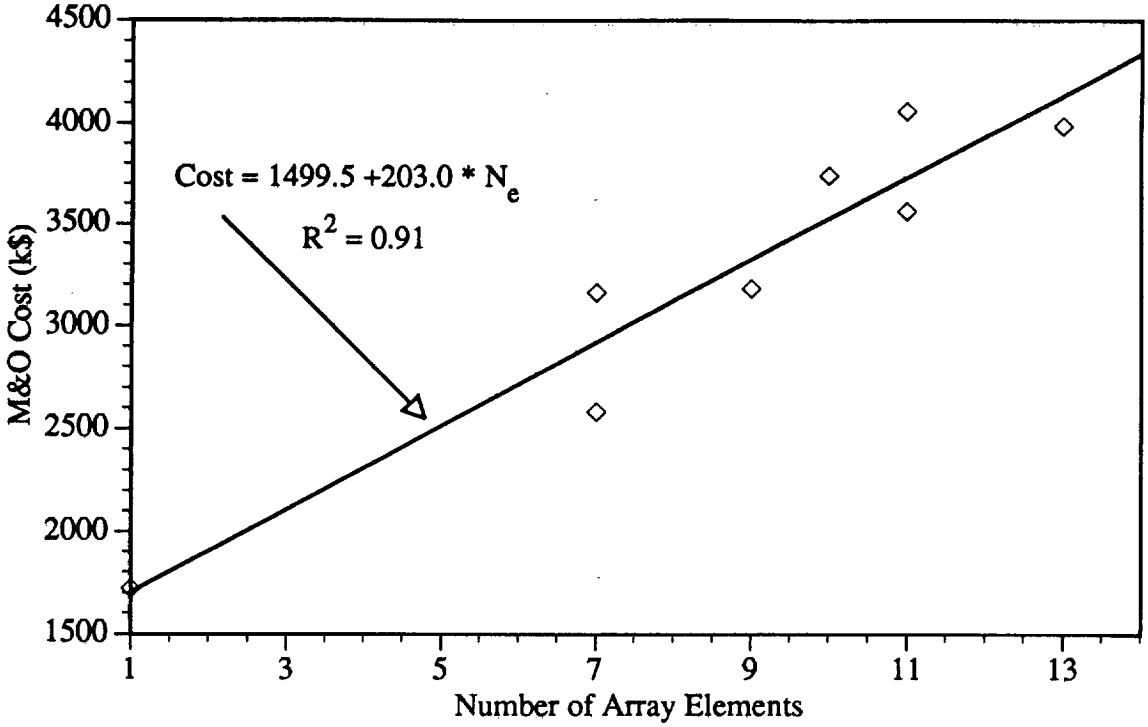

Figure 4.9-1. M&O costs as a function of the number of array elements (from the LAAS study).

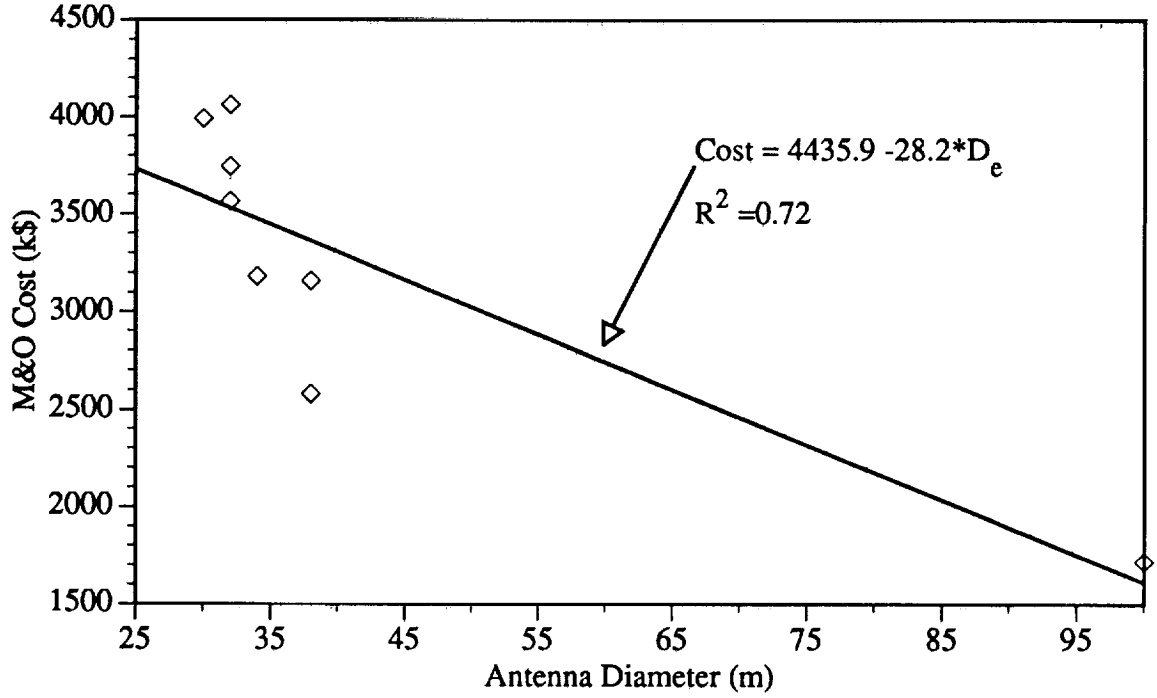

Figure 4.9-2. M&O costs as a function of array element diameter (from the LAAS study).

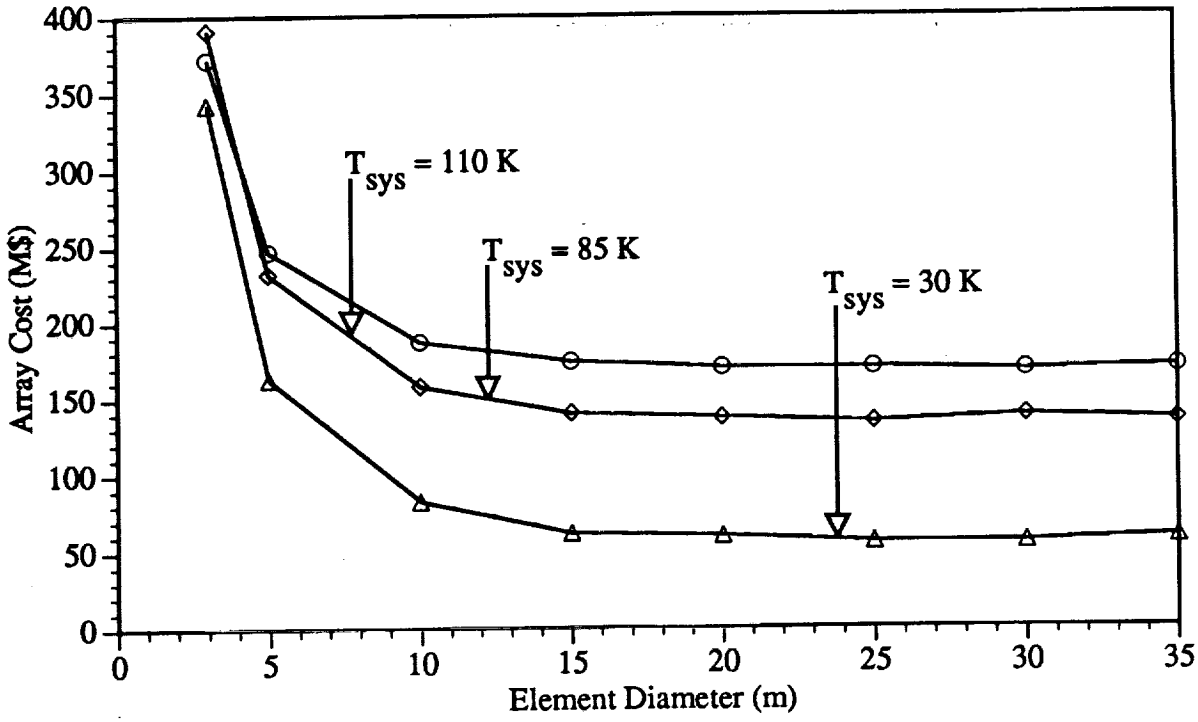

Figure 5-1. Total system cost as a function of antenna element diameter for an array that synthesizes the G/T of a DSN 70-m antenna at X-band.

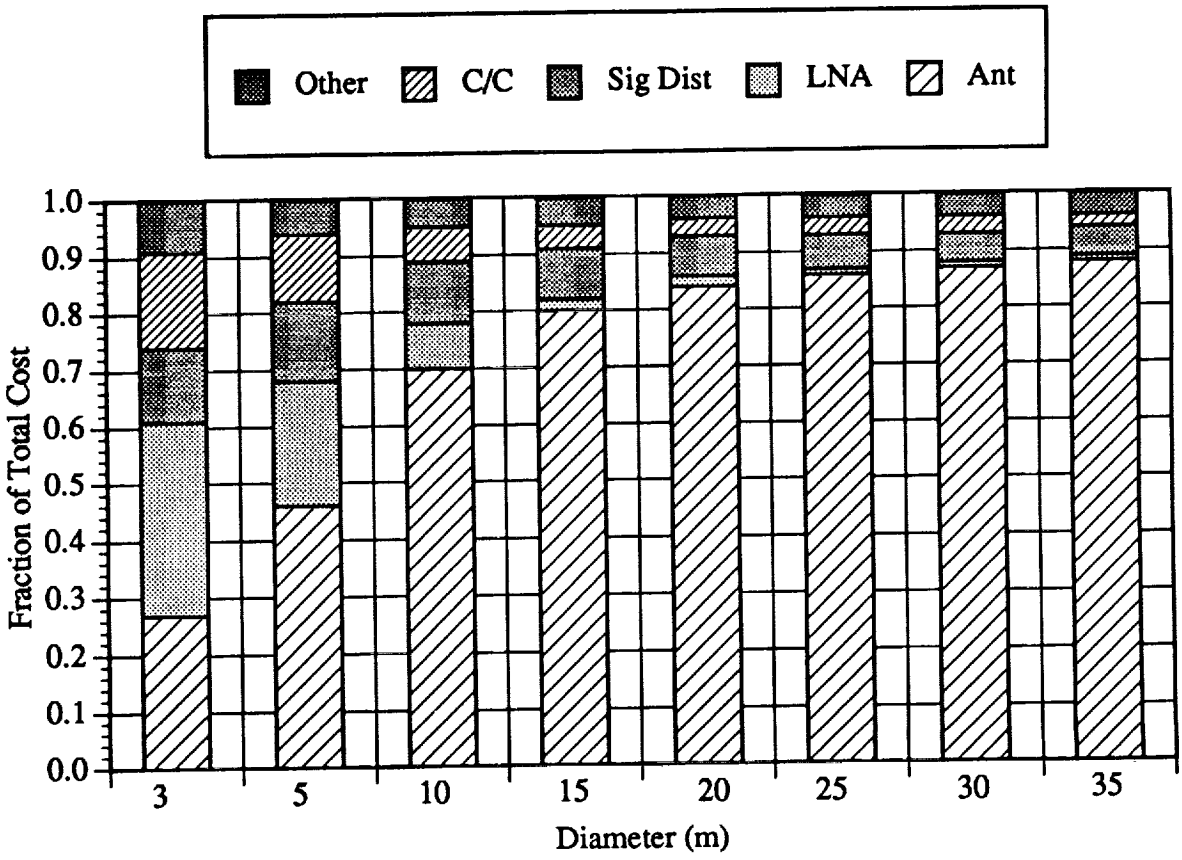

Figure 6-1. The fractional subsystem cost versus antenna diameter.

APPENDIX A
CONTRACTOR STATEMENT OF WORK

This is a summary of the STATEMENT OF WORK (dated Sept. 1992) that was sent to two contractors that had previously supplied antennas to the DSN. The final statement of work was modified by the JPL Procurement Office to include contractual details and cost.

I. PURPOSE

Jet Propulsion Laboratory is currently engaged in a study to develop a quantitative understanding of the performance, cost, and technical risks associated with synthesizing a large aperture from an array of smaller aperture antennas. The array will be a receive-only system, operating simultaneously at S-band and X-band. This Small Aperture Array Study will parameterize costs of the entire array as a function of the antenna element diameter for a prescribed G/T (gain divided by system noise temperature). As a benchmark, the prescribed G/T will be that of a small number (one to three) of Deep Space Network 70-m antennas. Costs for the complete system will be parameterized. These include the antennas, radio and intermediate frequency amplification, signal distribution, combiner electronics, and the monitor and control needed to operate the array in a synchronous fashion. (Further background information was included in the JPL Study statement attached to the Statement of Work.) This Statement of Work outlines a cost study of the antenna elements to be performed by TIW Systems, Inc.

II. NUMBER OF ANTENNAS, OPTICS, AND COST BREAKDOWN

The number of antennas needed to synthesize the G/T of a 70-m antenna is a function of the antenna diameter and system noise temperature. Shown in Table A-1 is the range of the number of antennas needed for the eight diameters considered in this study. This range allows both cooled and uncooled amplifiers to be parameterized, as well as a range of G/T for 1 to 3 different deep space stations.

The antenna optics are broken into two regimes. For small-diameter antennas, a frequency selective subreflector is used to separate S-band, arranged as a prime focus system, from X-band, arranged as a Cassegrain system. For larger diameter antennas, both bands operate as a Cassegrain system, with the bands separated by either a dual-frequency (concentric) feed, or a frequency-selective surface diplexor. It is expected that the break will occur in the range of 10- to 20-m antenna diameters.

Antenna costs are to be broken into the following categories:

(A) Structure

(B) Main Reflector Surface

(C) Axis Drive
(D) Position Control
(E) Foundation
(F) Shipping and Installation
(G) Feed System (including possible frequency selective surface)
(H) Power Supply

Table A-1. Minimum and Maximum Antennas

Diameter (m)	Units	
	Minimum	Maximum
3	545	27,000
5	196	10,000
10	49	2,500
15	22	1,100
20	12	615
25	8	394
30	5	274
35	4	201

The specific tasks to be completed are as follows:

- For each diameter in Table A-1, production techniques will be investigated and a preferred design in each category will be specified.
- The design will include specifying antenna optics for each diameter size, based on cost, manufacturability, and performance.
- Each category will be further divided into nonrecurring and recurring costs.
- Because of the large number of antennas that could be fabricated (especially at the smaller diameters), it is expected that an economy of scale will be encountered. This cost study should outline breakpoints in production where costs drop for a given diameter as more antennas are fabricated.
- As part of the JPL Small Aperture Array Study, a probabilistic determination of the number of antennas needed to maintain a prescribed G/T margin is being calculated for a given array and reliability of antenna elements. To assist in this calculation, this cost study should outline antenna components which critically affect reliability and detail the costs of critical components as a function of reliability.

III. PERFORMANCE REQUIREMENTS

The performance requirements are summarized in Table A-2.

IV. DELIVERABLES AND SCHEDULE

Following the agreed commencement date,

A. There will be a conference of TIW and JPL personnel after 3 weeks to discuss and clarify issues developed in the study.

B. A final conference of TIW and JPL personnel after 6 weeks will be held to discuss results of the study.

C. The final report will be delivered after 6 weeks.

Table A-2. Performance Requirements

Parameter	Specification
Operating Frequency	From S-Band to X-Band
Axis Coverage: Elevation Azimuth	 0° to 90° ±200°
Reflector Surface	Solid aluminum
Environments: Precision Operation: Wind Rain Temperature Normal Operation: Wind Rain Temperature Survival: Wind Seismic Hail Temperature Drive-to-Stow	 10 mph gusting to 12 mph 2 inches per hour 0°F to 115°F 30 mph gusting to 36 mph 2 inches per hour 0°F to 115°F 100 mph (stowed) 0.3 G horizontal and 0.15 G vertical Up to 1 inch diameter stones –20°F to 180°F 60 mph
Maximum Tracking Rates: Velocity Acceleration	 0.4°/sec $0.4°/sec^2$
Maximum Slew Rates: Velocity Acceleration	 0.4°/sec $0.2°/sec^2$
Site Location	Australia
Soil Conditions	3,000 psf bearing capacity at 3 feet below grade (no piles required)
Axis Configuration	Elevation over Azimuth
Pointing Accuracy: Precision Operation Normal Operation	 0.1 beamwidth 0.2 beamwidth
Surface Accuracy: Precision Operation Normal Operation	 0.030 inch RMS 0.035 inch RMS
Concrete Foundation	Minimum height (no building room required)

APPENDIX B
ANTENNA AVAILABILITY IN THE DSN

The DSN defines the availability of a system A_T, as the percentage of time that the system produces the required data for **scheduled** support. Thus, the downtime required for scheduled maintenance is not counted. One might imagine a situation in which a very old antenna requires 6 days/week of maintenance in order to be "available" for a single day. Therefore, the availability is only related to the reliability. However, when defined in this way the availability has the great virtue of being directly measurable.

Normally a spacecraft link is supported with a single antenna and a string of many other subsystems along a serial data path. Failure of any subsystem that results in loss of data requires the generation of a Discrepancy Report (DR) that is kept in a database. It is this database that we will use to estimate the availability of various subsystems rather than DSN Document 810-5 [1991], which lists specifications. The reader should keep in mind the limitations of the data. For instance, when an antenna fails for some long period of time, the tasks that were assigned to it are re-scheduled for another antenna and the availability as it is used here does not suffer. Clearly, the availability as defined above is at most an upper bound on the reliability, but they are the only data that are readily available.

The DR database is analyzed by Donald Custer of the Allied Signal Corp. and published periodically in thick books titled "DSN Performance Study: Telemetry Data Loss" [1993, 1990] that cover a period of time on the order of 2–3 years. Tables B-1 and B-2 summarize the DR data by subsystem for two periods. Table B-1 contains the data spanning the period 1 Jan. 1986 to 31 Jul. 1990, and Table B-2 covers the period 1 Jan. 1989 through 31 Dec. 1992. Both tables cover all DR types and all flight projects that were scheduled for the telemetry data type. However, Table B-1 contains data from all of the antennas in the DSN whereas Table B-2 contains the data from the 70-m and 34-m networks (i.e., DSSs 16, 46, and 61 are not included). It has been noted by others that the availability of the DSN is a function of time, typically increasing during such critical events as planetary encounters and decreasing during cruise periods.

The first column of each table contains the 3-letter acronym for the subsystem. The subsystem name appears in the second column for those readers who are unfamiliar with the acronyms. The third column lists the number of hours of data that was lost, according to the DR's count. At the bottom of this column, these hours are summed to give the total hours of data that were lost and the overall system availability. The cumulative availability is listed in column 4. For each subsystem row, the cumulative probability is calculated by summing the hours lost for the particular subsystem to the top of the table, dividing the sum by the total hours that were

scheduled, and subtracting this ratio from one. The last column in the table is the individual subsystem availability, i.e., the product of which yields the total system availability.

There are several things worth noting in these tables. First, the top five subsystems (in terms of losing data) are the same in both lists, and taken together account for about 70% of the total hours that were lost. Also, the antenna is in the number-two spot on both lists and has an availability of 0.993 in the older data set and 0.9956 in the more recent data set. A true believer in statistics might be tempted to conclude that as our antennas get older they get more reliable, but the reader has already been forewarned about the dangers in these statistics and certainly would not succumb to that temptation. Finally, the total system availability is in the range 0.97–0.98, which I believe is the number that has been used as the system availability per antenna in the current version of the data return calculations.

TABLE B-1. From Jan. 86 to Jul. 90, 142744.75 scheduled hours, all projects, all antennas, telemetry data type.

Abr.	SUBSYSTEM NAME	Hr. lost	Cumulative P	P_i
DTM	DSCC Telemetry Subsystem	1240.75	0.9915	0.9915
ANT	Antenna	963.53	0.9846	0.9930
RFI	Radio Frequency Interference	715.82	0.9795	0.9949
RCV	Receiver-Exciter	474.92	0.9762	0.9966
UMV	DSCC Antenna Microwave Subsystem	459.38	0.9730	0.9967
FAC	DSCC Technical Facilities Subsystem	143.13	0.9720	0.9990
TXR	DSCC Transmitter Subsystem	102.60	0.9713	0.9993
DMC	DSCC Monitor and Control Subsystem	68.40	0.9708	0.9995
NSS	NOCC Support Subsystem	42.18	0.9705	0.9997
GDC	DSCC Digital Communications Subsystem	39.63	0.9702	0.9997
DTK	DSCC Tracking Subsystem	38.13	0.9700	0.9997
FTS	DSCC Frequency and Timing Subsystem	29.72	0.9697	0.9998
N/A	Not Applicable	28.70	0.9695	0.9998
UND	Undefined	24.27	0.9694	0.9998
DSP	DSCC Spectrum Processing Subsystem	8.80	0.9693	0.9999
NTM	NOCC Telemetry Subsystem	5.10	0.9693	1.0000
GIA	GCF Intersite Analog Comm. Subsystem	4.22	0.9693	1.0000
DCD	DSCC Command Subsystem	3.70	0.9692	1.0000
GVC	GCF Voice Subsystem	0.83	0.9692	1.0000
MFR	Multifunction Receiver Subsystem	0.50	0.9692	1.0000
DTS	DSCC Test Support Subsystem	0.18	0.9692	1.0000
NTK	NOCC Tracking Subsystem	0.07	0.9692	1.0000
	Total hr lost =	4393.81		
	System Availability =	0.9692		0.9692

The subsystem availability should be calculated in a slightly different manner when the DSN provides arraying support. An array is a parallel architecture so its reliability is conditional. If we denote the availability of all the parallel subsystems (e.g., the antenna and probably the microwave subsystems) as a_i, then the total availability can be written

$$A_T = a_i \cdot \prod_{i=2}^{N} A_i$$

The composite availability of the antenna and microwave subsystem from the data base summarized in Tables B-1 and B-2 is 0.992, so now all we have to do is figure out how to calculate the conditional probability.

TABLE B-2. From Jan. 89 to Dec. 92, 148382.12 scheduled hours, all projects, DSS 12, 14, 15, 42, 43, 45, 61, 63, and 65, telemetry data type.

Abr.	SUBSYSTEM NAME	Hr. lost	Cumulative P	P_i
DTM	DSCC Telemetry Subsystem	1009.85	0.9933	0.9933
ANT	Antenna	620.70	0.9890	0.9956
RCV	Receiver-Exciter	293.22	0.9870	0.9980
RFI	Radio Frequency Interference	270.33	0.9852	0.9982
UMV	DSCC Antenna Microwave Subsystem	230.48	0.9837	0.9984
UND	Undefined	133.08	0.9828	0.9991
FAC	DSCC Technical Facilities Subsystem	95.18	0.9821	0.9993
DMC	DSCC Monitor and Control Subsystem	87.00	0.9815	0.9994
TXR	DSCC Transmitter Subsystem	81.30	0.9810	0.9994
NSS	NOCC Support Subsystem	48.37	0.9807	0.9997
GDC	DSCC Tracking Subsystem	46.10	0.9804	0.9997
DTK	DSCC Tracking Subsystem	32.72	0.9801	0.9998
FTS	DSCC Frequency and Timing Subsystem	27.07	0.9799	0.9998
N/A	Undefined	27.03	0.9798	0.9998
DCD	DSCC Command Subsystem	5.80	0.9797	1.0000
GIA	GCF Intersite Analog Comm. Subsystem	5.53	0.9797	1.0000
DPS	DSCC Power Subsystem	5.17	0.9797	1.0000
DSP	DSCC Spectrum Processing Subsystem	4.57	0.9796	1.0000
NTM	NOCC Telemetry Subsystem	1.72	0.9796	1.0000
GVC	GCF Voice Subsystem	0.72	0.9796	1.0000
GDR	DSCC Test Support Subsystem	0.18	0.9796	1.0000
NTK	NOCC Tracking Subsystem	0.06	0.9796	1.0000
	Total hr lost =	3026.18		
	System Availability =	0.9796		0.9796

TECHNICAL REPORT STANDARD TITLE PAGE

1. Report No. 94-15	2. Government Accession No.	3. Recipient's Catalog No.
4. Title and Subtitle Synthesis of a Large Communications Aperture Using Small Antennas		5. Report Date July 1, 1994 6. Performing Organization Code
7. Author(s) G.M. Resch, T.A. Cwik, V. Jamnejad, R.T. Logan, R.B. Miller, and D.H. Rogstad		8. Performing Organization Report No.
9. Performing Organization Name and Address JET PROPULSION LABORATORY California Institute of Technology 4800 Oak Grove Drive Pasadena, California 91109		10. Work Unit No. 11. Contract or Grant No. NAS7-918 13. Type of Report and Period Covered JPL Publication
12. Sponsoring Agency Name and Address NATIONAL AERONAUTICS AND SPACE ADMINISTRATION Washington, D.C. 20546		14. Sponsoring Agency Code RF 212 BG-315-91-60-10-07

15. Supplementary Notes

16. Abstract

In this report we compare the cost of an array of small antennas to that of a single large antenna assuming both the array and single large antenna have equal performance and availability. The single large antenna is taken to be one of the 70-m antennas of the Deep Space Network.

The cost of the array is estimated as a function of the array element diameter for three different values of system noise temperature corresponding to three different packaging schemes for the first amplifier. Array elements are taken to be fully steerable paraboloids and their cost estimates were obtained from commercial vendors. Array loss mechanisms and calibration problems are discussed. For array elements in the range 3 to 35 m there is no minimum in the cost versus diameter curve for the three system temperatures that were studied.

17. Key Words (Selected by Author(s))	18. Distribution Statement
Ground Support Systems and Facilities (Space) Communications Systems Analysis	Unclassified; unlimited

19. Security Classif. (of this report)	20. Security Classif. (of this page)	21. No. of Pages	22. Price
Unclassified	Unclassified	132	